

الجامعة
البريطانية في
دبي



The
British University
in Dubai

The Energy Performance of the Double Skin Façade in a Conventional Residential Building in Irbid, Jordan

الأداء الحراري للواجهات الزجاجية المزدوجة في المباني السكنية التقليدية في مدينة
إربد, المملكة الأردنية الهاشمية

by

AHMAD DAUD OMAR ABBADI

**A dissertation submitted in fulfilment
of the requirements for the degree of
MSc SUSTAINABLE DESIGN OF THE BUILT ENVIRONMENT**

at

The British University in Dubai

**Dr. Riad Saraiji
July, 2018**

DECLARATION

I warrant that the content of this research is the direct result of my own work and that any use made in it of published or unpublished copyright material falls within the limits permitted by international copyright conventions.

I understand that a copy of my research will be deposited in the University Library for permanent retention.

I hereby agree that the material mentioned above for which I am author and copyright holder may be copied and distributed by The British University in Dubai for the purposes of research, private study or education and that The British University in Dubai may recover from purchasers the costs incurred in such copying and distribution, where appropriate.

I understand that The British University in Dubai may make a digital copy available in the institutional repository.

I understand that I may apply to the University to retain the right to withhold or to restrict access to my thesis for a period which shall not normally exceed four calendar years from the congregation at which the degree is conferred, the length of the period to be specified in the application, together with the precise reasons for making that application.

Signature of the student

COPYRIGHT AND INFORMATION TO USERS

The author whose copyright is declared on the title page of the work has granted to the British University in Dubai the right to lend his/her research work to users of its library and to make partial or single copies for educational and research use.

The author has also granted permission to the University to keep or make a digital copy for similar use and for the purpose of preservation of the work digitally.

Multiple copying of this work for scholarly purposes may be granted by either the author, the Registrar or the Dean only.

Copying for financial gain shall only be allowed with the author's express permission.

Any use of this work in whole or in part shall respect the moral rights of the author to be acknowledged and to reflect in good faith and without detriment the meaning of the content, and the original authorship.

Abstract

This paper aims at investigating the thermal performance of double skin façade (DSF) for a residential building known as “Amara” in Irbid, Jordan. This city, is the second largest city located in the northern part of Jordan, usually experiences a hot dry summer with high solar radiations and a cold-wet winter. Being the DSF the globe’s active trends that is applicable in both new and refurbishment of old buildings as a passive solution, this paper addresses aspects of applying the DSF on an inhabited building in Irbid considering the windows glazing type and cavity thicknesses on the energy consumption of the adjacent conditioned zones. In this work, a comparative study is carried out on a base case and several models of DSF to systematically assess whether this system could work as a passive strategy. This papers also reviews literatures from cities share similar climate conditions. The majority of research results show that the DSF functions efficiently during winters, while the summer overheating between the two skin layers is highly predictable due to the excessive solar gains and its performance is not guaranteed during summer. Hence, special focuses were implemented on the different geometry shapes of the DSF to achieve the maximum benefits possible in attaining the thermal comfort zones with the minimal usage of the fossil-fuels based equipment.

Simulation using IES VE software confirmed that both the cavity width and geometry of the DSF played a massive role in obtaining a relatively moderate thermal zone during winter seasons and an acceptable indoor temperature during summer seasons. Results of simulations are presented and discussed for several geometry types, cavity widths, and ventilation modes. The results also highlighted the potential of energy saving in comparison to the existing façade (single skin façade). The impact on the occupant’s thermal satisfaction is also investigated.

Results showed that the box-window DSF type with 300mm cavity width is the most candidate facade that saves energy around 37.22% coincides with increasing occupant's thermal acceptance by 8.15% from 63.01% in the base case.

ملخص البحث

يهدف هذه البحث بدراسة الأداء الحراري في نظام البناء بالواجهه المزدوجه لمبنى سكني تقليدي المعروف باسم (العماره) في مدينه اربد, الأردن. هذه المدينه والتي تقع في القسم لشمالي في المملكه, تتمتع بمناخ حار وجاف في فصل الصيف واشعاع شمسي كبير نسبيا مع فصل شتاء بارد ورطب. وبما ان هذا النظام الذي يمكن تطبيقه في المباني الحديثه وكوسيله لتحديث مبنى مأهول والذي يمتاز بقبول عالمي في اتجاهات تخفيض كلف الطاقه التشغيليه للمبنى, هذه العمل يعنون طرق تطبيق هذه النظام في مبنى مشغول باخذ عين الاعتبار نوعيه الزجاج المستخدم في هذه النظام وايضا يعزم بدراسه سمك الفراغ ما بين الواجهه الاصليه للمبنى والواجهه المضافه وتأثيرهما على الاستهلاك الكلي للطاقه للغرف الداخليه. وايضاً, بني هذه البحث على مبدأ المقارنه ما بين الاستهلاك الكلي للطاقه مع دراسه مدى الارتياح الحراري للسكان في الوضع الحالي وبين مدى تحسنها او تدهورها بعد تطبيق نظام الواجهه المزدوجه على المبنى.

وتم اخذ بعين الإعتبار الاوراق البحثيه السابقه التي تمحورت حول استخدام هذه النظام في بيئيه مناخيه مماثله. بعض هذه الأبحاث اكدت فعاليتها في فصل الشتاء بينما الزيادة المفرطه في درجات الحراره خلال الصيف كانت متوقعه نتيجته للاشعاع الشمسي الكبير في هذه المناخ وادائه في هذه الظروف غير مضمونه. بناءً على ذلك, تمت الدراسه بالتركيز على عده هياكل شكلية للنظام حسب ما تم اقتراحها في الاوراق البحثيه في هذه السياق ومسافه البعد لهذه الواجهه الاضافيه عن الواجهه الاصليه للمبنى.

أكدت نظام المحاكاه الحاسوبية باستعمال برنامج (IES VE) على كفاءه عمل هذه النظام بحيث يوفر بيئه معتدله حراريا خلال فصل الشتاء وبيئه مقبوله الى حد ما في فصل الصيف. نتائج المحاكاه الحاسوبيه سوف يتم عرضها وسوف تناقش عده جوانب كهياكل مقترحه للواجهه الزجاجيه, سمك الفراغ ما الواجهه الاصليه والواجهه الزجاجيه المضافه, نوعيه التهويه التشغيليه. ومستويات الراحة الحراريه للسكان ايضاً سوف يتم مناقشتها ايضاً.

وأظهرت النتائج بان استعمال الواجهه المزدوجه التي لها شكل الصندوق الزجاجي (box-window) والتي تبعد مسافه 300 مم عن الواجهه الاصليه بانخفاض الاستهلاك الكلي للطاقه بنسبه 37.22% مقارنة في الحاله الاساسيه مع رفع درجه الارتياح الحراري للسكان بنسبه 8.15% مقارنة ب 63.01% في الحاله الاساسيه.

In the name of Allah the most Gracious the most Merciful

Acknowledgment

First of All, I would greatly thank **Allah Almighty** for his countless mercy and his will for giving me the ability to reach this stage. All praises and thanks be to **Allah**, the lord of the worlds.

Secondly, I would like to extend my sincere gratitude to my principal supervisor, **Dr. Riad Saraiji** for his tremendous support, patience, and mentor advice throughout this work. Thank you for your valuable guidance and efforts given for reaching this piece of work. I appreciated and owe you a lot for this.

To my parents (**Daoud & Khawla**) for their tremendous moral support and all tenderness over the entire of my life. Indeed, no words can express my deep love for both of you for your continuous giving. To my sister (**Doa'a**), who without her support and assistance throughout this work, this work and previous works would never been completed. Special thanks to my brothers (**Mohammad, Yazan, and Omar**) for their moral support and encouragement.

Special thanks to my Fiancé **Hala Al Sharawi** (Wife to be) for her support and understanding during the implementation of this long work over the past eight months. Thank you for your patience and support and your insistence on ending this work to the fullest.

Lastly, I would like to acknowledge the moral support given from ECG staff in Al Andalus Site office. Special thanks to my manager, my friend, our project Resident Engineer, Mr. **Shareef Kholief** for his understanding, support, and encouragement until this work had completed.

Table of Contents

1.0	Introduction.....	1
1.1	Overview.....	1
1.2	Jordan Sustainability Program	5
1.3	Research Aims and Objectives.....	5
1.4	Research Framework.....	6
2.0	Literature review	8
2.1	Definition and history of the Double Skin Façade.	8
2.2	Double Skin Façades classification and categories	9
2.3	Double Skin Façades as a Refurbishment of old building and their geometry types.	12
2.4	Double Skin Façade Example in Jordan	17
2.5	The significance of the study in the residential buildings sector in Jordan.....	18
3.0	Overview of the Hashemite Kingdom of Jordan, and Jordanian Energy Profile.....	20
3.1	Climate of Irbid/Jordan: An overview of Irbid City.....	22
4.0	Methodology	27
4.1	Research Approaches applicable to investigating the performance of the DSF.....	28
4.1.1	Experimental Approach	28
4.1.2	Computer/modeling Approach	29
4.1.3	Mixed-mode methodology	30
4.2	Justification of the selected approach.	30
4.3	Limitation of the study.....	31
4.4	Research Methodology	32
4.5	Simulation Software Selection	34
4.6	Building Sector in Irbid	35
4.7	Overview of the Base Case	38
4.7.1	Site Analysis.....	38
4.7.2	Description of the base case	40
4.8	Development of base case model	43
4.8.1	Setup the simulation model	43
4.8.2	Model exporting to IES VE.....	44
4.8.3	Building envelope definitions.....	45
4.8.4	Internal heat gain	47
4.8.5	Thermal profile of the base case	47

4.8.6	Windows and door openings scheme.....	49
4.8.7	Energy consumption evaluation methodology	50
4.9	Development of the double skin façade model.	51
4.9.1	Simulation procedures	51
4.9.2	Simulation Process.....	53
4.9.3	Façade vents and external window openings definitions	53
4.9.4	Energy consumption evaluation	56
5.0	Results of the simulation models	57
5.1	Findings of the base case	57
5.1.1	Indoor air temperature vs indoor relative humidity	57
5.1.2	Thermal comfort evaluation	59
5.1.3	Airflow rates and heat gain	63
5.1.4	Solar heat gain	64
5.1.5	Surface temperature	65
5.1.6	Heat gain through conduction.....	65
5.1.7	Energy consumption	66
5.2	Double skin façade simulation models results	69
5.2.1	Multistory DSF type 600mm cavity width.....	73
5.2.2	Corridor DSF 600mm cavity width	76
5.2.3	Shaft DSF 900mm cavity width	78
5.2.4	Box-window DSF 300mm cavity width	81
6.0	Discussion	84
6.1	Thermal behavior of the double skin façade.	84
6.1.1	Cavity air temperature.....	84
6.2	Thermal behavior of internal spaces.	87
6.2.1	Average behavior in summer.....	88
6.2.2	Average behavior in winter	95
6.3	Cooling and heating loads summary.....	104
7.0	Conclusion	107
7.1	Recommendation and future works	111
8.0	References.....	112

List of Figures

Figure 1:	Increase in electricity consumption in TeraWatts. (Source: MOEMR, 2016)	03
Figure 2:	Different types of double skin facade. (Source: Alberto et al. 2017, p. 88)	04
Figure 3:	The main structure of the double skin façade. (Source: Knaack, et al. (2000), P.29).	08
Figure 4:	Heat transfer and airflow through a ventilated DSF system. (Source: ALS & TT, 2014)	09
Figure 5:	Schematic diagram of DSF. (Source: http://new.fatare.com/double-curtain-wall-facade/)	10
Figure 6:	30 ST Mary Axe. (Source: fosterandpartners, 2015)	16
Figure 7:	One Angel Square. (Source: Colt Group, 2015)	16
Figure 8:	Capital Gate, Abu Dhabi (Source, Eileen, 2016)	16
Figure 9:	Building facade for both residential and commercial buildings of The Abdali Boulevard in Amman.	17
Figure 10:	Full glazed facades of Rotana Amman Hotel. (Source: http://reset-studio.com/portfolio/items/amman-rotana-hotel)	18
Figure 11:	Population distribution of Jordan. (Source: MEMR, 2015)	20
Figure 12:	Percentage of the electricity consumption in the Jordanian different sector	21
Figure 13:	Local production share of the total energy requirements 2015	21
Figure 14:	Map of Jordan. The red line indicates the City of Irbid. (Source: DOS, 2016).	22
Figure 15:	Jordan map of Köppen climate classification. (Source: Kotteck et al. 2006)	23
Figure 16:	Psychometric chart of Irbid (Source: Climate Consultant 6.0)	25
Figure 17:	Research methodology	33
Figure 18:	Dominant housing type in Irbid. a) Villa, b) High standards apartments, and c) Dar	35
Figure 19:	Number of houses per housing type and their annual energy costs in Jordan and for Irbid. (Source: DOS, 2016)	36
Figure 20:	Suggested u-values for walls, roof, exposed floors, and windows types by Energy-efficient Building code of Jordan.	37
Figure 21:	Site location and analysis of the chosen case study building	39
Figure 22:	Base case building selected for assessment	40
Figure 24:	Typical floor plan	42
Figure 23:	Cross view of Al Majd-1 Building.	42
Figure 25:	Base case model as modeled in Sketch up software.	44
Figure 26:	The base case as illustrated in IES VE software.	45
Figure 27:	Acceptable operative temperature ranges for conditioned spaces. (Source: ASHRAE-55, 2010, P.14)	48
Figure 28:	Windows open/close control diagram	49

Figure 29:	Energy consumption calculation methodology for the base case. Note T_{IN} is the indoor air temperature.	50
Figure 30:	Different geometry types of double-skin facades.	51
Figure 31:	Multistory type double skin facade building as appear in IES VE software	52
Figure 32:	Airflow modes studied for the assessment of the double skin facade.	53
Figure 33:	Methodology diagram of DSF thermal assessment	53
Figure 34:	Monthly PPD ranges of the shaft type DSF with 300mm cavity width in term of the mode of ventilation.	54
Figure 35:	Facade's and external windows' vents controlling diagram.	55
Figure 36:	The process of controlling the facade vents in case of overheating in summer season.	55
Figure 37:	Energy consumption calculation methodology for DSF.	56
Figure 38:	The relationship between the annual average dry-bulb temperature with the annual average room air temperature when the windows are opened and closed	58
Figure 39:	The relationship between the outdoor RH% with room RH% when the windows are either opened or closed	58
Figure 40:	Psychrometric chart indicating the winter and summer comfort zones (ASHRAE-55 (2010), P8)	59
Figure 41:	Maximum and minimum air temperature versus average mean annual air relative humidity: (a) external windows opened, (b) external windows closed.	60
Figure 42:	The annual operative temperature of the base case (4th floor) when, a) windows are opened, b) windows are closed	61
Figure 43:	Predicted percentage of dissatisfied (PPD) for both windows open/close modes for the base case.	62
Figure 44:	Assigned PPD for the base case	63
Figure 45:	Volume flow rate of the air entering the building's openings	63
Figure 46:	Heat gain through airflow entering the building's openings.	64
Figure 47:	Monthly solar heat gain on the external facade.	64
Figure 48:	External walls and windows surface temperatures.	65
Figure 49:	Heat gained through conduction	66
Figure 50:	Boiler and chiller systems loads.	68
Figure 51:	Energy consumption for the base case	68
Figure 52:	Comparison between base case PPD and other facade's type according to cavity widths	70
Figure 53:	The development of double skin façade simulation models in Sketchup software: a) Multistory, b) Corridor, c) Shaft, and d) Box-window.	72
Figure 54:	Volume flow rate of air entering the building and multistory DSF building	73
Figure 55:	Heat gain through airflow entering windows openings from Multistory 600mm façade's cavity width.	74
Figure 56:	The annual solar gain of the multistory type DSF building	75
Figure 57:	Conduction gain through external walls of the multistory DSF type building	75

Figure 58:	Volume flow rate of air entering the building and corridor DSF building	76
Figure 59:	Heat gain through airflow entering windows openings from corridor 600mm façade's cavity width	77
Figure 60:	The annual solar gain of the corridor type DSF building	77
Figure 61:	Conduction gain through external walls of the corridor DSF type building	78
Figure 62:	Volume flow rate of air entering the building and shaft DSF building	79
Figure 63:	Heat gain through airflow entering windows openings from shaft 900mm façade's cavity width	80
Figure 64:	The annual solar gain of the shaft type DSF building	80
Figure 65:	Conduction gain through external walls of the shaft DSF type building	81
Figure 66:	Volume flow rate of air entering the building and box-window DSF building	82
Figure 67:	Heat gain through airflow entering windows openings from box-window 300mm façade's cavity width	82
Figure 68:	The annual solar gain of the box-window type DSF building	83
Figure 69:	Conduction gain through external walls of the box-window DSF type building	83
Figure 70:	Annual average dry-bulb temperature vs the annual average cavity air temperature for each DSF geometry type according to the lowest PPD	85
Figure 71:	CFD image for the airflow velocity entering the external windows after utilizing the box-window DSF.	86
Figure 72:	Average airflow inside the facade's cavity during the cooling months.	86
Figure 73:	Velocity contour of the magnitude (m/s) of airflow entering the box-window DSF cavity	87
Figure 74:	Annual comparison between the indoor air temperature of the Base Case and after utilizing a various type of DSF with the outdoor air temperature. Red rectangles indicate the period selected for the hottest and coldest week.	88
Figure 75:	Air temperature and solar direct irradiance on a horizontal surface for the period from May 1st to September 30th. The rectangle indicates the week selected for the detailed analysis.	89
Figure 76:	Indoor air temperature for the period from May 1st to September 30th.	89
Figure 77:	Outdoor air temperature, relative humidity, and solar irradiance on a horizontal surface for the period between June 28th and July 4th	90
Figure 78:	Indoor air temperature for the period between June 28th and July 4th.	91
Figure 79:	Predicted percentage of the dissatisfied (PPD) as a function of the predicted mean vote (PMV). (Source: Knaack et al., 2007)	92
Figure 80:	PMV calculated for the 4th floor for the period between May 1st and September 30th. The black bounds represent the recommended values as per ASHRAE 55 standard for general comfort.	93
Figure 81:	PMV calculated for the 4th floor for one-week interval for the peak period in summer from June 28th to July 4th.	93
Figure 82:	PPD calculated for the 4th floor for one-week interval for the peak period in summer from June 28th to July 4th.	94
Figure 83:	Air temperature and solar direct irradiance on a horizontal surface for the period from January 1st to April 30th, and from October 1st to December 31st. The rectangle indicates the week selected for the detailed analysis.	95
Figure 84:	Indoor air temperature for the period from January 1st to April 30th, and from October 1st to December 31st	96

Figure 85:	Outdoor air temperature, relative humidity, and solar irradiance on a horizontal surface for the period January 1st to April 30th, and from October 1st to December 31st	96
Figure 86:	Indoor air temperature for the period between January 7th and January 13th	97
Figure 87:	PMV calculated for the 4th floor for the period between January 1st to April 30th, and from October 1st to December 31st. The black lines bound the recommended values as per ASHRAE 55 standard for general comfort.	98
Figure 88:	PMV calculated for the 4th floor for one-week interval for the peak period in summer from January 7th to January 13th.	98
Figure 89:	PPD calculated for the 4th floor for one-week interval for the peak period in winter from January 7th to January 13th.	99
Figure 90:	Typical plan floor of Al Majd 1 building. The box-window DSF is situated on all building sides.	100
Figure 91:	Section A-A	100
Figure 92:	View 1 details.	101
Figure 93:	Cross-section diagram of the box-window for both summer and winter modes.	101
Figure 94:	Rendered image of the building with box window type DSF.	103
Figure 95:	Boiler and chiller systems loads for the box-window DSF.	105
Figure 96:	Comparison between base case building and box-window DSF building for final energy consumption	106

List of Tables

Table 1:	The advantages and disadvantages of double skin façades found in different literature sources	11
Table 2:	Monthly air temperature ranges and solar irradiance on the horizontal surface of Irbid city	24
Table 3:	Sky cover ranges, rainfall, and relative humidity of Irbid City	24
Table 4:	Wind speed and prevailing direction of Irbid	25
Table 5:	Recommended strategies to achieve the thermal comfort of Irbid City (Source: EnergyPlus V3, 2018).	26
Table 6:	The numbering system for a typical apartment	41
Table 7:	Geometrical properties for all volumes, windows area, and window to wall ratios	43
Table 8:	Building model properties	46
Table 9:	Optical material properties	46
Table 10:	Internal heat gain	47
Table 11:	Double skin facade glazing properties.	52
Table 12:	Monthly thermal comfort zone boundaries	66
Table 13:	Summary of monthly energy profiles as defined in IES VE.	67
Table 14:	The monthly average of airflow for Multistory and the comparison with the base case in the ventilated months	73
Table 15:	The monthly average of airflow for Multistory and the comparison with the base case in the ventilated months	76
Table 16:	The monthly average of airflow for Multistory and the comparison with the base case in the ventilated months	79
Table 17:	The monthly average of airflow for box-window and the comparison with the base case in the ventilated months	82
Table 18:	Average PPD for summer, winter, and annual.	99
Table 19:	Upper and lower temperature limits for the box-window DSF building type.	104
Table 20:	Temperature and ventilation profiles defined in IES VE for the assessment of box-window DSF.	105
Table 21:	The similarity between findings from the literature and their relation to this research findings	110

1.0 Introduction.

1.1 Overview

The building sector constitutes a relatively large proportion of the global energy consumption of a nearly of 40 percent (Pomponi et al. 2016). The building total life cycle energy consumption including the construction stage, embodied energy, and operational energy is the main contributors of depleting the global natural resources, greenhouse gas (GHG) emissions, and then the challenges related to the Global Warming. With the global growth concerns for the sustainable use of energy and the energy efficiency of buildings, these interests have directed all the parties on a different scales to redefine the building performance standards corresponding the architectural thinking of buildings to develop new constructive solutions (Inan et al. 2016). One of the most paramount importance for that the sustainable designs in the built environment and their development principles seek is to reduce the energy demand and consumption by maximizing the use of renewable and sustainable energy. However, building façade's systems can introduce significant benefits in affording efficient energy management, better thermal insulation, providing thermal comfort, enhance the visual contact with the outdoor environment. One of these systems is called the "Double Skin Façade".

Double Skin Façade (DSF) has recently become the promising trends that emerged in energy efficiency and improve the indoor thermal comfort without affecting the primary functionality of the building. DSF is an architectural element recognized as an effective solution to obtain a better thermal insulation, blocking solar radiation, enhance the occupants' thermal comfort without breaking the indoor environment linkage with the outdoor. With the global growth concerns in analyzing the energy performance of DSFs, various studies with a different type of approaches were proved the energy saving with DSF. The top important areas in assessing the DSF performance were concentrated on the natural ventilation and thermal performance.

The modern DSF systems act as an external envelope that typically comprises two transparent glass façades separated by an intermediate air cavity. The ventilated cavity can improve indoor air quality and energy efficiency during summer and the sealed cavity helps in minimizing the heat loss and maximize the solar energy gain. Astorqui & Amores (2016) have defined the DSF as the additional sheet of the building that dissipates the absorbed heat from the direct solar radiation when it falls which,

consequently, reduces the temperature on the internal skin and therefore enhances the interior spaces temperature of the building.

The DSF systems can be applied to new buildings or as a renovation and refurbishment of old buildings. However, the internal skin usually consists of actual building façade, glazed, or semi-glazed skin and the external skin consists of the full transparent glass. The air gap between the two skins behaves as an insulating barrier against the undesirable ambient microclimatic conditions. This gap, that varies from 0.2m to 2m, has been defined by Jiru and Haghighat (2008) as the thermal buffer at which enhances the unwanted heat gain during the summer seasons, heat loss during the winter seasons, and raise the thermal comfort due to unequally thermal radiation between the two seasons. Two driven-force the cavity of façade can generate according to the cavity openings' configuration; temperature-generated thermal force and wind-induced pressure force. The former occurs during the sealed cavity while the latter occurs in the ventilated cavity. The cavity between the two skins may be ventilated with three different modes: mechanical, fan-supported (hybrid), or naturally (Pasut & Carli, 2012). According to Shamari et al. (2011), several DSF typologies were classified according to their air gap ventilation mechanism, fixed or adjustable inlets and outlets. However, the sealed air cavity enhances the greenhouse effect in winter while the ventilated air cavity decreases the heat gain in summer.

Jordan is a non-oil country that heavily depends on the foreign assistance and subsidies which faces serious energy security. For instance, it has been noticed that the construction of buildings is significantly grown over the past few years in the city of Irbid, Jordan. Due to the political disturbance within its neighboring countries that led to the emergence of large numbers of refugees that raising the urban population and then increases the pressure on the housing demand in the city. In Jordan, the annual electricity demand is increasing by 4-5%, and it has soared by 7.5% in the year 2017. The electricity consumption is attributed to be increased due to industrialization and development of the built environment being massively witnessed in the country in the past few years. According to Ministry of Energy and Mineral Resources statistics, the electricity consumption for all sectors in Jordan over the past 31 years has eightfold from 2151 to 7448 TW (Figure 1) since 1985 to 2016. The building sector is responsible for more than 45% of the total share electricity consumption in the kingdom. Within the public electricity consumption domain, the household stands out as the most energy consumer.

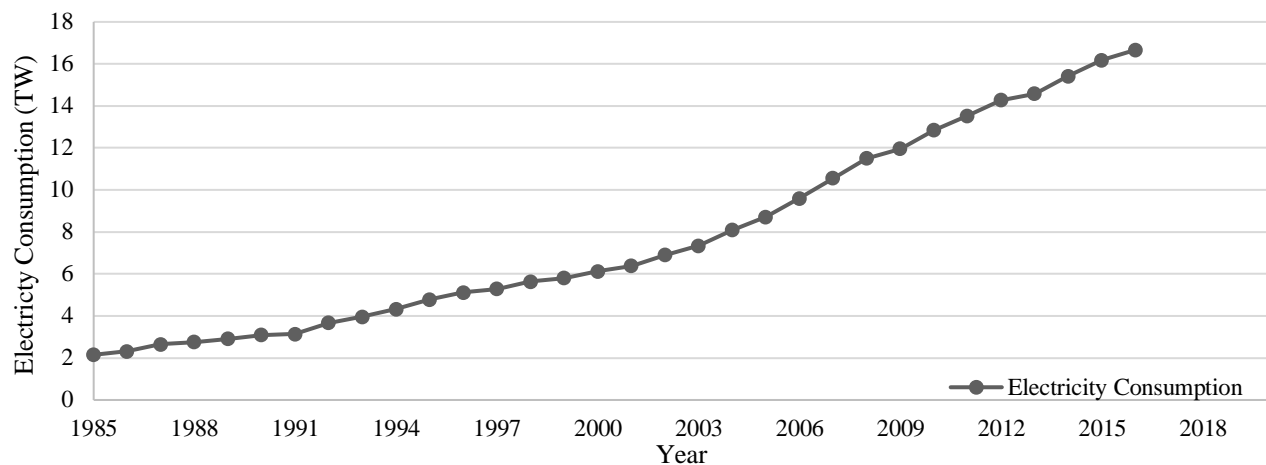


Figure 1: Increase in electricity consumption in Tera Watts. (Source: MOEMR, 2016)

In this context, a sustainable development in Irbid’s built environment regarding the energy saving in the building sector is strongly crucial. Investigating the DSF system potentials as promising passive technology in Jordan is important where the country experiences a relatively high solar radiation in summer reaching 5 kW.h/m² which cause overheating in this particular season. Generally, the system is expected to perform efficiently in winters but overheating related issues during summer is not guaranteed.

On the other hand, the Mediterranean regions are classified as a hot arid climate which characterized by large solar gain and high air temperature. In such climates, overheating and large energy consumption of buildings are the main issue to be managed. Jordan has been specified as the Csa region according to Koppen-Geiger’s climate classification system in which the country characterized by a dry temperate to cold winter wet warm to hot summer.

This paper targets to explore the various benefits of applying the DSF to an existing residential building in a Mediterranean climate. This paper main goals are to study the thermal performance of an existing residential building and simulate the annual energy consumption after applying the DSF. Pomponi et al. (2016) declared that research for the energy performances on the DSF in the temperate climate is crucial due to the knowledge gap in the available literature and lack of conclusive results in this area. Nevertheless, many studies have been conducted on investigating the performance of the DSF, no clear standards were been developed on the DSF design as the designing of the DSF is highly affected by the individual climate conditions of the building location. A study conducted by Lee & Chang (2015) showed that buildings with DSF with particular conditions obtained an energy saving by around 23.2% in the cooling season. A supportive proof for the DSF has been carried on by Larsen et al. (2015) shows that

the overheating period in the Mediterranean climate can be avoided by the appropriate selection of the façade's glazing.

The application of the double-skin façade arose at the early of the 20th century. This DSF acts as an alternative solution to improve the energy performance of the building instead of using the traditional single skin façades (Alberto et al. 2017). The double-skin façade is a sort of complex concept which mainly classified based on several factors and assumptions. However, there are primary there parameters that mainly contribute to the performance of the DSF such as the ventilation modes, air-cavity configuration, and air movement inside the cavity. Further to its transparent aesthetics, the DSF can provide the desired solution if appropriate design strategies are applied. Moreover, the three secondary parameters that characterize the double-skin façades are; the width of the cavity, shading devices, the height of the façade itself, and automated operable inlets & outlets. Accordingly, Alberto et al. (2017) have also categorized the DSF into four main distinct groups: Box-Windows, Corridor, Shaft-Box, and Multi-Story as shown in Figure 2.

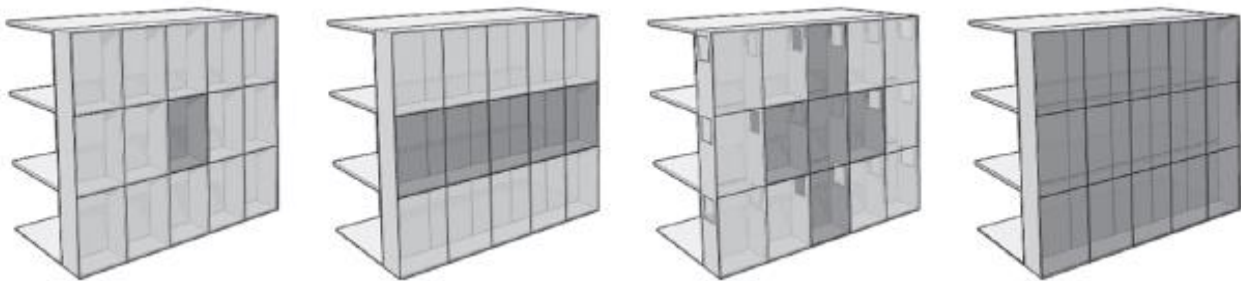


Figure 2: Different types of double skin facade. (Source: Alberto et al. 2017, p. 88)

The computer simulation is the chosen methodology for the performance investigation of the DSF. However, a group of assumptions for configuring the DSF is wisely selected for manipulating the six parameters along with the four DSF groups in this study in order to predict the optimum DSF efficiency, energy demands reduction, and for best users' thermal comfort experience. However, DSF is considered one of the promising passive cooling and heating technology to control the consumption of energy as well as enhance the thermal comfort for occupants. As Agrawal (1989) declaration, a reduction of 2.35% of total energy consumption can be avoided by utilizing the proper passive design for buildings. At the same time, on account of the complexity of the DSF working principles, independence of the system where the design of the DSF in a particular city is not necessarily applicable in another city, and also

there are no noticeable studies or assessments of the DSFs in Irbid especially in the residential sector. Thus, this report is quite important to investigate the performance of this system.

Generally speaking, this study showed that the DSF would be able to provide a significant heating loads reduction and a slight cooling energy reduction of the residential building. Furthermore, the system also able to achieve an 80% thermal comfort during the whole year.

Finally, general aspects of the system were drawn up, key outcomes and recommendations were also set out, research limitation and future works were described as well.

1.2 Jordan Sustainability Program

Jordan roadmap for sustainable development for tackling the energy scarcity has been developed. The program main aims to increase the contribution and exploiting of renewable energies to its total primary energy mix to reach 10% in 2020 and working on setting higher percentages by 2030 (MOEMR 2017). In that context, the Government of Jordan has set the targets to lessen the energy consumption from 0.296 to 0.276 toe in 2030. However, in order to maximize and optimize the building energy efficiency, Jordanian building codes were modified to codes that comply with green building regulations such as Energy Efficient Buildings Code and Jordan Green Building Code.

For that purpose, the Jordan Renewable Energy and Energy Efficiency Fund (JREEEF) that established in 2012, plays a local supportive firm in providing citizens with green financing to achieve the desired energy efficiency and reroute the reliance on energy towards renewable and sustainable energies, thus building awareness of the efficient use and conservation of energy and protecting energy infrastructure.

The Jordan's GHG emissions were reached approximately 28.7 million tons per year contributes to 0.06% of the global emissions. Consequently, the country CO₂ emissions per capita reached 4.41 tons during 2016 and expectations predict to reach 5.59 tons by the end of 2030.

1.3 Research Aims and Objectives

The research aims in investigating the thermal performance of several geometry types of DSF applied in a residential building located a warm to hot summer and cool to cold winter climatic conditions. More specifically, the assessment of the façade will be based on the most façade that affords better thermal insulation, natural ventilation, and able to enhance the occupants' annual thermal comfort.

The work aims to conclude with results that identify the followings objectives:

- 1- To study the importance of the various geometric shape of the DSF.
- 2- To investigate the potential of the system's performance in heating loads in winter and cooling loads reduction in summer.
- 3- To assess the importance of the cavity width that affects the system performance.
- 4- Determine the thermal comfort boundaries that comply with ASHRAE 55 standards to achieve 80% thermal satisfaction.
- 5- Examine the conduction heat gain before and after applying the DSF.
- 6- Study the effect of solar gain on the building's thermal performance.
- 7- Study the effect of the airflows and the related heat gain.
- 8- Evaluate the overall energy reduction after the selection of the most appropriate façade geometry along with the optimal cavity width.

1.4 Research Framework.

This research was built based on a simulation process where detailed computational simulation models based on IES VE software was developed to comprehensively investigate the energy performance of the double skin façade on a reference building located in Irbid, Jordan. The heat transfer, airflow, conduction and solar gain, and overall thermal acceptance were adopted to investigate the corresponding performance simultaneously.

To meet the objective of this study, this work will be divided as per the following guidance:

Part one provided an introduction of the double skin façade as passive solution technique in warm Mediterranean regions, indicating Jordan as a country that the DSF would be a promising solution that tackles the huge energy being consumed in the residential buildings in the country. Also, the research aims and objectives also covered in this part.

Part two covers the current body of relevant literature review related to investigating the thermal performance of DSF in several climatic conditions. Also, introduces the history and the working principles of the DSF. This part concludes some design guidelines and recommendations previously found in order to achieve the desired benefits of the DSF.

The **part three** describes the climatic conditions of Jordan in general and Irbid city in particular and discuss the weakness of current Jordanian building construction styles. However, this part also introduces some examples of DSF projects in commercial buildings in Amman.

Part four defines the proposed methodology in investigating the energy performance of DSF. Additionally, it describes the process of developing the computer simulation model in order to investigate the chosen base case and DSF models.

Part five presents and discusses the research outcomes based on the parametric study of various types of the DSF. It concerns in delivering the interpreting outstanding results showing the significance of DSF in achieving better performance in comparison with the base case model.

Part six concerns in integrating all results gathered from previous parts in selecting the façade's type that achieves the lowest energy consumption as well as the highest possible thermal acceptance level of occupants.

Part seven draws the general conclusion of the entire research including the major outcomes that might be benefiting the residential sector in Jordan, a comparative study between this research results with others concerning similar climatic conditions, and future works opportunities are also included.

2.0 Literature review

Benefits associated with the double skin façade systems have been described in several articles, reports, and books to gather more information to determine the efficient factors to enhance the principle airflow movement within the DSFs. These factors are physical such as the outdoor wind pressure or technical such as façade materials, cavity width, inlet/outlet sizes, and windows glazing types. Several previous works describing the benefits of natural ventilated double skin façade are presented as the following.

2.1 Definition and history of the Double Skin Façade.

Double Skin Façade system has been introduced in several references and being recognized in modern buildings as an additional layer - mainly glass - installed over the existing building façade and an intermediate gap separating the two skins (Figure 3). This gap between the two skins mainly known as the façade's cavity acts as an air channel ranging from 0.2m to several meters are often creates thermal buffer zones that serve in insulating the building from the external conditions such as overheating caused by excessive solar heat gain. This thermal buffer zone facilitates the circulating of the solar gain into internal spaces to offset the heating requirements during winters, while the ventilated cavity allowing the air to pass to mitigate the solar radiation and decrease the cooling loads in the summer period.

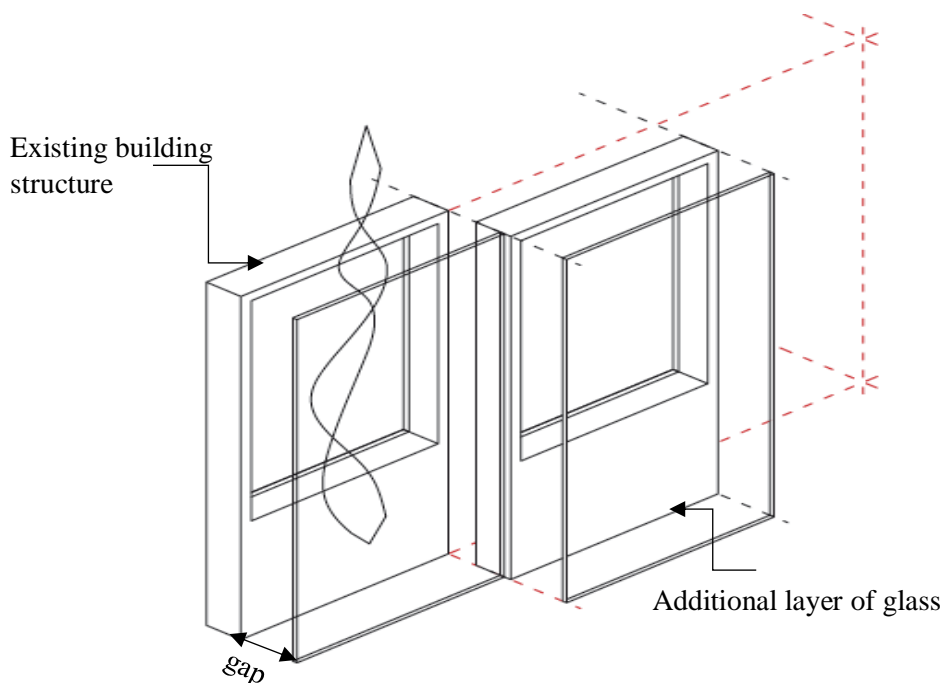


Figure 3: Main structure of the double skin façade. (Source: Knaack, et al. (2000), P.29).

The DSF first appear is in 1903 in Giengen, Germany (Poirazis, 2006). The main purpose of the structure was to maximize the daylight, enhance the thermal efficiency of the building, and protect the building from the strong winds. However, after the success of the system, two additional DSF buildings were built in 1904 and 1908. The system got attention in the 90's due to the increased environmental concerns that pushing the architectural design towards “green building”. By the end of 20th century, the DSF was spread in the European countries as an environmental solution for climatic building moderator. Recently, DSF has been used in cold to moderate regions and the concerns regarding the performance in harsh and hot climates more critical nowadays.

2.2 Double Skin Façades classification and categories

The classifications of the Double Skin Façade based on their categories were extensively mentioned in the literature. However, several aspects responsible for categorizing the system based on the type of construction and the mechanism of the air flow in the cavity.

Arons (2000) defined the DSF based on the airflow modes of the façade; airflow façade and airflow windows. The airflow façade is the airflow movement type that is continued for at least one-story height at which the inlets and outlets of the façade is placed below and above of the floor level of the story, respectively, while the airflow window is that façade that the spacing between the inlets and outlets is less than ceiling height of the floor. Magali (2001) differentiate the system by the system can be working as a full structure for the whole building or it has an individual working principle per the separated floor level. The difference between the two categories is the horizontal partitioning of the air cavity. Figure 4 shows a cross-section of the corridor or box-window DSF type.

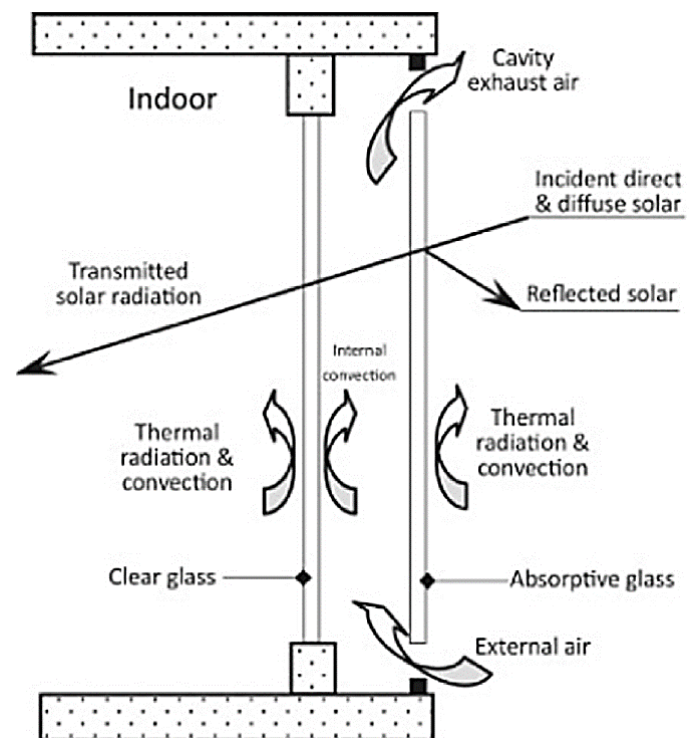


Figure 4: Heat transfer and airflow through a ventilated DSF system. (Source: ALS & TT, 2014)

Kragh (2000) categorized the DSF system upon the ventilation mode of the cavity into three different type; naturally ventilated wall, active wall, and an interactive wall. The naturally ventilated wall mainly depends on the amount of ambient airflow in which reduces the absorbed solar gain. This type of façade is not recommended in hot climates due to the risk of overheating of the cavity air. The active wall working principles significantly rely on the heat exchange between the outdoor and indoor air temperature where the inner glass remains close to the indoor air temperatures, in which this type of façade is preferable for cold climates. Lastly, the interactive wall working principle is similar to the naturally ventilated wall, but the outdoor ambient temperature is driven force of the system rather than the stack effect presented in the ventilated walls. This system is ideal for such a hot climate with relatively high cooling demands.

The Belgian Building Research Institute (BBRI) 2002 recommends classifying of the DSF by considering a detailed mode of operation of each compartment such as the type of ventilation, the source of airflow, movement of airflow, the width of the cavity, and the horizontal partitioning as illustrated in Figure 5

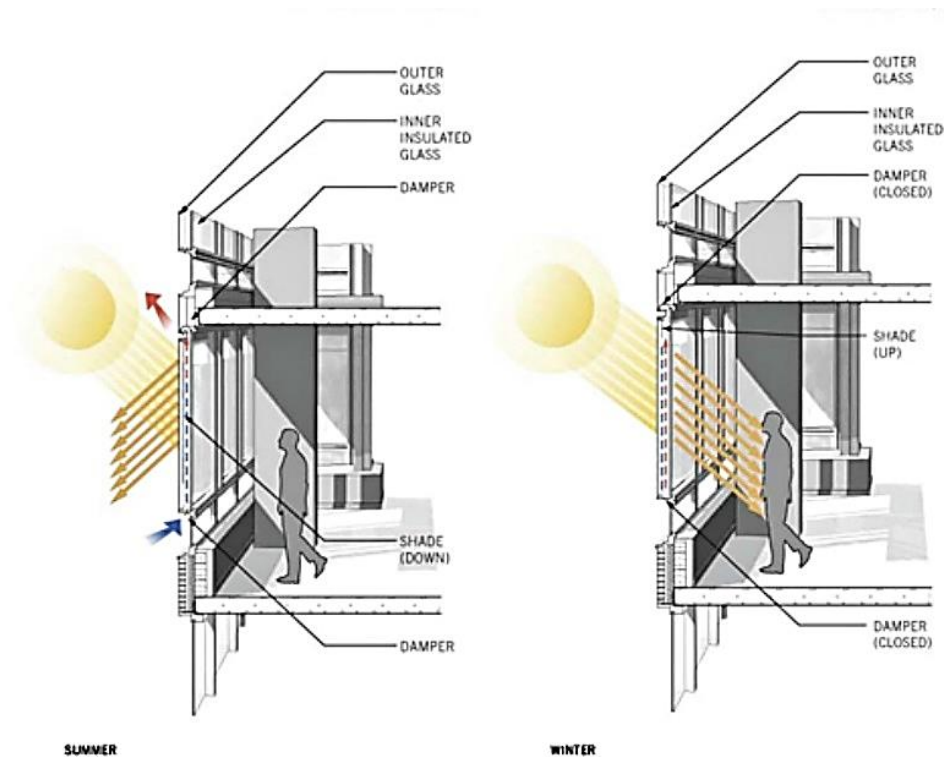


Figure 5: Schematic diagram of DSF. (Source: <http://new.fatare.com/double-curtain-wall-facade/>)

The advantageous and disadvantageous of the DSF were widely described in the literature that clarified the strength and weak points that used as a benchmark in proper designing of the DSF. Well-designed DSF can provide pros and cons, Table 1 shows the summary of some of the advantages and disadvantages mentioned in the literature.

Table 1: The advantages and disadvantages of double skin façades found in different literature sources

	Type	Description
Advantages	Lower Construction Cost	DSF proved its efficiency in delivering environmental solutions and achieve a quality of variability with lower capital cost compared to electrochromic, thermochromic, or photochromic panes,
	Acoustic Insulation	DSF acoustic performance is efficient in which the reducing the sound transmission from outdoor resources capable of delivering acoustic comfort.
	Thermal Insulation	Due to the additional outer skin, the system can provide a thermal insulation from the outdoor conditions.
	During winter	The reduced airflow speed and the increased air temperature of the air inside the cavity responsible for raising the heat exchange resistance.
	During Summer	The absorbed radiation that heats the cavity air is drained by the natural stack effect resulted from the ventilation of the cavity. Selection of the façade's compartment is crucial to avoid the overheating of the cavity.
	Night time cooling/ventilation	DSF can be an energy efficient solution in reducing the overheated air cavity caused in hot summer by exploiting the night natural ventilation. (Lee et al. 2002)
	Energy saving and reduce environmental impacts	DSF minimizes the solar radiation loads at the external perimeter of the building leading to reduce the U-value and then reduce the cooling loads. DSF can also extend the period in which natural ventilation can be more exploited. (Arons 2001)
	Wind pressure reduction	DSF facilities in lowering the short-term pressure fluctuation resulted from gusts of winds (Oesterle et al. 2001)
	Transparency	DSF provides an aesthetic, modern, and preserving the transparency of the building envelope without compromising energy performance and daylighting (Kragh, 2000)
	Thermal comfort	Since the cavity temperature is warmer than the outdoor air temperature, the indoor air temperature remains within close to thermal comfort levels during winter. Furthermore, the proper selection of glazing properties such as U-value and solar heat gain coefficient (g-value) so the cavity temperature will not incredibly increase during summer. The occupant thermal and visual comfort would be enhanced since such system provides a direct continuity to the outdoor environments.
Disadvantages	Higher construction costs	The construction cost of adding an additional skin is higher compared to conventional façade (Oesterle et al. 2001)
	Fire protection	Oesterle et al. (2001) claimed that the behavior of DSF buildings is not guaranteed against the fire protection in addition to smoke transmission control from room to room.
	Reduce indoor built-up areas	The size of the air cavity to reach the optimum DSF performance losses useful spaces.
	Maintenance and operational cost	DSF has higher cost regarding cleaning, inspection, servicing, and maintenance.
	Overheating	DSF initially introduced as a passive heating strategy, Hence, the possibility in transmitting the heat from the overheated air cavity is high if the DSF system is not properly designed. Jager (2003) recommended criteria to be considered during the initial design stage of DSF to avoid problems related to overheating including: a minimum of 200mm of cavity width and ventilation openings sizes, respectively.
	Uncontrolled airflow velocity	Apparently, in Multistory DSF, the increased airflow velocity led to instability of pressure distribution in the cavity caused inequality airflow paths into indoor spaces.
	Additional weight on the structure	To consider the additional weight to the structure mostly in case of refurbishment buildings
	Daylight	DSF can reduce in somehow the daylight entering the rooms as a result of additional skin.
	Acoustic	DSF can insulate the sound transmission from outdoor conditions, but the transmission from room to room or floor to floor is possible if the DSF is poor-designed.

2.3 Double Skin Façades as a Refurbishment of old building and their geometry types.

Zerefos (2008) defined the DSF as a system that involves adding multiple layers of glazing to the original façade (single skin) for maximizing the emitted daylight and improving the energy performance of buildings. Equally important, the buffer zone created between the two skins acts as multifunctional thermodynamics that combines both outdoor ambient conditions and building passive behavior. The DSF system has been utilized in many projects that reached a good reputation worldwide. The façade as a climate moderator firstly discovered by Le Corbusier in his project “Salvation Army Hostel”. His object was to study the indoor thermal performance of building located in Moscow after adding several membranes on the original skin of the building. The building with double membranes with a few centimeters spacing between them would maintain the interior membrane surface temperature at 18°C (Hamza, 2004). According to Barbosa et al. (2015), several scenarios of DSF were tested experimentally on an office building in Rio de Janeiro, Brazil. The testing parameters and variables were to verify the ability of DSF to maximize the acceptable comfort level in conjunction with reducing the energy consumption of an office building. The tested design parameters were categorized into four groups. The cavity physical configuration was the only parameter which supposed to be tested in the four groups. Additionally, the material specifications of the façade skins were also included as a variables to be tested with the cavity characteristics such as windows sizes, inner skin materials, windows positions, and shading devices. The result of the test showed that the by coupling the cavity with upper shading devices have then maximized the indoor comfort level of the occupancy working hours to 70%. On the other hand, the results showed that mixed-mode ventilation by the ease of mechanical ventilation is required to maintain the comfort level at 70% on peak summer time, where the natural ventilation of the DSF started to reduce its performance once the outdoor temperature exceeds 24°C.

Other work conducted by Shen and Li (2016) on the heat performance of three types of DSF. These types are the evacuated DSF, DSF with shading blinds, and pipe-embedded DSF. The three scenarios were tested by a numerical methodology to compute and compare the conjugated heat transfer between the three scenarios and coupled with shading blinds. The research main objectives were to investigate the effectiveness of the selected glazing materials in affecting the heat transfer between the DSF. The researchers concluded their research by the utilizing of shading blinds with particular angles would decrease the cavity air temperature between the two DSF from 57°C to 25.4°C while the using of the

pipe-embedded DSF reduces the average solar transmittance in which a reduction of 60% of cooling load is also achievable. The research has also tested the pipe-embedded technique on further types of glazing materials, where the result also showed that the performance of this technique can achieve a higher efficiency even if a poor quality of glass materials are used.

A study performed by Darkwa et al. (2014) on a multi-story building in Ningbo city in China. This city is classified by a subtropical climate condition. The research was aimed to investigate the potential of energy saving in both summer and winter seasons by the mean of natural ventilated DSF occurred by the pressure differences between the air and position of the inlets in both sides of DSF in all level of the building. The research conducted by the mixed-mode methodology using mathematical, computer simulation and experimental validation. The environment variables were simultaneously taken in the location by using a weather station and Pyrometer. The results of the work showed that DSF capable of supplying adequate natural ventilation to the upper levels of the building. In addition, a potential of cooling loads increment is likely predicted due to the overheating occurred since the DSF outlet air temperature reached 41°C in comparison to 36°C of ambient air temperature. The researcher conducted his research by suggesting a further work and thermal control management are required to configure the optimum inlet/outlet position which minimizes the excessive temperature in the cavity inside the DSF.

Larsen et al. (2015) have found that the solar heat gain which causing overheating inside the rooms in the Mediterranean climate can be eliminated if the glass materials of the DSF are adequately selected. The research result was based on a hypothesis where DSF was installed on the west side of an office building in Salta city, Argentina. The office building was modeled under the condition of no occupancy to completely assure that no human behavior or mechanical would affect the result of the research. The research outcomes were the using a low-e coating, or on the other hand, a higher insulation materials, would increases the possibility of heat gain reduction and also decreases the heat transfer radiation through the DSF glass. However, additional protection against the cavity heat gain can be achieved by placing an extra painting layer on the external surface of DSF, which is considered the most economical options in order to achieve the highest efficiency. And according to Joe et al. (2014), the façade configurations have been tested in order to obtain the maximum thermal efficiency design criteria. A multi-story building in Seoul, South Korea constructed with DSF has been investigated using computer simulation called EnergyPlus. The simulation was based on testing several parametric factors; cavity

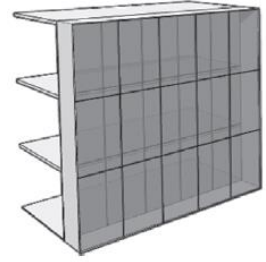
depth and windows glazing types, where multi-cavity thicknesses along with several window glazing materials were tested to optimize the best combination among them. The results of the research show that the cavity thickness and depth play a significant role in the energy consumption, where the total energy decreased by decreasing the depth of the cavity. This cavity might also influence by climatic and environmental conditions. Also, a larger reduction in energy consumption was occurred by changing the outside surface of the internal layer of the DSF windows glazing while a smaller reduction was obtained by changing the inside surface of the internal layer. The gross reduction in energy consumption was reached with optimized case up to 5.62% annually.

Lee et al. (2015) had investigated the potential of energy saving by placing shading devices between the façade's cavities. The study showed that the shading devices also helped in balancing of natural ventilation while maintaining the energy saving rates. Choi et al. (2012) found the integration between the HVAC system and multistory DSF provides a significant energy saving. Alberto et al. (2017) investigate the overheating related issues caused in the façade cavity in the southern European climate. The study concluded that reduction of the cooling loads occurs only if careful consideration was taken during the designing stages of factors such as airflow path, cavity width, and solar heat gain in which then the cavity overheating can be prevented.

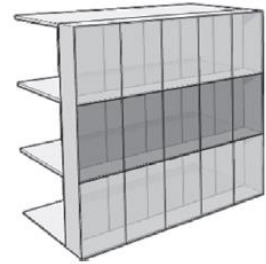
Overall, these studies had evaluated the energy performance of building with precisely double skin façades, where the energy saving in both cooling and heating purposes was, however, the in common subject along with all researchers. The majority of research concluded by a recommendation for further work and study for the cavity thickness/depth and glazing types of the DSF to achieve the highest possible energy saving. Also, all the work conducted in several cities around the world and the achieved results might not necessarily applicable to a certain city or country.

According to the relevant literature, four typologies of DSF were set based on cavity configuration. These typologies are the most common types and used through most of the recent publication. The four geometries types as appeared in Oesterle et al. (2001) are:

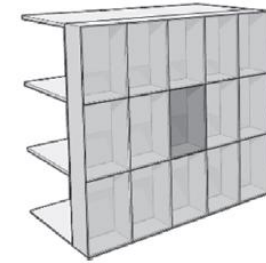
1. Multistory (MS) Façade: it is the most common DSF which mainly comprises from a full solid glazed placed with a certain cavity distance with no any horizontal or vertical partitions between the two skins. The façade's openings usually placed in the bottom and the roof of the façade. The air circulates across the entire façade area within the cavity between the two façades.



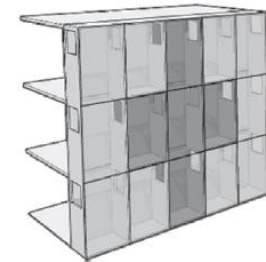
2. Corridor (CO) Façade: the façade's air cavity is channeled horizontally across one story level or several adjacent zones. According to Barbosa (2014), the façade inlets and outlets in external façade should be suited near the floor and ceiling levels. This type is realized for more acoustical insulation, fire security, or ventilation reasons. Special care should be taken into consideration to avoid the exhaust air from one room to be entered in the room above.



3. Box-windows (BW) Façade: a group of horizontal and vertical partitions that divide the façade in several independent boxes. Each box-window requires its own openings for intake and extract of airflow (Hamza, 2004). Thus, this type can provide an individual airflow through natural ventilation towards the external windows of the building. Furthermore, this typologies affords a safer environment in term of fire and smoke transmission from room to room if the compartmentalization is designed properly.



4. Shaft (SH) Façade: separated vertical partitioning or group of box-windows façades placed vertically with no horizontal spacing. The airflow principle is similar to the mechanism of solar chimney or the stack effect in which the air exhausts out through the roof. This system afford better noise insulation compared to box-window DSF and offers lower risk of fire distribution compared to Multistory.



Example of the distinguished buildings utilized the double skin façade in the United Kingdom are the One Angel Square in Manchester (Figure 6) and 30 ST Mary Axe in London (Figure 7). Further to its aesthetic appearance, the ventilated façade delivers several benefits on the environment in reducing the energy demand of a building through the openable vents that according to the controllable programmed weather data. An example from the Middle East that utilizes the DSF technology is the Capital Gate in Abu Dhabi, UAE (Figure 8). The integrated DSF with the HVAC system facilitates the reduction the solar heat gain and mitigate the dependency on the air-conditioning system by the recycling the air inside the façade's cavity- which has a temperature lower than the outdoor air temperature – towards indoor facilities (Schofield, 2012).

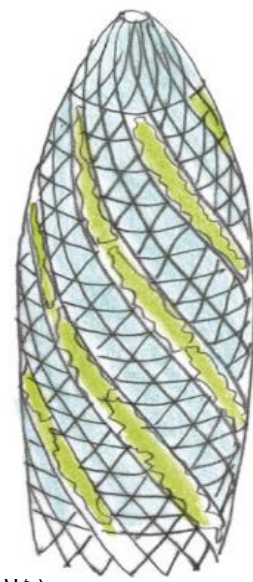


Figure 6: 30 ST Mary Axe. (Source: fosterandpartners, 2015)



Figure 7: One Angel Square. (Source: Colt Group, 2015)

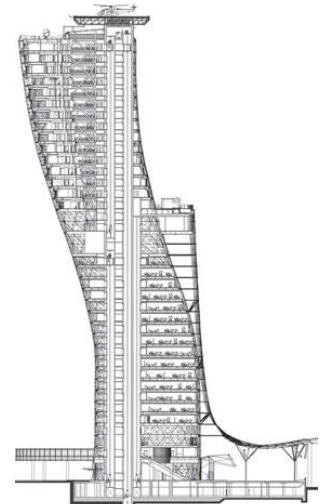


Figure 8: Capital Gate, Abu Dhabi (Source, Eileen, 2016)

2.4 Double Skin Façade Example in Jordan

- Al Abdali Boulevard in Amman Downtown.

Al Abdali Boulevard as shown in Figure 9 is the largest mixed-use development compound located in heart of Jordanian capital, Amman. The compound with a total built-up area of 2 km² became recently an active hub consisting of residential, commercial, and serviced apartment. The city's new urban framework plan is equipped with latest innovative building techniques and environment advancements such advanced Building Management System (BMS), fire protection, grey water treatment, and energy efficiency that entitled the country plan of 2025. The compound comprises from several blocks and each has four buildings. The five-stories building has a single-side double skin curtain wall constructed on its façade. However, each single-side façade has internal and external skins made from a clear glass separated by 0.75m. This gap is equipped with integrated active solar shading elements. These elements were a combination of stone, metal, and glass louvers that keep the cavity from increasing the internal radiant temperature. The main aims of the double skin curtain wall were to control the image of the Al Abdali development district, enhance the daylight, and to control the heat loss (Musa, 2014).



Figure 9: Building facade for both residential and commercial buildings of The Abdali Boulevard in Amman.

- Rotana Amman Hotel.

Rotana Hotel is a landmark in the Amman new downtown as shown in Figure 10. The ambitious 48 story high rise serviced apartment building adopted effective sustainable techniques utilized as a part of the core functions of the tower. The curtain walls with double glazed elements integrated with aluminum louvers are one of the sustainable features, which functions to shade the inner spaces from the excessive

solar heat and to enhance the natural air circulation inside the façade. However, there is no detailed description available concerning the DSF performance and their impact on the energy performance as well as the thermal comfort.

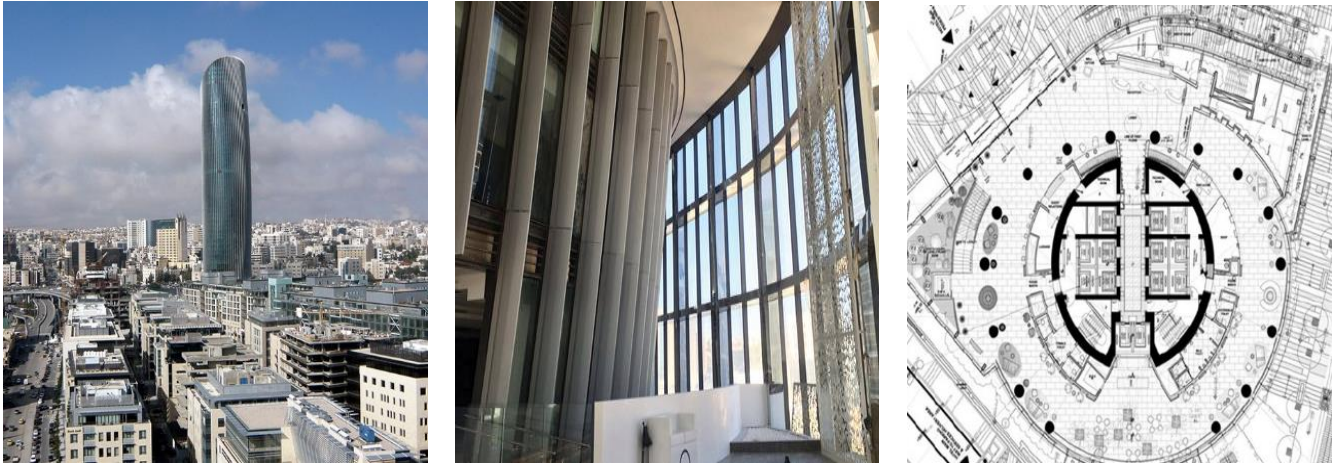


Figure 10: Full glazed facades of Rotana Amman Hotel. (Source: <http://reset-studio.com/portfolio/items/amman-rotana-hotel>)

2.5 The significance of the study in the residential buildings sector in Jordan

Passive heating and cooling strategy towards achieving the optimum energy efficiency and indoor thermal comfort is highly desirable in such country like Jordan that faces critical and limited local energy resources. For instance, residential buildings were responsible for 45% of the total energy consumption in the country in 2016 and the demand on electricity for the household sector is expected to increase with a growth rate of 5.1% by the year 2025 (MOEMR,2017). Despite there is no clear statistics regarding the energy consumptions for space heating and cooling purposes in residential buildings in Irbid, the energy consumption is expected to have a significant portion of the total energy consumed by such buildings with excessive hot conditions during summer and cold winters of the city.

Subsequently, the double skin façade as a promising passive technology that being introduced to buildings in cold climate and having acceptable performance in hot conditions, the DSF as described in literature is expected to perform positively in such country that is; (1) experiencing a hot dry summer with intensive solar radiation levels, (2) relatively cold winter with ambient air temperature that is usually reach under zero, (3) occupants thermal discomfort throughout the year with poor and/or traditional building standards, (4) noticeable building construction growth rate, and (5) acute crisis in the local

energy resources, is considered as a unique environmental solution. Even though there are no noticeable record or standard guidelines regarding the energy performance of DSF conducted in buildings in Irbid city (or any Jordanian cities nor cities have similar climatic conditions in the Levant “Al-Sham” region), therefore, as the residential building consumes more than one-third of the total electricity consumption of the country, the potential of energy saving in the residential sector by investigating the performance of the double skin façade system is crucial as it is not yet obvious if the system would properly work over the climatic conditions in such city especially in summer. Additionally, all the previous work conducted in several cities around the world might not necessarily applicable to a certain city or country. In regard to thermal comfort, the system is expected to provide an acceptable thermal comfort during winter while, on the other hand, artificial cooling loads still required despite the ability of the DSF to reduce, to some extent, the cooling loads.

3.0 Overview of the Hashemite Kingdom of Jordan, and Jordanian Energy Profile.

Jordan is a developing country located in the Middle East. It is a landlocked country with a total cross area of 89,213 km². The population of the country according to the recent census statistics carried out by the Department of Statistics (DOS) 2016 was estimated to be 9,531,715 with a growth rate of 3.1% per annum. Amman, the capital of Jordan presents that largest population share with a total population of 4,007,526 (42.06%) followed by the city of Irbid with a total population of 1,770,158 (18.57%) as appear if Figure 11. Statistics also revealed that the population of the Kingdom has multiplied ten times in the last 55 years. However, the total residential units registered in Irbid was 173,697 with the average family size of 4.8 persons.

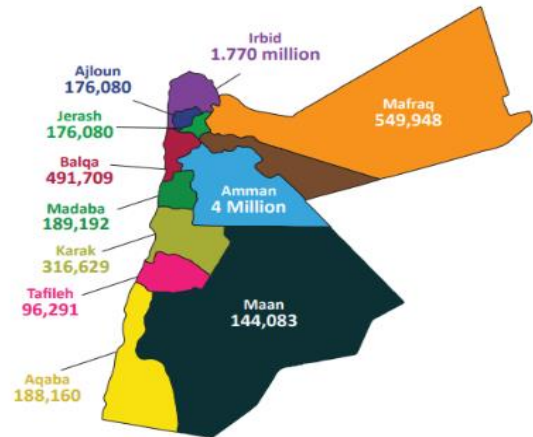


Figure 11: Population distribution of Jordan. (Source: MEMR, 2015)

Jordan faces a considerable crisis in energy resources. According to the annual energy report of the year of 2016 organized by the Ministry of Energy and Mineral Resources, Jordan imports nearly of a 95% of its energy need from the neighboring countries and the local resources contribute for less than a 5% including the generated energy from the small-scale renewable energy plants in the country as presented in Figure 13. A key challenge factor facing the energy sector in Jordan is the high annual growth rate in energy demand compared to global levels.

In a period of 5 years, the demand for electricity had considerably escalated. The growth rate of the consumed electricity was touched the 17%, where the generated electricity for the period starting from 2012 to 2016, was increased from 16595 GW_h to 19390 GW_h. Accordingly, the Ministry of Energy and Mineral Resources (MOEMR) (2016) declared that the household sector in Jordan was responsible for 7448 GW_h representing a 45% of the total electricity consumption share during the year of 2016. This consumption in the residential sector mainly includes the space heating and cooling using the air conditioning, lighting, water pumps, etc. However, the demand for electricity is likely to increase with the expected growth percentages reaching 5% and 5.1% by the year 2020 and 2025, respectively (MOEMR, 2016). In the same context, and since the residential sector in Jordan accounts for almost the half of the gross electrical consumption and 20% of final energy consumption, it became crucial to

explore solutions for lessening the total energy consumption in this sector. General speaking, it has been a priority crucial to find building design that coupling in achieving climatic responsive buildings since more than 60% of the final energy is being used in households for space heating and cooling. Even though the energy consumption is likely to escalate due to the expanded constructional works to accommodate this rise in populations, enhancing the physical building envelope and the developing the adequate insulation barrier between the building and its external environment contribute in enhancing the energy efficiency in this sector. According to Jarad and Ashhab (2016), optimizing the physical building envelope material and the envelope smart designs in the Jordanian residential sector play a significant role in achieving an annual energy consumption and energy cost annual saving of 24% and 22%, respectively.

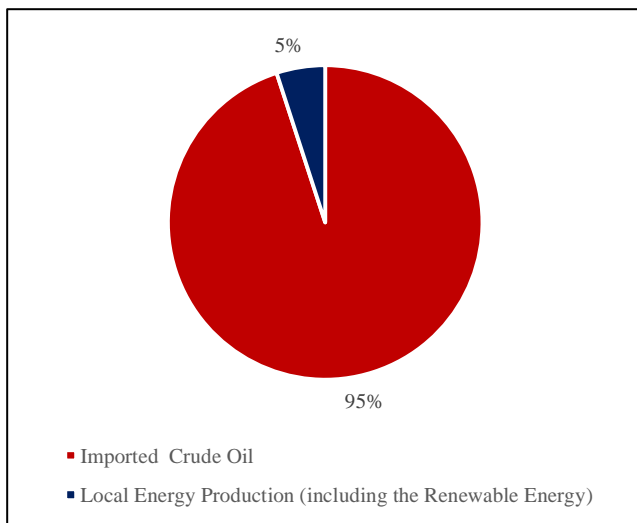


Figure 13: Local production share of the total energy requirements 2015

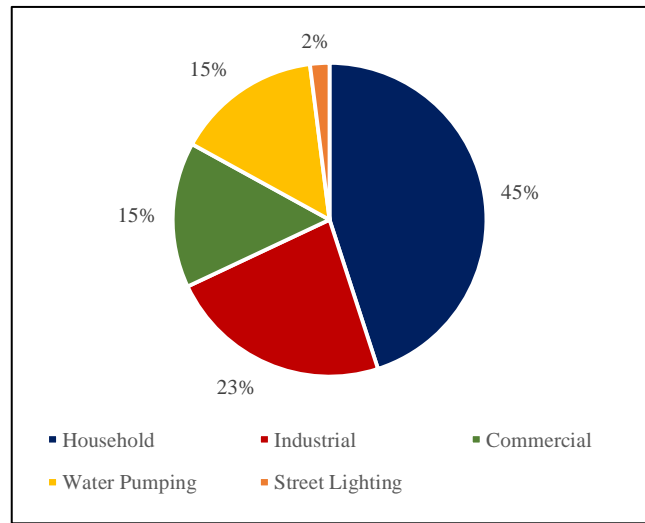


Figure 13: Percentage of the electricity consumption in the Jordanian different sector

In the current decade, more awareness for exploring sustainable solutions for the creation of energy efficient buildings is being distinctly noticeable in Jordan. For that manner, an Energy Efficient Building Code was published recently developed by the Building Research Center that mandated by Jordan National Building Council (Royal Scientific Society, 2009). However, those efforts still seem incompetent to be implemented in the existing traditional residential buildings (e.g. the Whitestone façades) especially for the space heating and cooling purposes.

Exploring passive architectural design plays significant roles in improving the premises' indoor thermal conditions to mitigate the dependency on the heating and cooling energy demands. According to the

(Handbook on Energy Conscious Buildings Pilot Edition: May 2006), the “passive building” regulates its indoor environment by utilizing resources of its direct surrounding which, on the other hand, provides a thermal barrier through passive heating and cooling techniques. In this regards, an additional skin to the existing façade of the building proposed as promising passive building technology to enhance the energy efficiency and then to improve the indoor thermal comfort simultaneously is investigated.

3.1 Climate of Irbid/Jordan: An overview of Irbid City

The city of Irbid (32.33° North latitude, 35.51° East longitude, and 616m above the sea level) is located in the Northern part of Jordan. The city has recorded the second largest metropolitan population share of 18.57% of Jordan total population that presents 1,770,158 after the capital Amman (Jordan Population & Housing Census, 2016). Irbid, however, has witnessed an escalated percentages in population due to fleeing conflict from neighboring countries, where 343,000 presenting a 27% of the total city’s population are non-Jordanians. The city is bounded by Syria from the North side and Palestine from the westside.



Figure 14: Map of Jordan. the red line indicates the City of Irbid. (Source: DOS, 2016).

Generally, Jordan accommodates difference topography at which classifies the Kingdom into five different bioclimatic zones. The major characteristics of the country’s climate fluctuate between the relatively rainy seasons from November to April and very dry weather for the rest of the year. Likewise, the city of Irbid is influenced by other climatic characteristics due to the state location lies in the merging boundaries of the Gulf Desert, North of Africa Desert, and the Mediterranean Sea regions. However, Irbid city as indicated in the climatic classification according to Köppen-climate map shown in Figure 15, which located in the northern part of the Kingdom is falling within the Mediterranean Csa category. However, the Csa refers to a climate that predominantly features a mild temperate that has dry hot summer season and wet cool in the winter season.

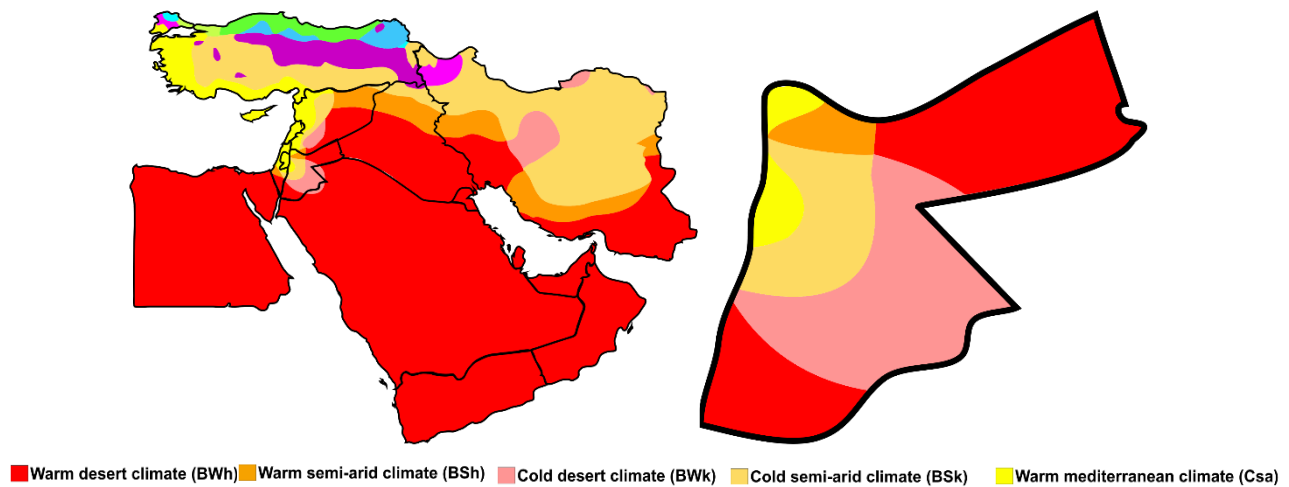


Figure 15: Jordan map of Köppen climate classification. (Source: Kotteck et al. 2006)

The climate of Irbid City has a moderate weather condition that is predominantly dry (Suliman and Beitou 2014). In summer months starting from May until September, the average high temperature usually ranging between (29.94°C - 36.70°C) and the temperature could exceed 40°C in summer in many days. The average low temperature for the same period ranges from 10.73°C - 17.04°C. In particular, the country's long summer reaches a temperature peak during August. This month usually has moderate to hot blowing air resulting from the subtropical air pressure difference in which it is characterized by the highest average temperature. However, the average temperature is liable to increase as stated by Matouq et al. (2013) as the average local temperature in Jordan has increased by 1.5 to 2°C in the last 25 years. Winter's temperatures have an average of 3.74°C and sometimes it could reach below the freezing points by 6 degrees Celsius. Those months mainly have mild to cold spells, light winds to heavy storms, and occasional snow. The average high and low temperatures in the winter season usually ranging between (12.27°C - 19.86°C) and (0.81°C - 4.97°C), respectively.

In the same context, Table 2 also presents that the average monthly global solar radiation in the Irbid City. The minimum and maximum average solar radiation are ranged between 0.46 – 1.0 kW/m² and annual average is about 0.76 kW/m². The solar radiation could reach sometimes to 1.04 kW/m² as represented in June as a result of the Summer Solstice. However, this range reflects on Irbid land starting from May until August for more than 12 hours daily, followed by March, April, and September with 8 hours. The least months receives daily solar radiations are February and November with less 6 hours.

Moreover, the month of January and December are the only two months that are receiving global radiation ranged as mere as 115 W/m².

Table 2: Monthly air temperature ranges and solar irradiance on the horizontal surface of Irbid city

		Month	Jan	Feb	Mar	Apr	May	Jun	Jul	Aug	Sep	Oct	Nov	Dec	Year
Dry Bulb Temperature (°C)	Record high (°C)	17.4	21	27	31.9	38	37	38	40	43.4	30.7	24	21	43.4	
	Average high (°C)	12.3	13.0	18.1	23.1	29.9	32.8	35.2	36.7	33.9	25.6	19.8	14.5	24.59	
	Daily mean (°C)	6.30	7.46	11.1	14.6	21.1	24.5	26.4	26.2	23.5	17.7	12.3	7.21	16.53	
	Average low (°C)	0.81	0.46	4.46	5.24	10.7	14.9	17.1	14.8	12.6	9.3	4.97	0.92	8.02	
	Record low (°C)	-6	-6	0	-2	6.3	8.4	11.7	11.9	10	4	-3	-6	-6	
Global Solar Radiation (W/m ²)	Record high (W/m ²)	596	754	927	988	1025	1039	1032	1004	951	830	684	562	1039	
	Average high (W/m ²)	490	580	717	852	943	1006	1018	974	884	711	537	457	764	
	Daily mean (W/m ²)	115	153	202	259	303	339	337	307	261	197	135	110	227	

According to the sky cover range in oktas as illustrated in Table 3, it shows that the city of Irbid is a partially cloudy city. However, the minimum mean cloud cover of the summer season represents in July with a percentage of 0.07 oktas while the maximum sky cloud cover range appears in January with 4.54 oktas. Consequently, the city of Irbid is considered a sunny city where the percentage of annual mean cloud coverage does not exceed 2.15 oktas. Moreover, about 70% of the average rainfall seasons of Irbid falls between November and March; June through September often rainless. Summer relative humidity averaged at 44.25% and the winter’s relative humidity average at 67.31%. December and January are the most humid months concurrent with the rainy season.

Table 3: Sky cover ranges, rainfall, and relative humidity of Irbid City

Month	Jan	Feb	Mar	Apr	May	Jun	Jul	Aug	Sep	Oct	Nov	Dec	Year
Sky Cover (oktas*)	4.54	3.39	3.83	2.85	2.09	0.87	0.07	0.11	0.11	1.65	3.07	3.19	2.15
Rainfall** (mm)	25.2	12.5	24.4	9.3	4.8	0	0	0.2	0	5.1	15.2	31.5	10.68
Relative Humidity (%)	80.69	66.37	67.82	53.83	41.49	40.41	44.88	48.22	46.25	60.63	67.15	74.65	57.70

* : is a unit of measurement used to describe the cloud cover in which the sky is divided into eighths okta. (BBC, 2014)

** : Data gathered from (timeanddate.com, 2018)

The wind data illustrated in Table 4 shows the annual wind speed and prevailing wind direction for the city of Irbid. The recorded data shows that the prevailing direction of blew winds are often from the Southwest, Southeast, and barely from the South directions with a rate of 71% of total wind hours of the year. Moreover, for a one-year period, the monthly average maximum, mean, and minimum wind speeds

are 7.26 m/s, 3.33 m/s, and 0.74 m/s, respectively. The wind table also shows that the speed of blew winds could reach in some months to 17.5m/s and July is the windiest summer months.

Table 4: Wind speed and prevailing direction of Irbid

Month	Jan	Feb	Mar	Apr	May	Jun	Jul	Aug	Sep	Oct	Nov	Dec	Year
Wind Speed record high (m/s)	14.40	14.40	17.50	12.30	14.40	14.40	16.50	11.80	12.40	13.40	9.30	10.8	17.50
Wind Speed average high (m/s)	6.62	6.89	8.95	7.26	6.59	10.00	10.60	7.87	7.33	5.15	4.91	4.98	7.26
Daily Mean (m/s)	2.88	3.02	3.87	3.01	2.93	4.61	6.05	3.50	2.96	2.52	2.20	2.45	3.33
Wind Speed average low (m/s)	0.46	0.61	0.74	0.65	0.59	1.16	2.07	0.62	0.48	0.54	0.44	0.49	0.74
Prevailing wind direction (E of N)	148 (SE)	139 (SE)	189 (S)	193 (SW)	199 (SW)	215 (SW)	224 (SW)	218 (SW)	193 (SW)	172 (SE)	112 (SE)	133 (SE)	177.9

Figure 16 shows the Psychrometric chart for Irbid City based on data gathered from the EnergyPlus weather data files. This figure specifies the annual thermal comfort zone for both seasons based on the prominent and typical clothes insulation. The winter thermal comfort zone mainly ranges between 19.5°C and 25°C considering the winter clothes insulation index at 1.0 clo. In summer, on the other hand, the thermal comfort zone ranges from 24.5°C to 27.5°C based on the typical summer clothes index which is 0.5 clo. However, this chart also reveals that the occupants experience thermal comfort only 33.5% throughout the year in the ideal conditions, while a considerable part of the year does not fall within the designated thermal comfort zone, especially in the winter seasons, where a massive need of artificial heating energy is required during this period. Nevertheless, the cooling energy should not be discarded during the overheating period in summer.

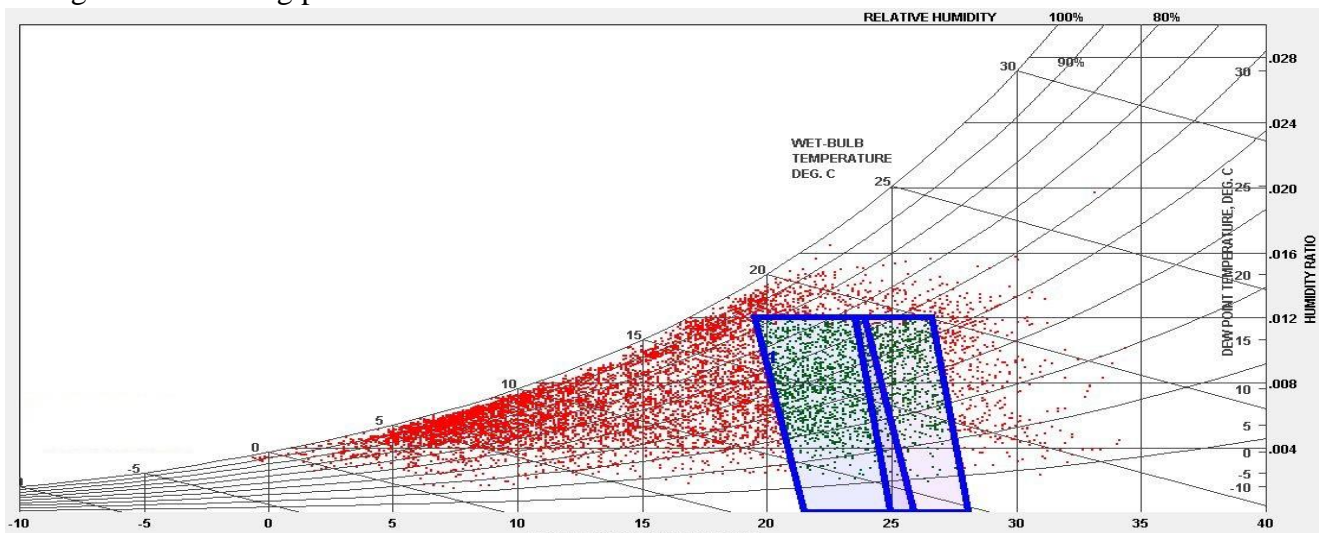


Figure 16: Psychrometric chart of Irbid (Source: Climate Consultant 6.0)

The comprehensive month-to-month analysis of the Psychrometric chart returns with recommendations as illustrated in Table 5.

Table 5: Recommended strategies to achieve the thermal comfort of Irbid City (Source: EnergyPlus V3, 2018).

Month	Acceptable Thermal Comfort (%)	Main Strategies recommended.
January	0.0%	Solar heat gain is mainly the most recommended strategy. The artificial heating system is still required.
February	0.0%	Solar heat gain is mainly the most recommended strategy. The artificial heating system is still required.
March	1.0%	Internal heat gain is one of the main recommended strategies. 66% of the heating load is required to achieve the thermal comfort.
April	13%	Internal heat gain and passive solar gain are still required, but windows' sun shading devices are suggested as a passive solution in conditional heat gain.
May	33%	Sun shading device is the main recommended passive strategy to achieve the thermal comfort.
June	43%	Cross ventilation is the highest recommended strategy to achieve indoor thermal comfort. Minimal usage of cooling loads and dehumidification devices are required in this months.
July	39%	Although mechanical cooling is not discarded, sun shading devices and dehumidification are also required in this month.
August	36%	Similar to July; artificial cooling, shading devices, and dehumidification are required, the cross ventilation and usage of high thermal mass for night flushed are the main recommended strategies to achieve the thermal comfort.
September	40%	Passive solar gain through the high material thermal mass is one of the recommended strategies. Sun shading and cooling are occasionally required.
October	41%	Internal heat gain and passive solar gain are still required, but windows' sun shading devices are recommended as a passive solution in conditional heat gain.
November	8.0%	Internal heat gain is one of the main recommended strategies. 66% of the heating load is required to achieve the thermal comfort.
December	0.0%	Solar heat gain is mainly the most recommended strategy. The artificial heating system is still required.

The implementation of the available passive heating and cooling strategies in buildings of Irbid could be sufficient solution to achieve in somehow the thermal comfort that helps in achieving the summer and winter thermal comfort with the minimum usage of energy. However, the thermal acceptance of each month of Irbid for the purpose of this study was based on thermal acceptability limits derived from the ANSI/ASHRAE 55 standards, which aimed in satisfying 80% of occupants. The comfort zones boundaries of each month were calculated through adaptive methodologies adopted from the experiments carried out on more than 21,000 prototypes around the world. The adaptive methodology defines the acceptable indoor ranges as a function of the average outdoor air temperature. The acceptability limits for typical building application can be calculated through the following equations:

- $Lower\ temperature\ limit\ (^{\circ}C) = 0.31 \times T_{OUT} (^{\circ}C) + 14.3$ Equation 1

- $Upper\ temperature\ limit\ (^{\circ}C) = 0.31 \times T_{OUT} (^{\circ}C) + 21.3$ Equation 2

Where:

$T_{OUT} (^{\circ}C)$; Mean monthly outdoor temperature.

4.0 Methodology

This section will discuss the different applicable methodologies that are applicable to assess and evaluate the performance of the Double Skin Façade. The prevailing literature towards energy-efficient building through the proper design of the DSF was spread out dramatically. Such projects encouraged the researchers to explore several techniques and approaches focusing in on the performance of the DSF with the emphasis with their advantages and positive impression with their fast reaction with the outdoor environment. The relevant literature of the key studies performed on the DSF's mainly involved empirical and experimental investigations, computer simulations approaches in which the performance of the DSF was assessed. A large number of researches were conducted to evaluate the efficiency of the DSF worldwide but very limited or often non-existent research in the same field was conducted in the Levant counties having similar climate conditions. Also, it worth mentioning that there is no published work nor assessment investigation concerning the performance of DSF in any of Irbid's building (commercial or residential) were conducted according to the available literature.

Benefits associated with the DSF buildings that first appear in the early 80s were involved in several articles, publications, and books. With the growing trends to design such building associated with DSF for energy conservation purpose, the different modeling approaches for the assessment of the DSF should be understood comprehensively. Since all the DSF elements interact with each other, the modeling and simulation of such a system are considered a complicated task since each element could influence the functionality of the façade's cavity. Thus, the difficulties related to the modeling process and simulation procedures including the airflow patterns, cavity thermal gradient due to the height difference, and daylight penetrations must be fully understand linked with the appropriate methodology to assure the well-designed of the façades. However, the daylight performance of the double skin façade is not a part of this dissertation.

The choice of suitable research methodology in assessing the performance of the additional glazed structure for the purpose of investigating the potential in lessening the energy consumption as well as enhancing the thermal comfort is very important to enable the existence of this paper. Therefore, this section will look over the utilized methodologies in evaluating the performance of the system in previous conducted works considering the following criteria:

- (1) It had to address the energy savings potential and the ability in achieving the thermal comfort associated with DSF on old or refurbishment buildings.
- (2) It had to refer to climates that the heating is required in winter and cooling is not discarded in summer.
- (3) It had to contain results built on the comparison with the preliminary results of a base case.
- (4) The paper should not be older than 18 years.

4.1 Research Approaches applicable to investigating the performance of the DSF.

The intellectual and creative development on the double skin façade recently led to appearing several pieces of research related to the positive aspects of the system. As mentioned earlier in the literature review section, and according to other research related to DSF, each study used a different method to investigate the parameters which were in the research question. However, the thermal performance of buildings utilized by a DSF was mainly conducted by either single methodology or by a combination of methodologies. Selecting the research methodology mainly depended on what the research aimed to or results that are expected to be achieved. In particular, the most common methodologies observed in investigating the performance of DSF are; experimental or laboratory approach, computer simulation, literature review, and mixed mode approach. Each research methodology has its pros, cons, limitations and also the accuracy may also differ from methodology to other.

4.1.1 Experimental Approach

Studies using the experimental or field measurement as a methodology allows the researcher to test the parameters, collect data, and evidence from the real life. Collecting data mainly occurred by special types of equipment. Experimental-based researches mainly required to isolate and control every independent variable on which the effects can be later observed when the conditions are manipulated. Campen 2009, declared that collecting data directly from the field allows the researcher to gather more accurate results in comparison to other methodology which may build up upon certain assumptions or designed for particular regions. Nevertheless, the result may also influence by human or equipment errors. The accuracy of any experimental research depends on the quantity of the installed sensors and the calibration of each equipment (Andelkovic et al. 2015). Moreover, the experimental method also gives the researcher a greater chance to control a large number of extraneous variables. However, for the cavity itself, the

researcher can determine the properties by placing several sensors on it, such as the velocity, the air temperature, and air pressure within the DSF cavity. This methodology also gives the researcher the flexibility to measure and manipulate several variables within the same unit for more accurate results. However, results obtained from this methodology usually give the researcher more confidence to declare their output, no like those performed the research by computer or mathematical which they might design their model upon some particular conditions. There are many limitations obstruct the experimental research on DSF. The availability of the testing devices is a major obstacle in hindering the course of the research. Also, as the investigation the performance of DSF usually takes a relatively long period, the financial support is also required for the equipment and also laboratory measurements to assure a steady and continuity of the research progress. The main obstacles facing the experimental research are issues related to the privacy, where the research sometimes unable to test or investigate particular variables without a prior permission from the premises being investigated. According to Andelkovic et al. (2015), an experimental study was performed in order to investigate the thermal efficiency and the energy performance of the building façade in Serbia. Several parameters were measured experimentally; three variables of air cavity (temperature, relative humidity, and velocity), the surface temperature of DSF, and indoor temperature and relative humidity.

4.1.2 Computer/modeling Approach

Computer simulation methodology was used in a large number of papers to investigate the thermal performance and energy performance of naturally ventilated DSF. Computer simulation in DSF mainly occurred by gathering information from other resources or by several assumptions which then be assigned to a single or multi-software to obtain theoretical results. The accuracy of the results strongly depends on the input reliability and precision. Through this approach, the evaluation of the performance of DSF building is mainly simpler than experimental methodology. It takes fewer efforts and can be performed in a faster manner. The simulation tools allow the researcher to test a large number of hypotheses and assumptions in a very short time. However, the results level of accuracy usually is lower than the experimental results. The software must be modified and all input must also be carefully assigned to obtain a maximum possible simulation. In the field of DSF, a wide range of computer simulation or developed numerical models is present in a wide range of complexity. Starting from a simple few equations to most complex as presents in CFD simulation, many types of computer software are

nowadays available as declared by (Poirazis, 2006 P.59) to test the performance of the energy of DSFs such as, IES VE, FLUENT, while Djunaedy et al. (2002) categorized the airflow modeling according to its complexity should be taken place by software such as building energy balance (BEB), zonal airflow network (AFN), and computational fluid dynamic (CFD).

4.1.3 Mixed-mode methodology

Mixed mode or multi-methodologies approach was also observed in large numbers of researches to test the energy performance of naturally ventilated DSFs. The mixed mode research mainly involves a mixture of both the quantitative and qualitative methods in one overall study. The combination of experimental and computer simulation was found on the majority of researches investigating the DSF where the researcher either combine the two methodologies to investigate the research question or validate the results obtained from one methodology by the other to answer the research question from a number of perspectives. Researchers usually tend to use the mix mode methodologies to show the obtained results from this combination have a complementary strength and no overlapping weaknesses (Tashakkori & Teddlie, 2003). Also, the researcher in the validation case tends to use the mixed mode methodology to corroborate and evidence of their research results.

4.2 Justification of the selected approach.

Research methodology is a route to systematically solve the research question (Kothari, 2004). Various types of methodologies are found applicable to the assessment of the performance of the Double Skin Façade. Among these types, the chosen methodology in investigating the performance of the DSF in a residential building Jordan is the computer simulation. The justification is described below in details.

Apparently, the term “simulation” refers to the controllable form of the re-creation of a certain type of system or process, often using a computer, in which the system variable could be evaluated by the mean of manipulating. This manipulation allows the researcher to have similar conditions of an experimental in an artificial form in which the hypothesis is being tested. Another definition by Nimlyat et al. (2014) was the means of initiating the performance of a certain system by means of an analogous model. Simulation and modeling approach was selected by the researcher due to several factors and benefits. Accordingly, Sahlin (2000) has described the simulation as the equivalent method of conducting real-life experiments with many benefits especially in the early design stages. Also, the simulation allows the system being simulated to be described virtually with mathematical equations in which the development

of the same system in new directions can be granted. In the building industry, simulation using computer has expanded and gained wider acceptance in the last few decades. The computer-based simulation in this industry conceptualizes the link between the developed model and the real system at which the simulation seems to remain beneficial and will continue to grow in use for early designs, operation, and maintenance processes of buildings. Nimlyat et al. (2014) confirmed that computer simulation techniques can be employed in building's at their early design stages as well as occupied old building, in which the success of using the simulation in assessing the energy performance of buildings substantially depends on professional integrating the various variables on the design stages and their influences on building lifespan.

Since the building simulation software provides an advanced treatment of the real-life energy process, the computer simulation approach was chosen in this research. Perhaps, the research restrictions as the time constraints, fewer equipment resources and materials, and no large amount of capitals are needed were the main reasons. Most importantly, the unavailability of the researcher on the place of the building being investigating was played a significant role in selecting this approach where one of the main computer simulation's advantages is that not necessarily require the presence of the researcher in the same place at which the prototype is being examined. Nevertheless, the initial stages of developing the simulation configurations considered one of the disadvantages of this approach, where complicated processes and assumptions take a longer time to develop appropriate simulation boundaries according to the prototype conditions to be examined.

4.3 Limitation of the study

As any research constrained with time-frame, several restrictions and limitations would influence the research outcomes; in which these limitations must be avoided in future works. Most limitations were directly linked to the time constraints and limited availability resources. Following points highlight these limitations:

- (1) It was impossible to conduct any experimental work as the researcher was not at the same place the building being investigated, in which the absence of validation of simulating results against the experimental data could not be performed.
- (2) Fewer precision results could be extracted as the simulation software only provides results based on the hourly basis.

- (3) The thermal comfort boundaries measured for the individual month may vary from year to year,
- (4) The study was limited for airflow mechanism and air temperature within the DSF cavity where many factors might affect the performance.
- (5) All simulations were conducted by ignoring the influences of any adjacent buildings.
- (6) The study was limited to testing the DSF performance for three cavity's width intervals; 300mm, 600mm, and 900mm while the DSF cavity width could reach up to 2500mm.
- (7) To avoid simulation complexity and computational time, the study was only carried out for the fourth floor level of the building.
- (8) Due to time limitations, the daylight penetration and the related glare issues, fire security, condensation on the glazed surface, and maintenance and cleaning costs of the DSF were not covered in this thesis.

4.4 Research Methodology

This paper aimed at investigating the thermal performance of Double skin façade on an existing residential building in Irbid, Jordan. As described, the computer simulation approach deemed the most appropriate research approach in this study as this methodology complies with the scope of the research.

Initially, the different considerations that characterize the base case model related to the building with a single façade (natural-stone façade) were set. These considerations include the geometry, material specifications, and indoor and outdoor environmental conditions of the building. The base case model is used as a base reference for evaluating the performance when different and variables parameters are applied. Different geometry types of DSF then applied to this reference model. Then, a comprehensive analysis will be conducted aiming at evaluating the energy performance of the façade according to its geometry. The energy audits and indoor thermal conditions from the simulation outputs of the base case building and the different classification of DSF are essential in which a comparison study is established. This comparison allowed evaluating whether the applied DSF on the initial building would translate into passive strategy in term of energy saving and affording acceptable thermal conditions inside the building. Figure 17 represents the visual milestones of the methodology followed throughout this paper.

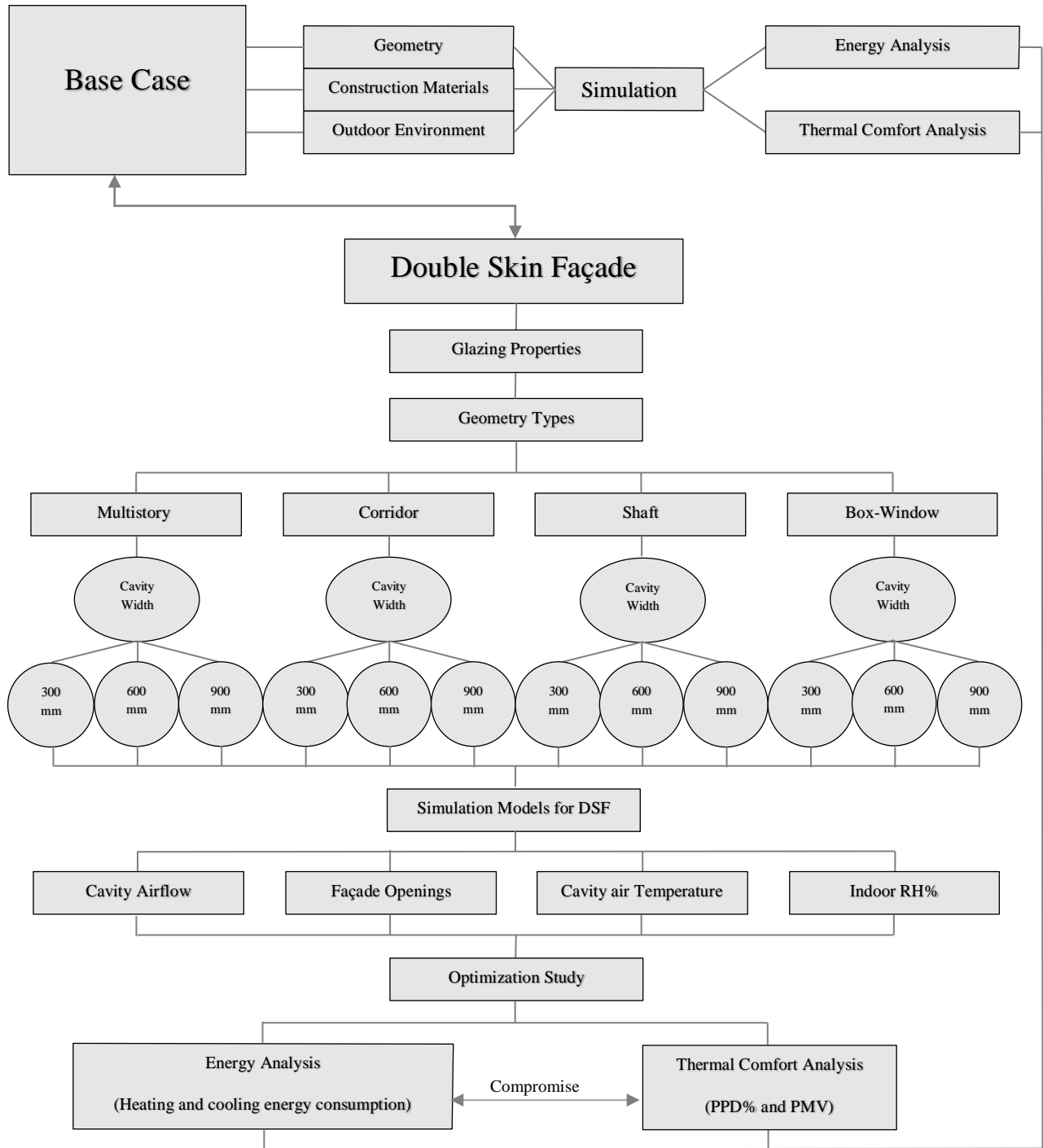


Figure 17: Research methodology

4.5 Simulation Software Selection

A software called IES VE (*Integrated Environmental Solution, Virtual Environment*), version 2017.3 is the chosen software for this work. This study provides the simulation process outlined different parameters to achieve the highest precision of the heating and cooling loads. The computational model of the base case building was mainly exploited as a comparative model to simulate and then assess the actual overall thermal performance of the building. However, this computational simulation developed to investigate trends in the tendency towards the heating and cooling loads saving potentials of the building by utilizing the DSF on their façade. The IES VE software features in delivering quantitative analytical results for various assumptions in a very short time. The software provides a series of sensitivity analysis on a wide range of design parameters that directly influencing the building performance (Sousa, 2012). These parameters include the building orientations, construction materials, different schemes of natural ventilation according to windows type and size, and shading devices. In this study, the performance of the base case building and the renovation of the building with DSF were assessed by the mean of six modules in the Software. Apache, SunCast, VistaPro, MacroFlo, and MicroFlo are the main software modules in which the thermal performance of the building is evaluated. The Apache is the tool in which it allows to assign the thermal load on different criteria in the building. The solar loads and shading calculations are performed using the SunCast. Moreover, VistaPro is the tool that gives a series of graphs, tables, and bar charts for the results obtained on inputs defined in the Apache. Additionally, the MacroFlo provides the ability to manipulate on the degree of all windows and doors opening based on a profile that previously defined, and the MicroFlo gives a visual data related to air temperature profile, air velocity profile, and the pressure difference known as CFD (*Computational Fluid Dynamic*).

The user-friendly interface software, IES VE, delivers unique tools and technologies that allow the Engineers to easily visualize and link results at a highly detailed level. In addition, the software provides a wide range of applications that assist in testing various design options, identifying the optimum passive solutions, and draw conclusions related to final energy use including detailed consumption of heating and cooling loads, thermal comfort, airflows in according to different building green rating systems.

4.6 Building Sector in Irbid

Following the significant growth in the population represented in the Kingdom, an overwhelming growth in constructional works is noticed to accommodate this rising in population. According to data provided by the Department of Statistics of Jordan in 2015 regarding the housing types in Irbid, the dominant residential building in Irbid are classified into three typical types; 1) Villa, 2) Dar, and 3) Amarah (high standard apartments in buildings that are more than 2 storeys) as shown in Figure 18. In case of Irbid, the most common house type is the house type “Dar” followed by the “high standard apartments” as illustrated in Figure 19 with their annual energy consumptions. The constructional growth towards the high standard apartment buildings seems to continue with the increasing of the Kingdom’s population where the most of the current housing projects are in the construction of high standard apartments.



Figure 18: Dominant housing type in Irbid. a) Villa, b) High standards apartments, and c) Dar

Al Asir et al. (2009) confirmed that the high standards apartments are the most energy consumer as they mainly equipped with central HVAC system regardless of the thermal efficiency of these housing types. Villa is expected to have higher thermal efficiency due to relatively higher construction standards. Figure 19 shows the number of house and their annual energy cost per housing type in Jordan and specifically the city of Irbid. For this purpose, and as the high standards apartments are the highest energy consumer, this research will only deal with this type housing as a step in lessening the huge energy bills being consumed for the space heating and cooling purposes.

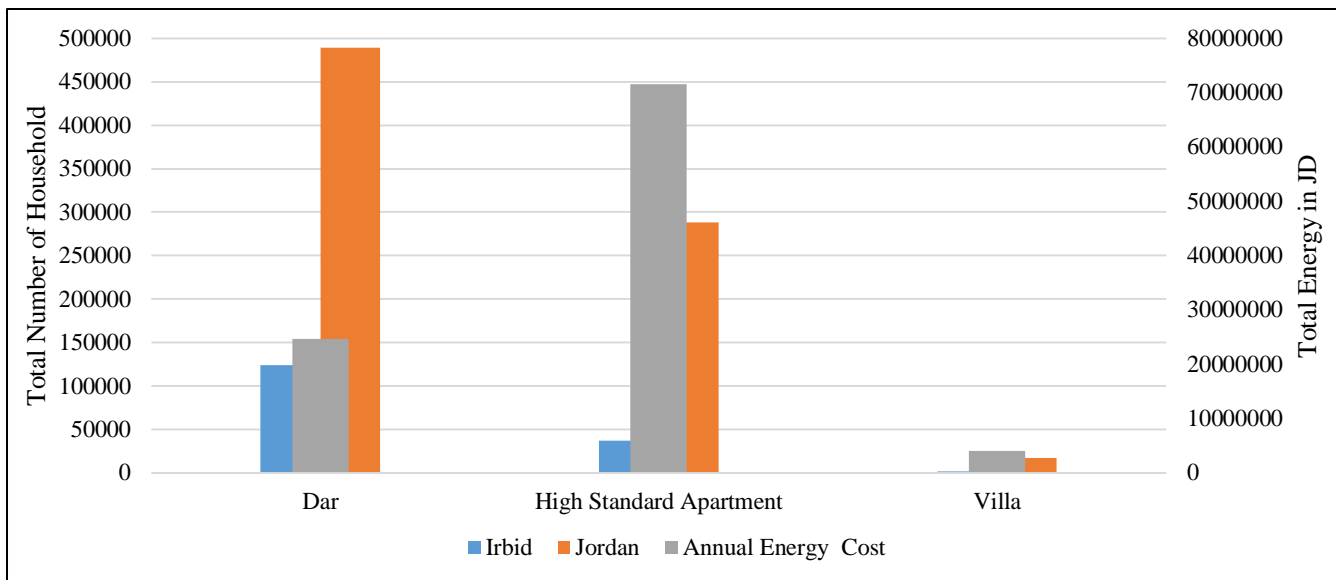


Figure 19: Number of house per housing type and their annual energy cost in Jordan and for Irbid. (Source: DOS, 2016)

In Jordan, the constructional sector is mainly controlled by building regulations called the national building code of Jordan that is focuses mainly on urban and rural design specifications. However, the buildings in Jordan in general and the residential units in particular, suffer poor indoor comfort conditions, moist, and unhealthy environment due to factors. These factors include lack of availability of materials, labor skills, and cost efficiency. For instance, the majority of external windows in conventional residential buildings in Irbid still come with a single glazed window in which create air infiltration as a result of the thermal bridge. In this matter, the Energy-efficient building code was promoted to further rationalize and optimize the energy efficiency of buildings. This code also aimed to achieve an acceptable thermal comfort and reduce the dependency on an active source of energy by the proper selection of construction materials, and optimizing the mechanical and electrical devices in the buildings. For instance, the suggested U-values for the building envelope is presented in Figure 20.

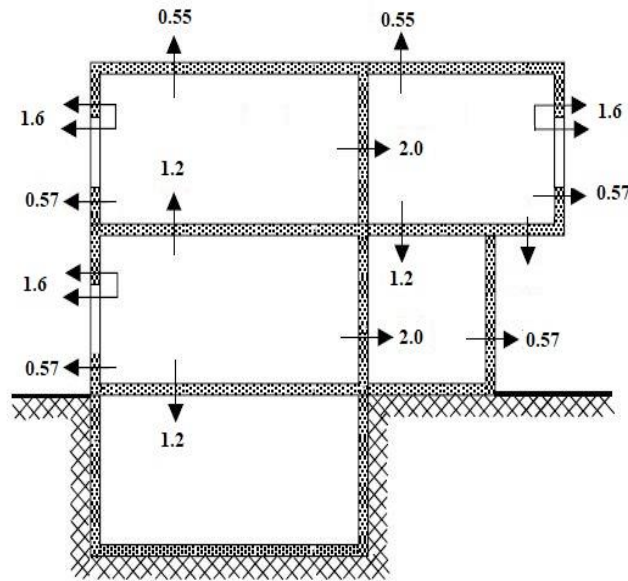


Figure 20: Suggested u-values for walls, roof, exposed floors, and windows types by Energy-efficient Building code of Jordan.

The Amarah building type (high standard apartments) in Jordan based on Al Asir et al. (2009) declaration, have typically a flat area ranged between 75m^2 to 225m^2 and an average of 140m^2 . Each floor accommodates two symmetrical facing apartments in which each apartment has three exterior façades. Most buildings in Jordan are constructed with a single shaft located in the middle of the building. This shaft mainly used as a driving force to promote indoor natural ventilation generated by buoyancy effect resulted from the temperature difference in the shaft and the entered airflow from external windows opening (Al Asir et al. 2009).

More specifically, building's external façade in hot to warm Mediterranean climates are foreseeable to be responsible for nearly 40% of the building's cooling loads (Hamza, 2004). In the same context, Shariah et al. (1997) confirmed a reduction of more than 40% both heating and cooling loads can be achieved by the proper thermal insulation for both ceiling and external walls in residential buildings. Therefore, and according to the climate of Irbid where the air temperature could reach 40°C in summers and to -6°C in winter, the investigation and the proper design of the external façade or the added façade (DSF) using efficient energy techniques would intensively provide façade the have the potential to decrease the energy demands as well as to passively enhance the indoor thermal comfort.

4.7 Overview of the Base Case

Briefly, this section presents the selected methodology for simulating the actual performance of the chosen case study. The general aim is to investigate the indoor thermal conditions along with the predicted occupants' thermal comfort. Also, all steps of the base case configurations based on relevant studies and general regulations for residential buildings in Jordan and recommendation derived concerning the definition of the Efficient Building Code in Jordan were covered in this section.

Remarkably, this work aimed to investigate and optimize the use of DSF in a residential building in Irbid/Jordan. The generated results from the analysis of the base case building using the computer simulation will be needed to conduct a comparative analysis with the difference DSF geometries applied to the reference building. However, the following facts will be generated from the simulation process of the base case;

- (1) The airflow rate fluctuations related to the changing of external windows level of openings,
- (2) The temperature of the indoor environment through the process of heat transfer towards the structure envelope influenced by conduction, convection, and radiation.
- (3) Assessment of occupants' thermal comfort.

4.7.1 Site Analysis

A residential building in Irbid was chosen to investigate its energy performance and compare with the same building after utilizing the double skin façade on its external envelope. The location and site geographical data as listed below have been used in the software to accurately simulate the energy performance of the system. The summer daylight saving was considered during the simulation for more accurate data acquisition.

Location Data:

- Latitude: 32°33`47``N
- Longitude: 35°52`52``E
- Altitude: 560 m
- Time Zone: +2:00 Hours (GMT)

Site Data:

- Ground reflectance: 0.20
- Terrain type: City/building
- Wind exposure: Normal (heating load by CIBSE)



Figure 21: Site location and analysis of the chosen case study building

4.7.2 Description of the base case

This study focuses on a typical residential building situated in the Eastern District of the Greater Irbid Governorate called Al Rawdah District of Irbid City, Jordan. Al Majd-1 building has the usual identical construction style of residential buildings which comprises of 4 multi-stories building height in compliance with the DLS Legislation issued in 1979. The 7 years old building has a total height from the ground of around 14.5m. However, the total typical floor area is equal to 335m² where the total built-up area is approximately around 1340m² distributed into 4 floors. The building was built with the traditional white Jordanian limestone layer on their four external facade and relatively well-sealed windows as shown in Figure 22.



Figure 22: Base case building selected for assessment

Each floor accommodates two apartments where the building’s total apartments are eight. All apartments have the same built-up area equivalent to 162m² including the external balcony (5.8m²) and differentiate in the orientation. Every apartment consists of 2 bedrooms, 1 master bedroom, living room, kitchen, 2 bathrooms, powder room, 3 corridors, and guest room. The typical apartment comprises of 12 spaces (volumes). The total number of spaces for the whole building is 96 volumes in addition to the shaft opening, lift lobby, and the staircase room. However, the lift lobby and the staircase room is considered as one integrated volume. The numbering system that prefixed for the one apartment is illustrated in Table 6.

Table 6: Numbering system for a typical apartment

Room type	Prefix	Window Prefix	Door Prefix
Guest Room	V01	W01	D2
Kitchen	V02	W02 & W03	D12
Living Room	V03	W04	D3 and D5
Bedroom 1	V04	W05	D6
Bedroom 2	V05	W06	D8
Master Bedroom	V06	W07 & W08	D10
Powder Room	V07	-	D4
Bathroom 1	V08	-	D9
Bathroom 2	V09	W09	D11
Corridor 1	V10	-	D1,D2,D3, and D4
Corridor 2	V11	-	D5, D6, D7, D8, and D9
Corridor 3	V12	-	D7, D10, and D11
Lift Lobby + Staircase	V13	W10	D13
Shaft Opening	V14	-	-

Each volume of each space in the building model was considered for the simulation. A numbering methodology was set for each room in each apartment for one floor in the purpose of ease referencing due to a large number of rooms in the model. However, the numbering of each room starts with: floor level, room’s prefix, and then the apartment’s type. For instance, 2 V07 (A) stands for the powder room on the second floor of type A, in the same context, 3 W04 (B) stands for window of the living room in the third floor of the type B. The window to wall ratio was defined as the ratio of the window area to the exterior wall area (Goia et al. 2013).

In reference to the typical floor plan shown in Figure 24, the flat on the left named type (A) while the one on the right named type (B). The main elevation of the building is facing the west direction.

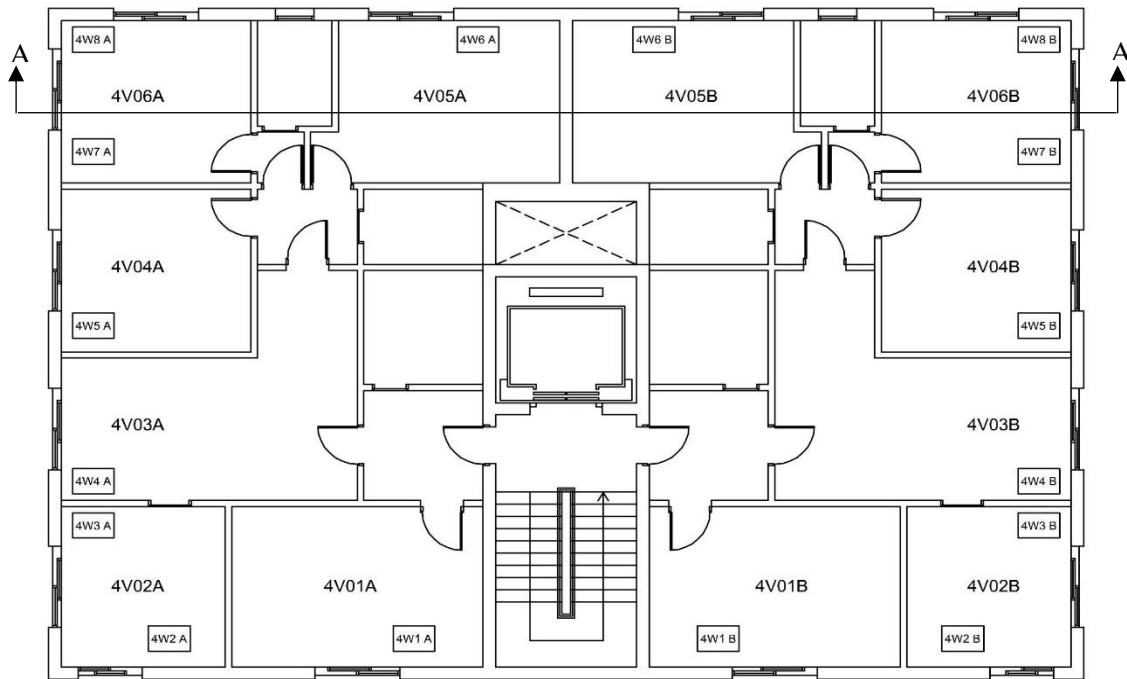


Figure 23: Typical floor plan

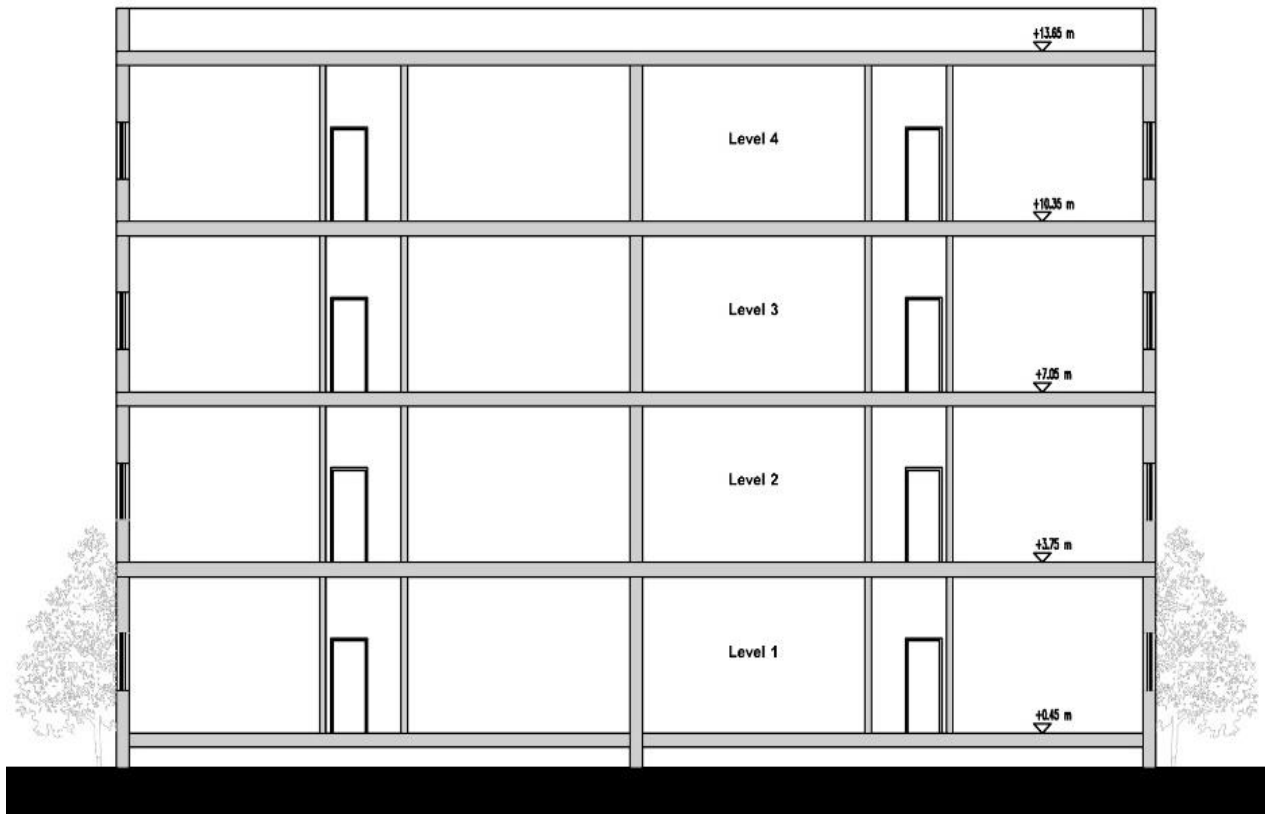


Figure 24: Cross view of Al Majd-1 Building.

Each volume of each space in the building model was considered for the simulation. A numbering methodology was set for each room in each apartment for one floor in the purpose of ease referencing due to a large number of rooms in the model. However, the numbering of each room starts with: floor level, room's prefix, and then the apartment's type. For instance, 2 V07 (A) stands for the powder room in the second floor of type A, in the same context, 3 W04 (B) stands for a window of the living room in the third floor of the type B. The window. The window to wall ratio was defined as the ratio of the window area to the exterior wall area (Goia et al. 2013). The geometrical properties for all volumes including the window area and the window to wall ratios are described in Table 7.

Table 7: Geometrical properties for all volumes, windows area, and window to wall ratios

Volume	Width x Length (m x m)	Floor Area (m ²)	Ceiling Height (m)	Window Area (m ²)	Window to Wall Ratio (%)
V01 (Guest Room)	5.9 x 3.95	23.31	3.3	2.4	12.33
V02 (Kitchen)	3.95 x 3.85	15.22	3.3	2x2.4	16.32
V03 (Living Room)	6.96 x 3.2 + 2.5 x 2.3	27.99	3.3	2.4	22.72
V04 (Bedroom 1)	4.45 x 4	17.80	3.3	2.4	18.18
V05 (Bedroom 2)	5.2 x 2.95	15.34	3.3	2.4	13.99
V06 (Master Bedroom)	4.45 x 2.95	13.13	3.3	2x2.4	17.20
V07 (Powder Room)	2.8 x 2.8	7.84	3.3	-	-
V08 (Bathroom 1)	2.8 x 1.7	4.76	3.3	-	-
V09 (Bathroom 2)	1.95 x 1.75	3.41	3.3	0.96	16.62
V10 (Corridor 1)	2.8 x 2.7	7.56	3.3	-	-
V11 (Corridor 2)	2.5 x 1.7	4.25	3.3	-	-
V12 (Corridor 3)	1.75 x 1	1.75	3.3	-	-
V13 (Lift Lobby + Staircase)	9.45 x 3.3	31.19	3.3	13.875	31.85
V14 (Shaft Opening)	3.3 x 1.7	5.61	3.3	-	-

4.8 Development of base case model

This section will describe and justifies the followed procedure in defining the base case in the simulation model. The geometric configuration, all optical and opaque dimensions, and model fabric materials were followed recommendations of the Building National Code of Jordan regulations defined for the building model. Also, this section will also cover all aspects related to thermal comfort evaluation, windows open/close definitions, energy consumption patterns, and internal heat gain loads.

4.8.1 Setup the simulation model

The building geometry was modeled in IESVE 2017 plug-in from Sketch Up, in which the thermal zones, the position of openings, windows and doors location, and wall sizing are defined. The developed model

in SketchUp is shown in Figure 25. Moreover, parameters including the building orientation, building geometry, thermal properties of the opaque, optical properties of glazing elements, internal loads, infiltrations, and occupancy schedules are also defined in the software to have more acceptable accuracy in predicting the energy performance of the building. As illustrated, the building was modeled by ignoring the presence of an adjacent building. However, this is considered one of the limitations of this study as Haase et al. (2009) disagreed with overlooking the influence of shading created by surrounding buildings.

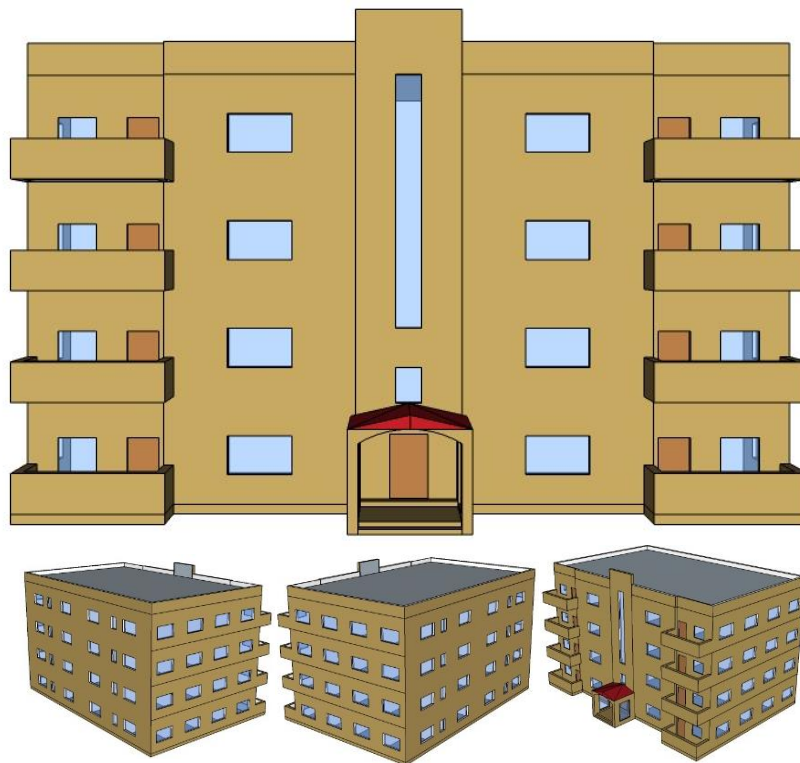


Figure 25: Base case model as modeled in Sketch up software.

4.8.2 Model exporting to IES VE.

Transferring the model to IES involves several procedures. Additional data are necessary to be defined in the software for more accuracy outputs. The generated file after exporting to IES VE is shown in Figure 26. This study focuses on the assessment of the performance of the double skin façade for energy saving potential in occupied space, which the external balconies were intentionally discarded due to their minimal influences on the overall indoor thermal performance of the building. Importantly, running the IES VE simulation requires a valid weather data for the chosen city. The weather file plays a significant

role in obtaining accurate and reliable results according to the site being studied. Unfortunately, the weather file of the city is not included in the software’s database where it was decisively important to add the weather-related information manually. However, the added data were extracted from the Jordan University of Science & Technology weather station located in Al Ramtha district located by 15Km from Irbid city center and it is the nearest weather station to the selected case study building. The obtained data includes temperature ranges, latitude, longitude, elevation, summer daylight saving, wind velocities, and solar radiation flux indexes.

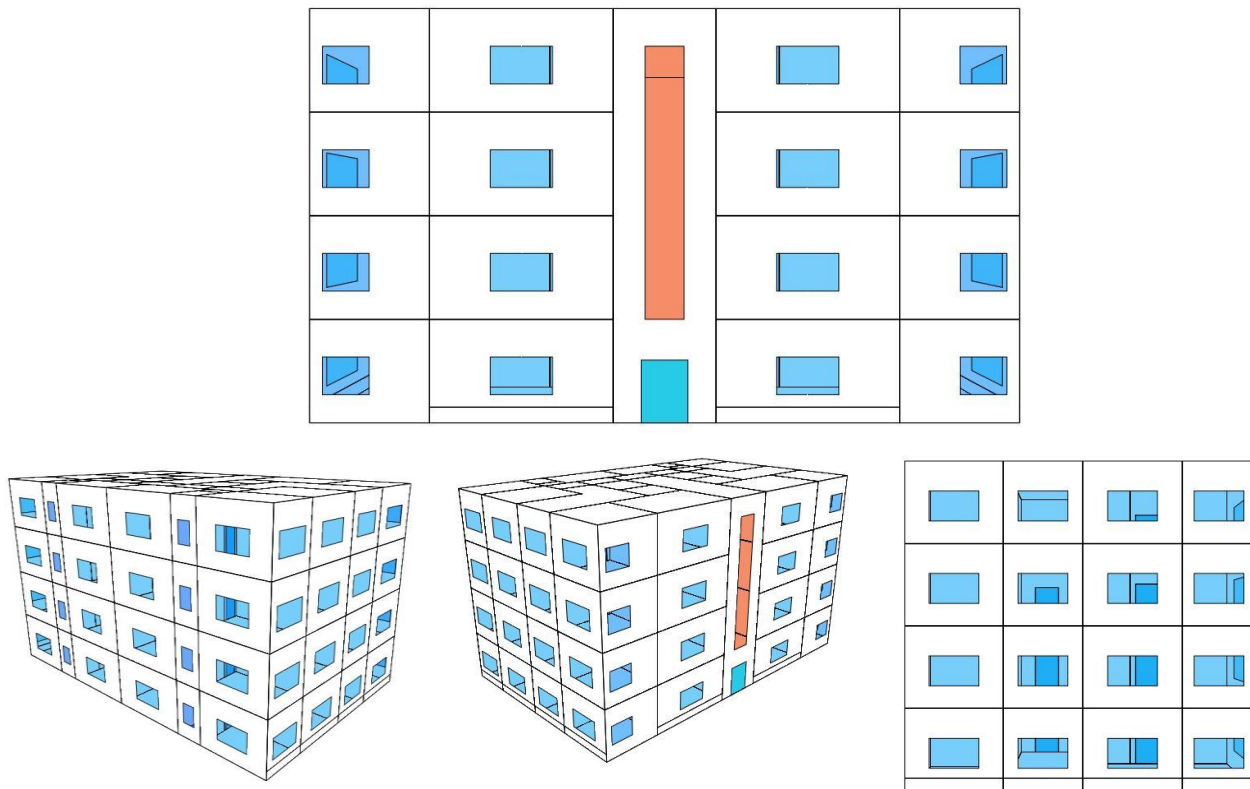


Figure 26: Base case as illustrated in IES VE software.

4.8.3 Building envelope definitions

The fabric materials and their properties of the base case were adopted from the recommendations from the National Building Code of Jordan (JNBC, 1993). The model conserved the typical Jordanian building typology with the usage of the prevailing construction materials. Following the national building code of Jordan, the construction materials including the masonry works, concrete works, and finishes works including their thermal properties that are assigned in the software are presented in Table 8.

Table 8: Building model properties

Type	Materials	Thickness (mm)	Conductivity (W/m.K)	Specific Heat (J/(Kg.K))	Density (Kg/m ³)	U-Value (W/m ² .K)
External Wall	Whitestone	50	0.7797	837	2580	1.8
	Cement mortar	100	1.400	1000	2000	
	Hollow concrete blocks	150	0.700	800	1200	
	Cement plaster	25	0.700	1000	1400	
Internal Wall	Cement plaster	25	0.700	1000	1400	2.108
	Hollow concrete blocks	100	0.700	800	1200	
	Cement plaster	25	0.700	1000	1400	
Roof	Concrete Screed	100	1.400	840	2000	2.19
	Asphalt-insulation	10	0.1	1000	2300	
	Reinforced concrete	250	2.3	1000	2300	
	Cement plaster	25	0.7	1000	1400	
Typical Floor	Terrazzo tiles	20	0.85	800	1900	1.69
	Concrete Screed	10	1.4	840	2000	
	Sand	50	0.3	840	1500	
	Reinforced concrete	250	2.3	1000	2300	
	Hollow blocks	50	0.7	800	1200	
	Cement plaster	10	0.7	1000	1400	
Ground Slab	Terrazzo tiles	50	0.85	800	2000	0.58
	Cement mortar	25	1.4	1000	2000	
	Concrete Screed	25	1.4	840	2000	
	Reinforced concrete	300	2.3	1000	2300	
	Polyurethane board	20	0.036	1400	20	
	Cellular polyurethane	20	0.03	1600	24	
Rooms Door	Pine Wood	40	0.14	2720	419	2.19
Main Door	Steel	40	50	480	7800	5.85

The properties of windows glazing of the building are crucial for obtaining accurate heating and cooling loads of the studied building. However, the assigned transmittance factor for the external single glazed windows was fixed at 0.78. The optical properties for all glazed surface of the building are demonstrated in Table 9.

Table 9: Optical material properties

Type	Materials	Thickness (mm)	Resistance (m ² .K/W)	Transmittance	g-value	u-value (glass) (W/m ² .K)	Net u-value (including frame) (W/m ² .K)
Single Glazed Layer	Clear float	6	0.0057	0.78	0.7062	2.94	3.17
	Air Cavity	12	0.1588	-			
	Clear float	16	0.0057	0.78			

4.8.4 Internal heat gain

The assessment of the thermal performance of any building may influence by the normal daily internal activities within the building envelope. To make this research more realistic, internal heat gain is considered. In residential buildings, the three most effective sources of heat gains are the presence of habitats, luminaires, and home-based equipment (PCs, washing machines, dishwasher, vacuum cleaner, refrigerators, TVs etc.). However, the DOS 2016 stated on their recent Census report that the occupancy density in Jordanian residential units considered a medium capacity where the average of the Jordanian family members is equivalent to 4.8.persons (3.2 people per 100m²). In this study, the assigned family-size set at 6 persons in the flat area of 150m² where the occupancy density set at 0.04 person/m². However, the software was assigned to manage the usage of all home-based equipment based on the occupancy profile defined in section 4.3.2. Although it is crucial to link the daily-operation heat gain according to occupancy actual presence in their premises. Heat gains related to people, luminaires, and equipment are listed in Table 10.

Table 10: Internal heat gain

Categories	Internal heat gain			Total (W/m ²)
	People	Luminaries	Home-based equipment	
Occupancy 00:00 to 24:00	420 W (70 W/person)	13 W/m ²	8.4 W/m ²	25

4.8.5 Thermal profile of the base case

Creating an acceptable thermal comfort for buildings' habitats is considered one of the main goals of the thermal design of buildings. This thermal comfort influences by factors linked with the Physiological state of humans in the livable spaces. However, the heat balance phenomenon for occupants is only achieved if the man-made Metabolism is equal to heat loss transferred to the ambient atmosphere.

Generally, the investigation of the indoor thermal comfort of the base case was assessed by the adaptive model developed by ANSI-ASHRAE 55 standards. The adaptive thermal model can be defined as the model that relates acceptable indoor air temperature ranges with outdoor meteorological parameters (ASHRAE 55, 2010). This technique based on a series of field studies derived from a global database of 21,000 experiments measurements conducted in commercial buildings. The adaptive model methodology can be applied in cases that match certain criteria, which fairly similar to the base case conditions, includes (1) the space should be equipped with operable windows that can be adjustable by occupants,

(2) the initial evaluation of thermal comfort must be assessed with completely absence of any mechanical cooling system, and (3) natural ventilation through the windows is the primary source of regulating the indoor thermal condition of the space. The adaptive model diagram is illustrated in Figure 27, in which the 80% acceptability limits are for typical applications while the 90% acceptability limits are for a higher desirable thermal comfort of spaces.

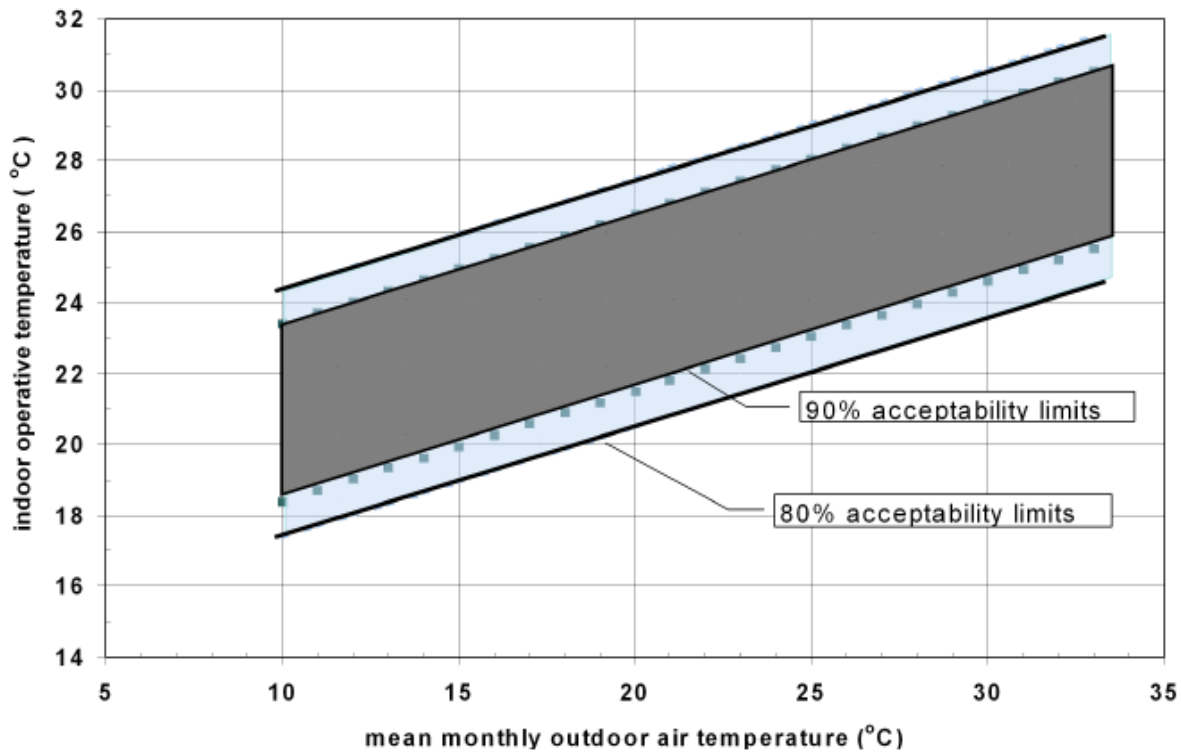


Figure 27: Acceptable operative temperature ranges for conditioned spaces. (Source: ASHRAE-55, 2010, P.14)

Considering the typical building application of the base case, the acceptability limits that satisfies 80% can be defined by the following equations:

- $LTL (°C) = 0.31 \times T_{OUT}(°C) + 14.3$ Equation 3

- $UTL (°C) = 0.31 \times T_{OUT}(°C) + 21.3$ Equation 4

Where:

LTL(°C): Lower acceptable temperature limits

UTL(°C): Upper acceptable temperature limits

T_{OUT} (°C); Mean monthly outdoor temperature.

Therefore, the assigned thermal profiles in the software considering 80% of the people perceive thermal comfort within these ranges in every month are defined as; (1) the heating loads kick in if the indoor temperature drops below LTL, the cooling loads kick in if the temperature exceeds UTL, and the spaces remain unconditioned if the indoor air temperature is between the two limits.

4.8.6 Windows and door openings scheme

The opening size and duration for all external windows and internal doors were taken into account due to their dramatic effect on the overall thermal performance of the building. The window opening strategies were assigned to follow the variation of cooling loads and ventilation scenarios defined in section 4.3.2. Consequently, all rooms' windows were programmed to be openable during summer only in a certain limit of time. According to the assigned geometry of windows, the software was defined to assume an opening of 50% of the gross area of the windows to be opened only if the indoor air temperature is below the UTL and the outdoor air temperature is above the LTL. Figure 28 shows the schematic diagram defined in the software for controlling the windows openings as a progression from the previous part.

In the same context, doors openings were also defined to follow certain assumptions during the year. However, the door of all of the kitchen, all bathrooms, and main apartment's door are considered closed the whole time, while the rest doors assumed to be fully opened the whole time.

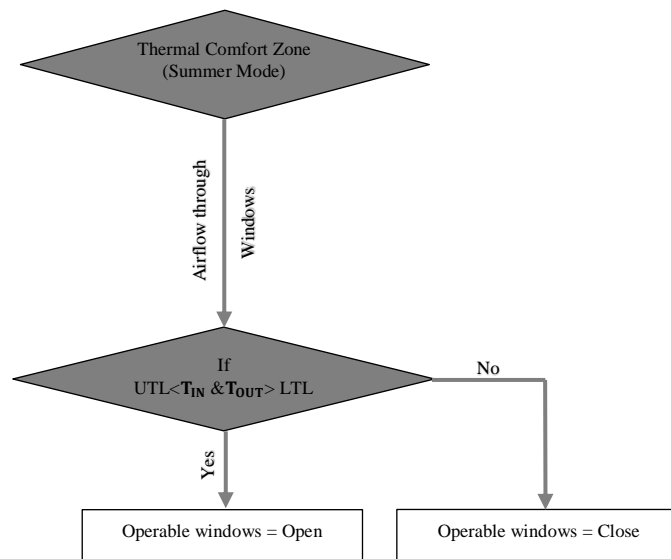


Figure 28: Windows open/close control diagram

4.8.7 Energy consumption evaluation methodology

In Jordan, the bottled LPG (liquid petroleum gas) is the major source of energy used in wide application such as space heating, water heating, and cooking. While the Air Conditioning system (A/C) is usually the main source of moderating the indoor temperatures during summer. In this study and for the ease of comparative analysis between the two loads, the electricity was assumed the main source of operating both heating and cooling loads. However, the electricity as the main runner of operating the (A/C) loads in the building, the Seasonal Energy Efficiency Ratio (SEER) is one of crucial factor affecting the evaluation of the system, where this ration indicates the total heat removed by the mean of cooling equipment during the annual cooling-season, expressed by kW/kW, divided by total electrical energy consumed during the same period (AHRI 2012). However, the assigned SEER for the base case was fixed at a rate of 4.25 kW/kW. Consequently, to assure achieve the optimum thermal comfort for occupants, the running of cooling and heating loads were set to be operated based on the upper and lower acceptable temperature limits. The control logic defined in the software is shown in Figure 29.

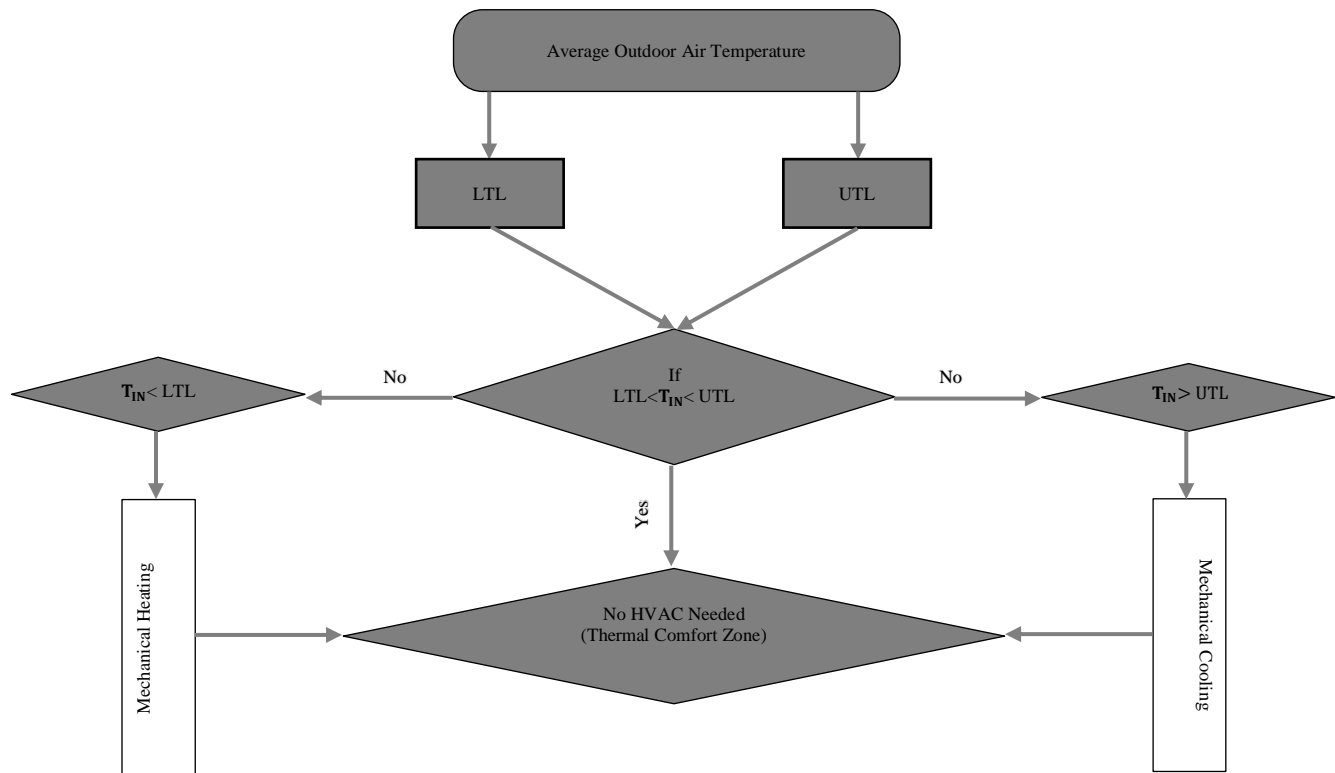


Figure 29: Energy consumption calculation methodology for base case. Note T_{IN} is the indoor aire temperature.

4.9 Development of the double skin façade model.

This study provides preliminary simulation results based on an additional glazing skin placed over a conventional building located in Irbid/Jordan. Double skin façades building commonly known as complex systems that require advanced analysis of their variables. This research will focus on testing and evaluation of four geometry types of façade structure on which several configurations of the cavity are evaluated in the modeling. The façade geometry types are; box-window (Figure 28a), shaft (Figure 28b), corridor (Figure 28c), and multistory (Figure 28d). The DSF formed on the building was modeled with additional glazing skin placed over the four-side elevations, covering the whole height of the building starting from 30cm above the ground floor. The space between the ground level to the bottom of the façade allows better air entrance from the bottom inlet opening of the façade, if needed, as well as to prevent the dust and particles that enter towards the cavity (Hamza, 2008).

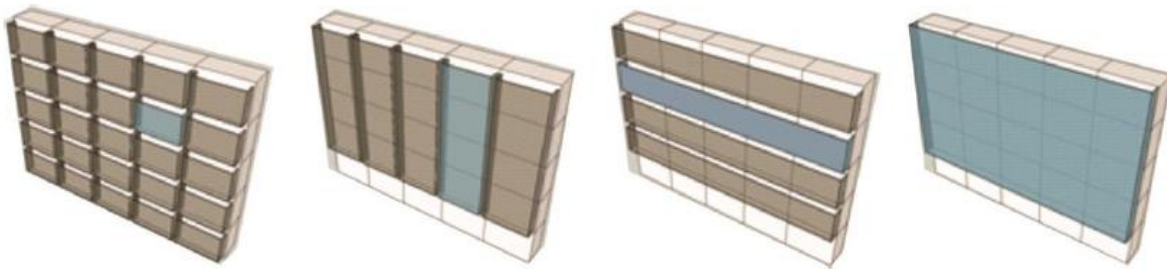


Figure 30: Different geometry types of in double-skin facades.

4.9.1 Simulation procedures

The geometry of the computational models of each DSFs was defined in SketchUp software, in which all of the thermal zones, positions, and areas of all of the external walls and transparent surfaces were defined before they were exported in IES-VE thermal simulation software. In IES, all the base case building properties were imported to the model and the DSF properties were the only variables modified in the program including the façade glazing type and properties, inlet and outlet opening sizes, and operational profile schedules of controlling of façade's openings. The main simulation results gathered from IES-VE were the airflows in and out from all the external windows and the façade openings, cavity air temperatures, indoor air temperatures, and thermal comfort indices. The selected glazing material properties of all DSF geometries are illustrated in Table 11.

Table 11: Double skin facade glazing properties.

Type	Materials	Thickness (mm)	Resistance (m ² .K/W)	Conductivity (W/m.K)	Transmittance	g-value	reflectance	u-value (glass) (W/m ² .K)
Double	Clear float	6	0.0057	1.06	0.78		0.07	
Glazed	Argon	12	0.1588	-	-	0.7062		2.94
Layer	Clear float	16	0.0057	1.06	0.78		0.07	

Figure 31 shows the model of the simulation scenario a multistory double skin façade type with a cavity width of 300mm.

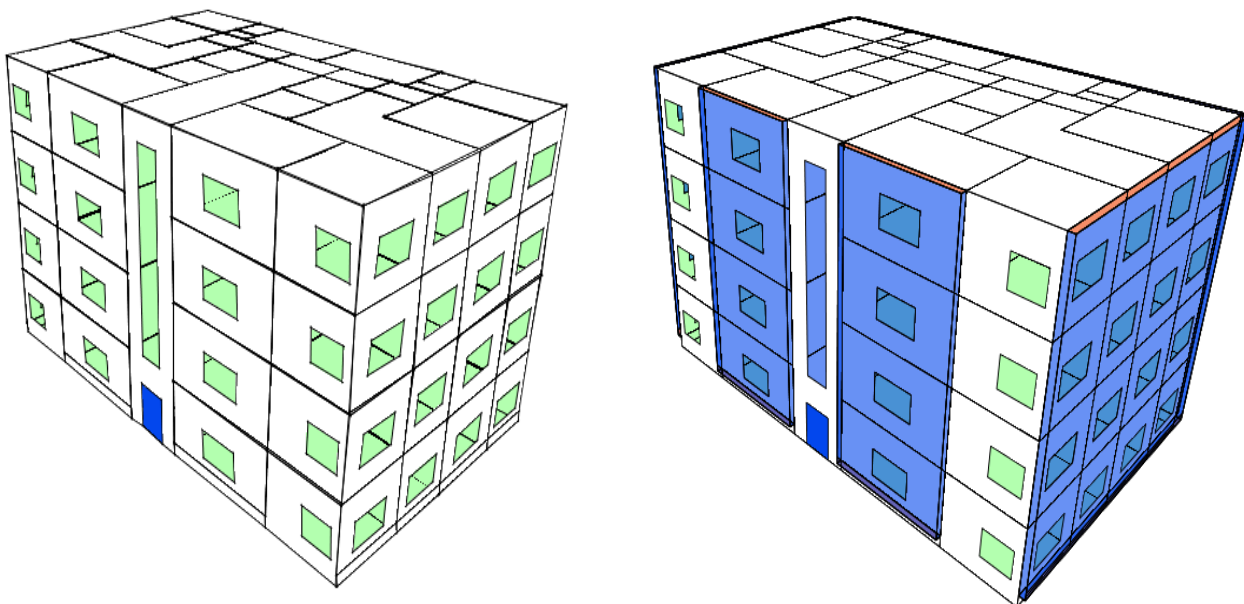


Figure 31: Multistory type double skin facade building as appear in IES VE software

After the simulation of the base case, different proposed types DSF were modeled. A total number of 48 simulations were conducted covering the individual performance of each geometry of DSF for every cavity thickness. Initially, the performance of the airflow was necessary of each façade for a better understanding of the performance of the building in the steady state conditions without any usage of energy loads. The analysis of the airflow included the effect of airflows on the indoor conditions when façade’s openings are opened vs external windows are opened, façade’s openings are opened vs external windows are closed, façade’s opening are closed vs external windows are opened, and façade’s openings are closed vs external windows are closed. The four configurations of controlling the façade’s openings and external vents are illustrated in Figure 32.

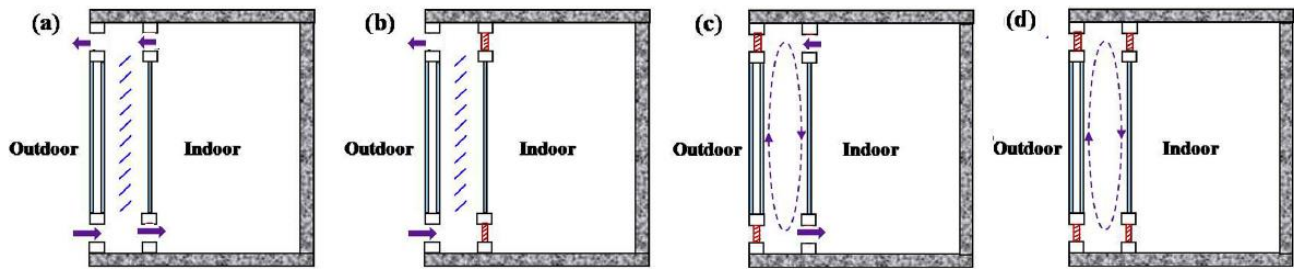


Figure 32: Airflow modes studied for the assessment of the double skin facade.

4.9.2 Simulation Process

Following a multiple of the tested performance of all geometries in corresponding to the cavity thickness, one optimized façade's geometry based on a combination of the four airflow parameters for each month according to the lowest PPD% (max thermal comfort) will be then selected for the rest of the comparative study. Figure 33 illustrates the methodology matrix of choosing the optimized façade geometry in terms of thermal comfort acceptability adopted from ASHRAE 55 standards using the *Predicted Percentage of Dissatisfied* index.

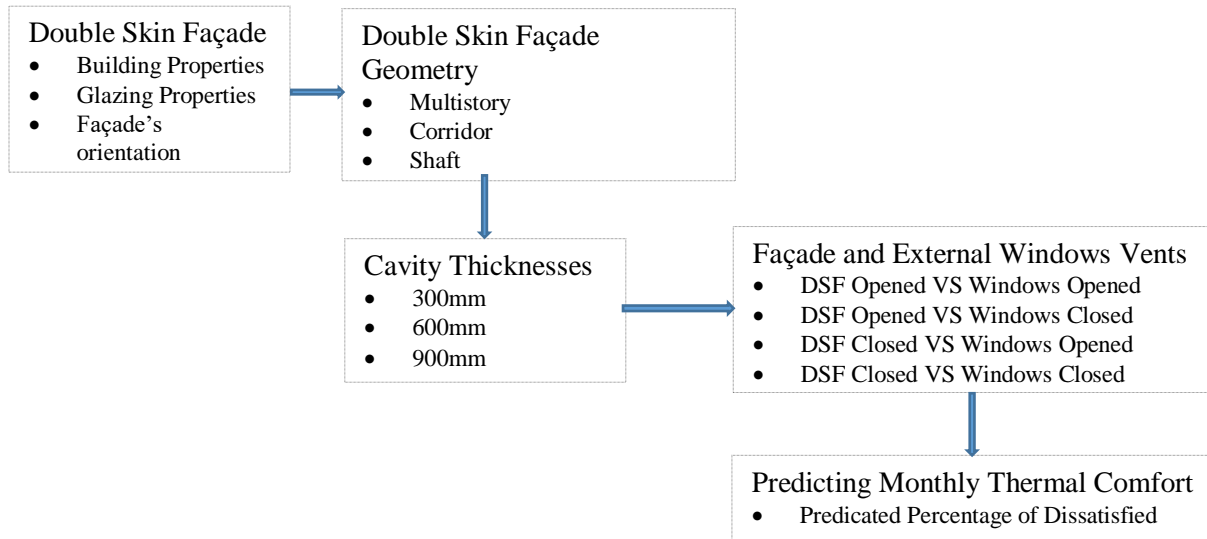


Figure 33: Methodology diagram of DSF thermal assessment

4.9.3 Façade vents and external window openings definitions

This study is highlighting the DSF technology in a conventional residential building located in Irbid. Given the complexity of heat transfer and air movement inside the façade chamber (cavity), it is recommended to include tools of computer simulation in the initial stages of façade design that allow in establishing dynamic strategies of modes of ventilation based on the climatic conditions. However, the

correct design inputs along with the appropriate operation of the system crucial in accomplishing successful outcomes of the performance of the DSF. One of the most parameters influencing the performance of the DSF is the controlling the opening and closure of the external windows and façade’s vents (inlets and outlets) based on requirements for the acceptable thermal indoor environment. Consequently, all rooms’ windows and façade’s vents were programmed to be openable on certain conditions. These conditions correspond to the lowest PPD in every month during the year. For instance, Figure 34 shows the distribution of all values of PPDs for every month in four modes of ventilation in case of shaft DSF with 300mm cavity width. Apparently, the percentages illustrated show that occupants feel thermal comfort in winter (January, February, March, November, and December) if both façades and windows vents are closed in winter, whilst thermal comfort of occupants can be achieved in summer if the openings are opened represented from May until September. More specifically, the months of April and October, which often represent the months of the summer and winter solstice, dual input assumptions should be considered during the simulation parameters definitions. The minimum PPD of the former happens if the external windows opening is either opened or closed. Regarding the latter, thermal comfort occurs if the façades vents are either opened or closed.

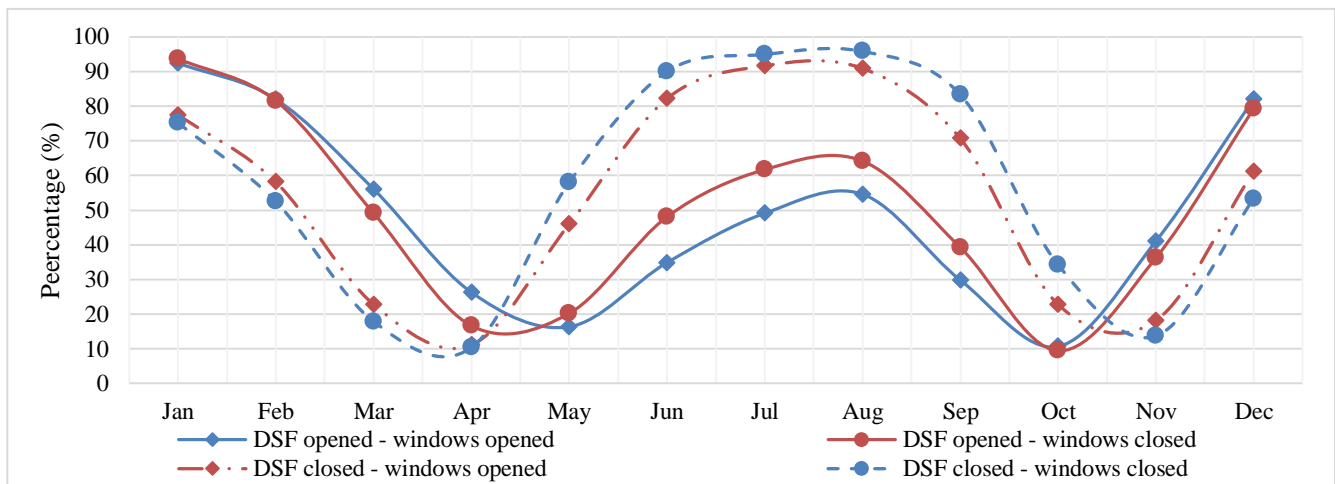


Figure 34: Monthly PPD ranges of the shaft type DSF with 300mm cavity width in term of the mode of ventilations.

The best way to reduce the uncertainties and to accomplish the reliability of simulation results is by the proper data definitions in the software, which provides extended control of airflow mechanism in order to achieve the maximum possible thermal comfort. Figure 35 outlines the airflow network control of the vents of both façade and external windows for all façade’s geometries.

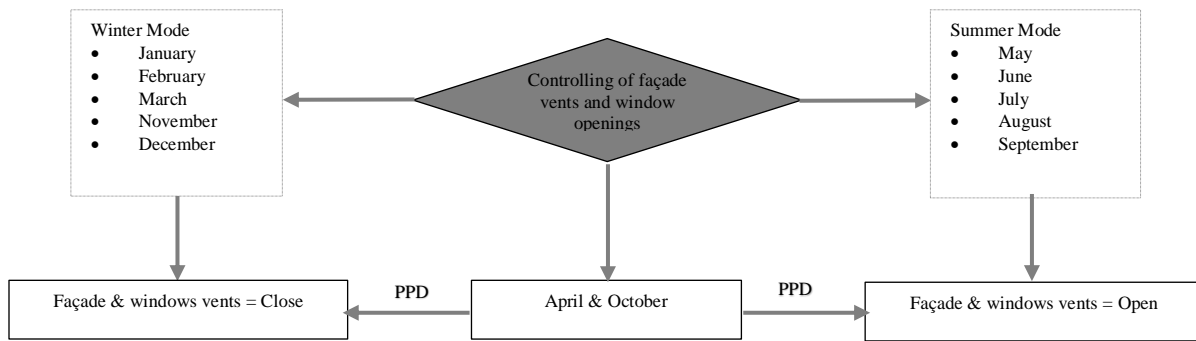


Figure 35: Facade's and external windows' vents controlling diagram.

4.9.3.1 Controlling of overheating

To prevent overheating of the interior spaces during summer which may cause unexpected thermal discomfort, the external operable windows were defined to be automatically closed if the cavity temperature exceeds a certain limit, which mainly the UTL of the internal spaces in this period. Since the flowing air into temperature is driven by the ambient temperature of the cavity, the UTL, in this case, is considered the average monthly cavity temperatures. The airflow windows temperature control diagram is presented in Figure 36.

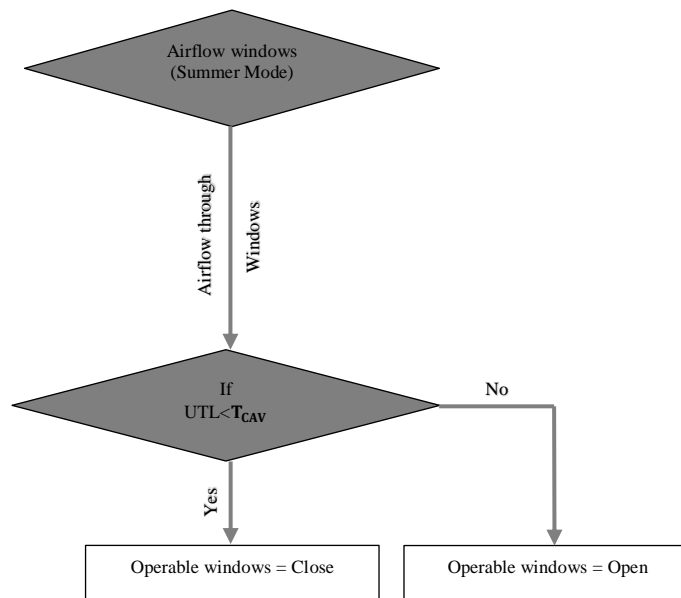


Figure 36: Process of controlling the facade vents in case of overheating in summer season.

4.9.4 Energy consumption evaluation

In the same manner, the assessment of the energy consumption will follow the criteria already defined in the base case. Due to the additional skin is built on the perimeter of the building, the building then no longer has direct contact with the outdoor ambient environment where, on the other hand, indoor air temperature is highly influenced by the cavity air temperature. However, special consideration to be drawn in the evaluation of energy consumption during winter as once the façade's cavity is sealed, a thermal dissatisfaction is expected as such very little cavity airflow occurs. Therefore, a set of complex thermal profile based on mathematical formulas were defined in the simulation software. The control diagram for computing the energy consumption in the case of DSF building as programmed in the simulation software is presented in Figure 37.

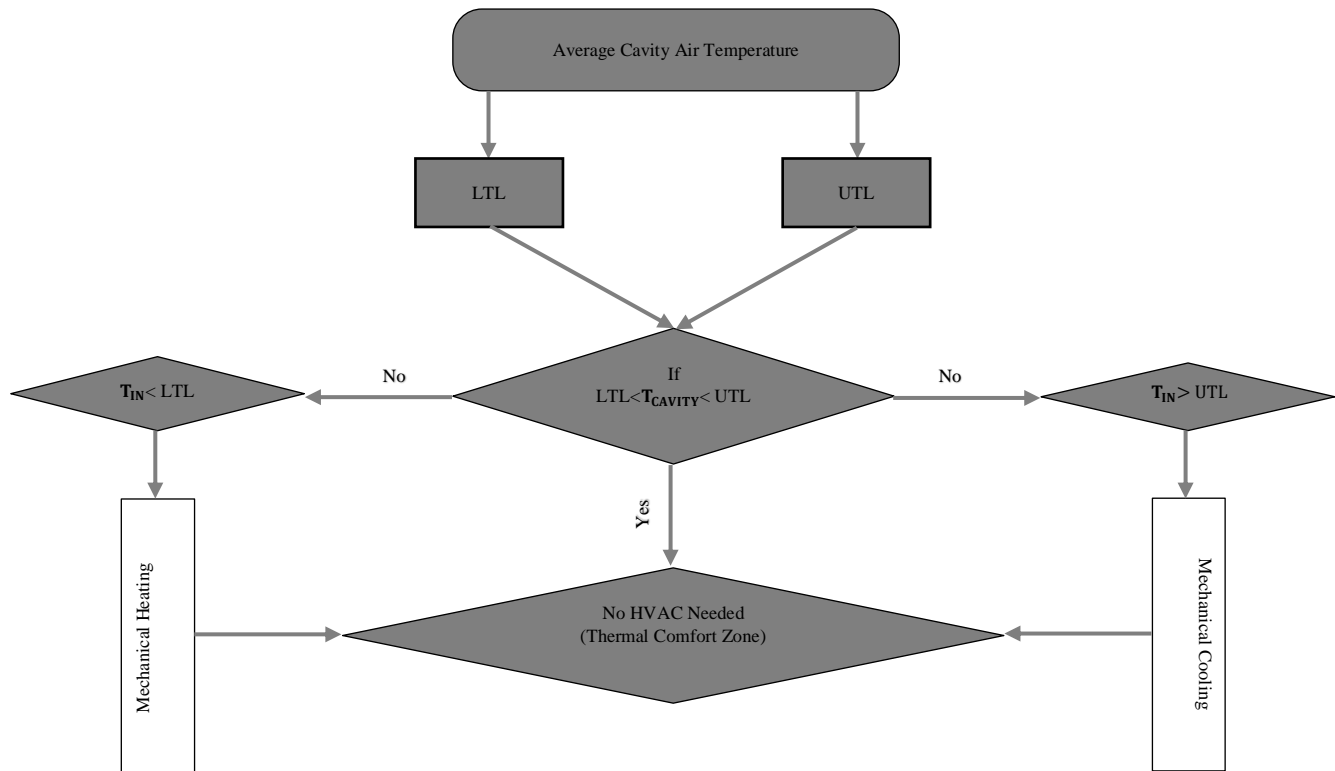


Figure 37: Energy consumption calculation methodology for DSF. Note T_{CAVITY} is the cavity air temperature

5.0 Results of the simulation models

This section will include the full results of this research and discussions for selecting the most appropriate façade that affords the lowest energy consumption in conjunction with the highest achieving of occupants' thermal comfort. The first section will initially present the results of simulations of alternative cases model related to the base case and all multiple simulations of different types of façade geometries. The comprehensive analysis of all related direct and indirect results of the building is crucial to a better understanding for any potential of energy reduction and thermal acceptance levels. The discussion section will present a comprehensive comparative study between the base case (single skin façade) and all other DSF types to highlight the benefits and constraints of the application of this system.

5.1 Findings of the base case

Thermal comfort can be evaluated by calculating the number of hours the indoor temperature in correspond to the relative humidity that will not exceed certain limits according to the psychometric charts of Irbid city. In this section, detailed results of the thermal performance of the base case are discussed separately. After running the simulation for the building in the IES VE program, results are illustrated in figures and tables below. By assuming the top floor is the most critical case, and for the symmetrical floor layout for all levels, the 4th floor was intentionally chosen for running the simulation and gathering results

5.1.1 Indoor air temperature vs indoor relative humidity

The window opening profile plays a significant role in fluctuating the indoor air temperatures. According to Figure 38, the indoor air temperatures follow the behavior similar to the outdoor air temperature when the windows are opened, whereas the indoor temperature has risen when the windows are closed. Moreover, the difference in temperature between the dry-bulb temperature and indoor air temperature during closing windows expands in summer by 5°C, while it narrowed by 2°C in winter seasons. Although the annual average air temperature while the windows are closed is higher than when the windows are opened, the indoor air temperature maximizes at 33.32°C, while the air temperature while the windows opened rose to 36.08°C. This can be explained by the positive effects of the natural ventilation in moderating the indoor air temperature which forces the average air temperature to be lower than the closed-window scheme. Moreover, the minimum air temperatures for the opened and closed windows are 0.21°C and 7.35°C, respectively. However, the diagram shows that the air temperature

profile for both cases starts to increase gradually until the mid of May, then the air temperature profile behaves steady until mid of September, and the temperature starts to gradually decrease. The graph's results illustrate the importance of properly selecting the of the window openings schemes based on the occupant's response to accuracy and efficiency of the model.

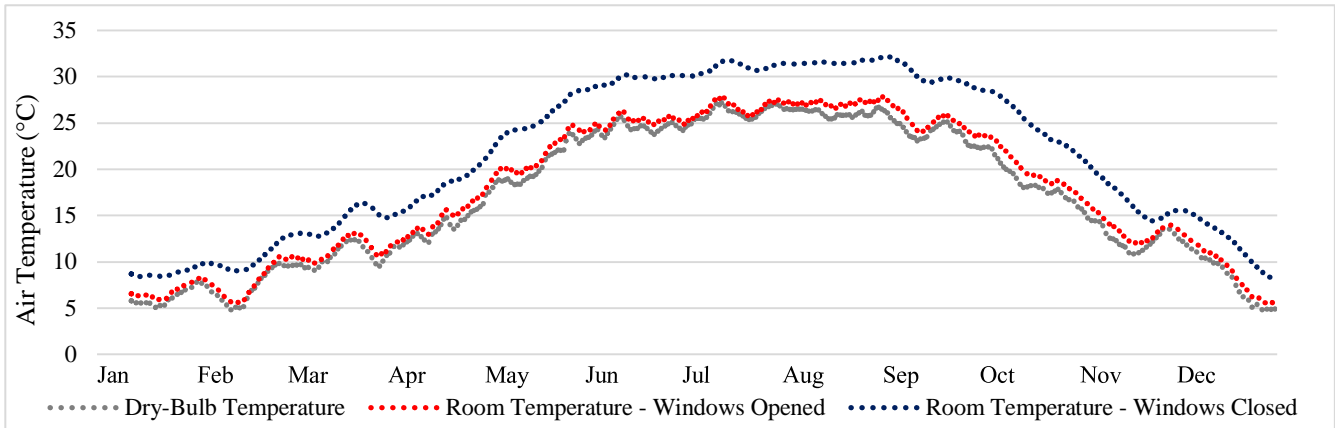


Figure 38: The relationship between the annual average dry-bulb temperature with the annual average room air temperature when the windows are opened and closed

In the same context, Figure 39 illustrates the relationship between the outdoor air relative humidity percentages with the indoor air relative humidity in both case; windows are opened and closed. The diagram shows that indoor relative humidity is highly dependent on the outdoor air relative humidity where the annual average indoor air relative humidity maintained very similar to the outdoor relative humidity. However, closing windows preserves the indoor air relative humidity ranging between 40% and 10%. The slight rise in relative humidity properly resulted in moisture penetrated through external walls.

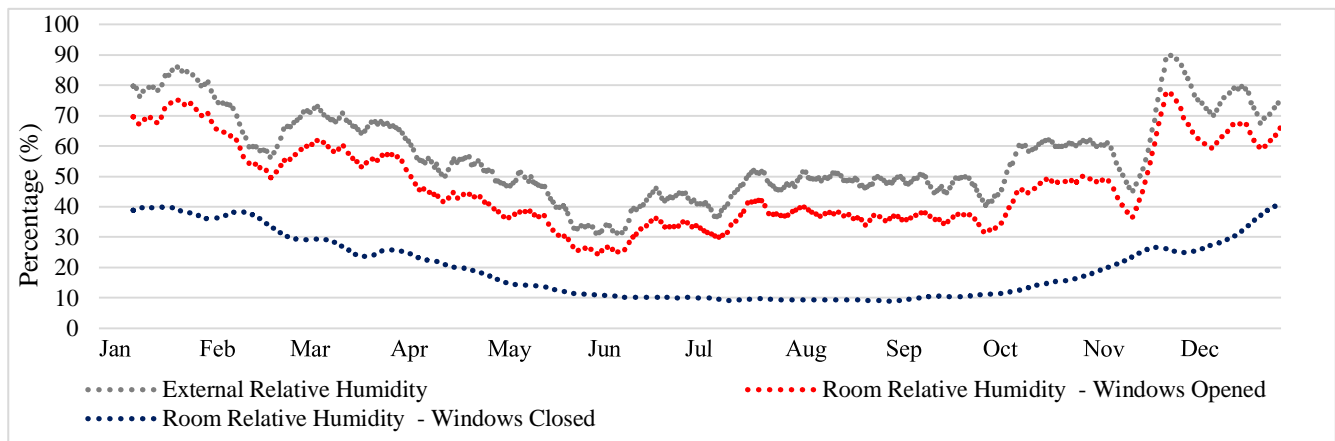


Figure 39: The relationship between the outdoor RH% with room RH% when the windows are either opened or closed

5.1.2 Thermal comfort evaluation

In order to predict the actual thermal performance of the building, the average maximum and minimum air temperature for both openings schemes were delineated in the Psychrometric Chart adapted from Climate Consultant Software as shown in Figure 40. The comfort zones represented on the two blue boxes located based on an assumption that occupants clothing insulation values are 1.0 clo in winter season (left-side of the light-gray box) and 0.5 clo in summer season (right-side of the dark-gray box), the metabolic rate is 1.1 Met units, and that the indoor air maximum speed equals 0.1 m/s.

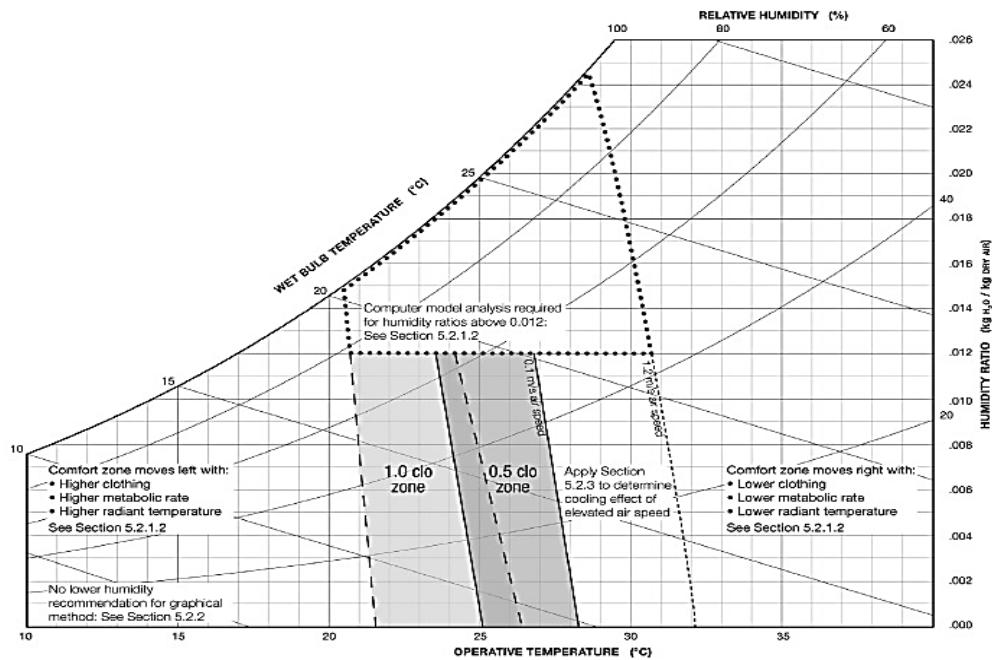


Figure 40: Psychrometric chart indicating the winter and summer comfort zones (ASHRAE-55 (2010), P8)

Perhaps, considering the annual indoor air relative humidity conditions is crucial due to differences in openings modes, the average mean annual relative humidity for opening and closing windows are 46.682% and 20.39%, respectively. For the ease plotting, the annual average mean relative humidity for both cases were assumed to be 50% and 20%, respectively. Figure 41 indicates the poor thermal performance of the building when all windows are considered opened and closed during the study year period. The diagram illustrated in Figure 41a shows that the lowest temperatures of summer season starting from June until August are fallen within the comfort zone. Similarly, the highest temperatures of both April and October are fallen within the comfort zone. However, the thermal behavior of the 4th floor while closing windows keeps both April and October indoor air temperature within the comfort zones as shown in Figure 41b. The chart also shows that the lowest air temperature of May and September

are fallen within the boundaries of the comfort zone. It is concluded that the occupants of the building probably are voluntary in achieving their thermal comfort if the temperature reaches its maximum in April and October only, which they are mainly the transition seasons. Other months including heating and cooling season, natural ventilation and/or mechanical ventilation are necessary.

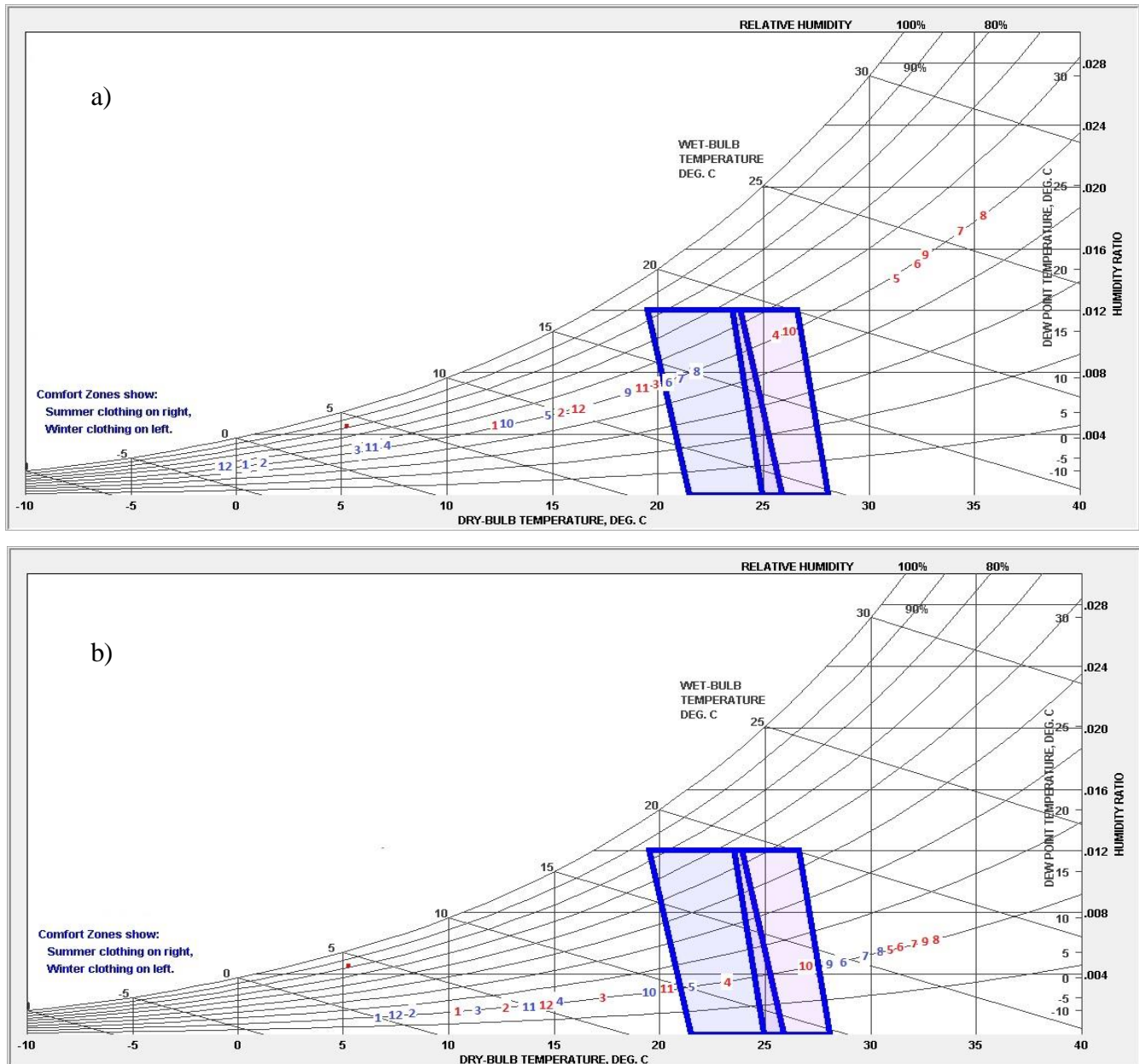


Figure 41: Maximum and minimum air temperature versus average mean annual air relative humidity: (a) external windows opened, (b) external windows closed. The number represent months of the year on sequence, the red color indicates the average maximum temperature while the blue color indicates the average minimum temperature.

The comfort zones boundaries of each month were calculated through adaptive methodologies adopted from ANSI/ASHRAE as discussed earlier. Figure 42 shows the thermal comfort matrix for the base case (4th floor) based on the adaptive thermal model calculated by using equations (1) and (2). It indicates whether the operative temperatures for both opening modes are falling within or outside the thermal acceptable limits. However, the thermal acceptability limits based on an assumption that 80% of people feel thermal satisfaction within these ranges. The diagram illustrates the majority of the operative indoor air temperatures are not within the acceptability limits. In case of closing windows, a slight improvement can be achieved during the heating seasons while it worsens in the cooling season due to the fact that comfort zone boundary varies with temperature/air-speed combination (ASHRAE-55 2010).

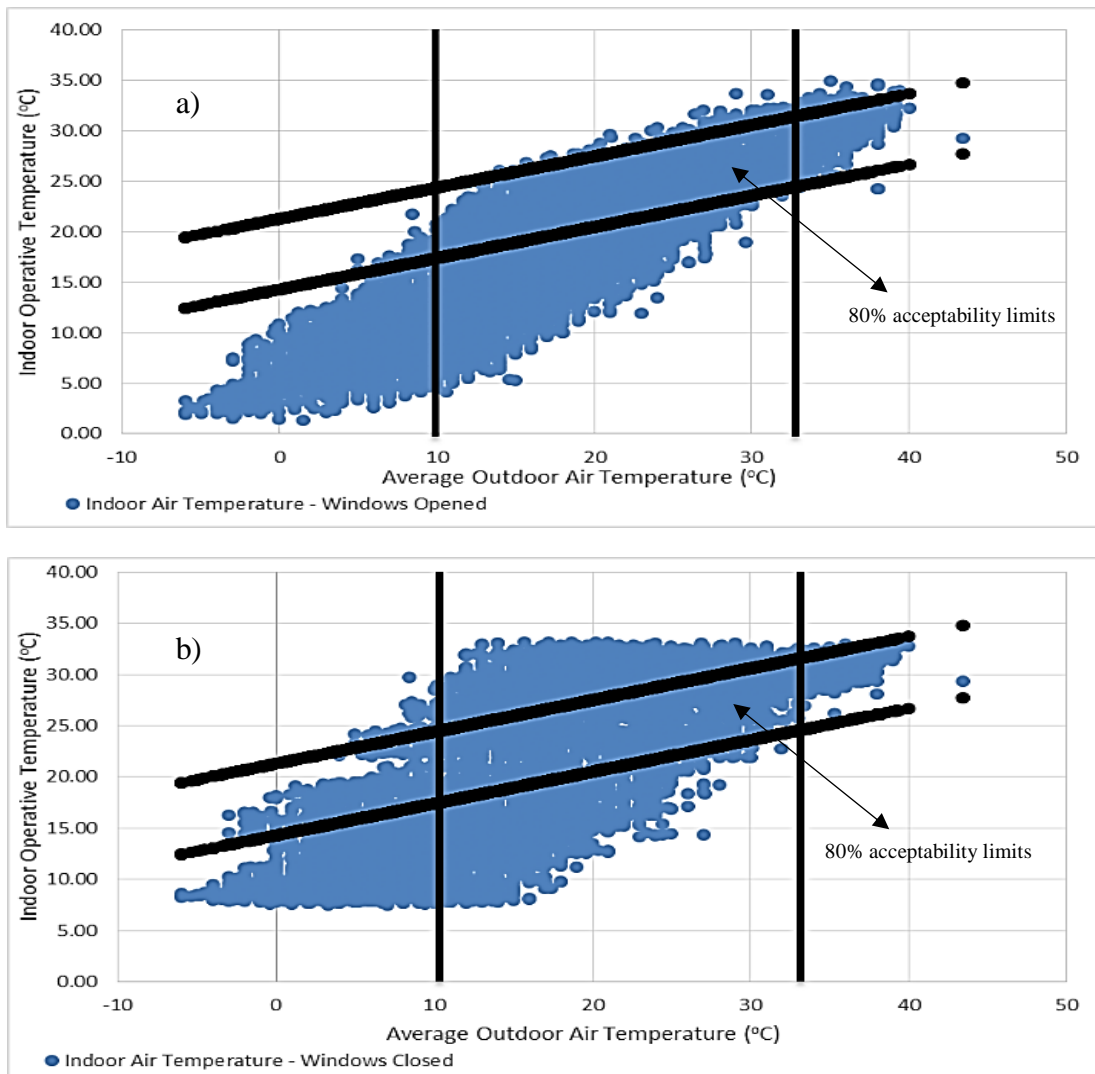


Figure 42: Annual operative temperature of the base case (4th floor) when, a) windows are opened, b) windows are closed

Consequently, the percentage of the annual operative indoor temperatures that are not falling within the comfort zone boundary can be represented in Predicted Percentage of Dissatisfied (PPD) graph. The PPD can be defined as the index that can predict the percentages of people that feeling thermal discomfort during a particular month. Figure 43 shows that PPD% for both windows open/close modes. The percentages illustrate that the base case occupants prefer closing windows for months starting from January to April and November to December while opening the windows is more preferable during the summer season starting from May to September. The diagram indicates the poor thermal satisfaction of occupants in January, February, and December where the percentages indicated by a very high rate of dissatisfaction. Moreover, the month of October is the only month where the PPD% for both cases were having the same rates. It can be concluded that the base case in both windows opening modes showing a poor thermal performance where the annual average PPD for windows opened and closed are 47.92% and 50.58%, respectively.

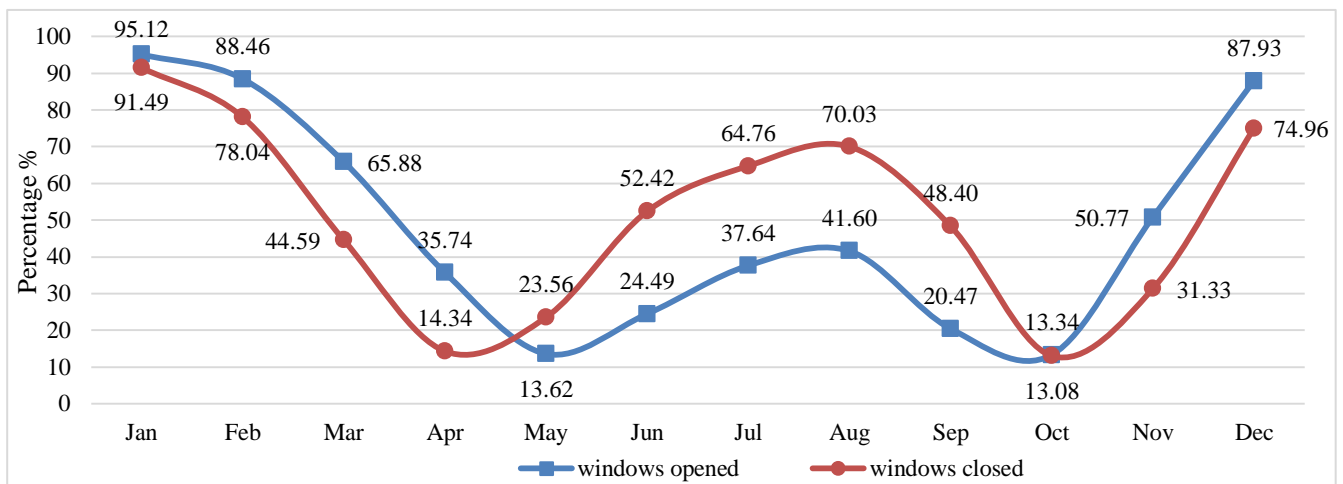


Figure 43: Predicted percentage of dissatisfied (PPD) for both windows open/close modes for the base case.

The annual energy demand of the base case needed to achieve an 80% of occupants satisfaction will be measured upon the lowest PPD. However, the lowest percentages indicated in each month represent the highest optimal indoor conditions that can be sensed by the occupants. In order to facilitate the scope of this research, the assumed “thermal dissatisfied curve” in parallel with the preferable window opening mode in each month is shown in Figure 44. This curve will be used as a benchmark to indicate whether implementing of several DSF have the potential to enhance the overall thermal comfort before assessing the total energy demand for that purpose. This figure also demonstrated that the annual PPD for the occupants’ in the case study building averaged at 40.47%.

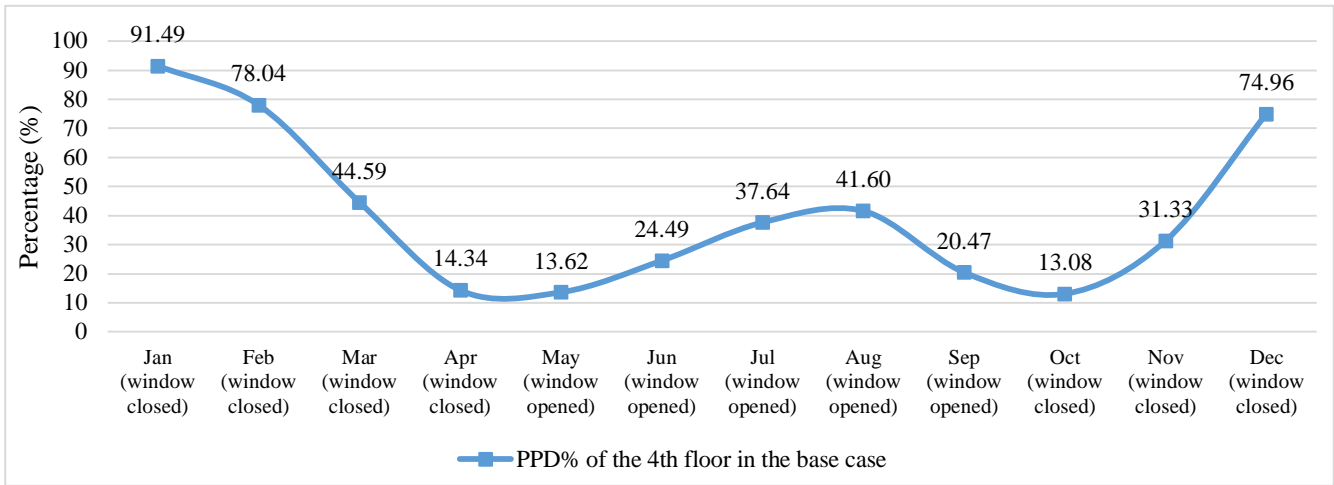


Figure 44: Assigned PPD for the base case

5.1.3 Airflow rates and heat gain

The airflow rates entering through the building’s openings during the ventilation months can give a prediction of the relationship between the airflow and thermal behavior of the indoor environment. Investigating the airflow during the hottest months (May to September) based on the PPD values that stated that the occupants prefer all the external windows to be opened during the hottest seasons (May to September). By considering the windows are fully opened (50% equivalent area), the mean annual net airflows entering the building’s opening during the ventilation period is shown in Figure 45. The monthly airflows across the building gradually increase and peaks on July with an average airflow rate of 8670 l/s.

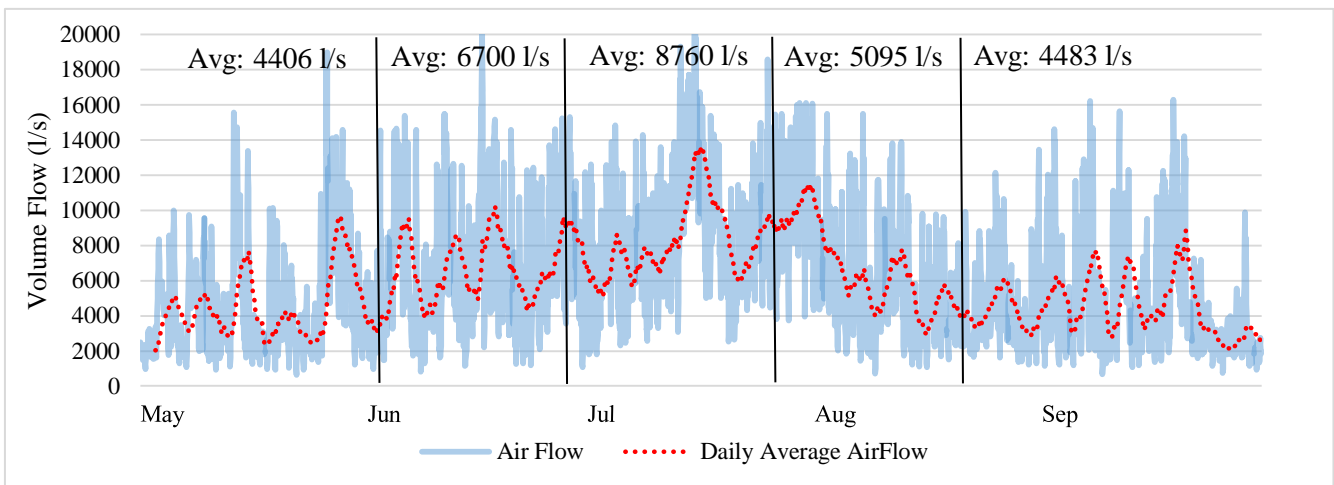


Figure 45: Volume flow rate of the air entering the building's openings

Specifically, Figure 46 shows the heat gain profile associated with the airflows entering the building spaces over the hottest period from May to September. The simulation results illustrate the potential of the entered air in reducing the excessive indoor heat where the monthly average of the heat gain is -0.269 kW. The negative value signifies the ability of the entered airflow to eliminating or rejecting the heat inside the spaces. The diagram illustrates that the airflow in July and August have the lowest effect of heat rejection as the average net airflow heat gain is -0.233kW and -0.246kW, respectively.

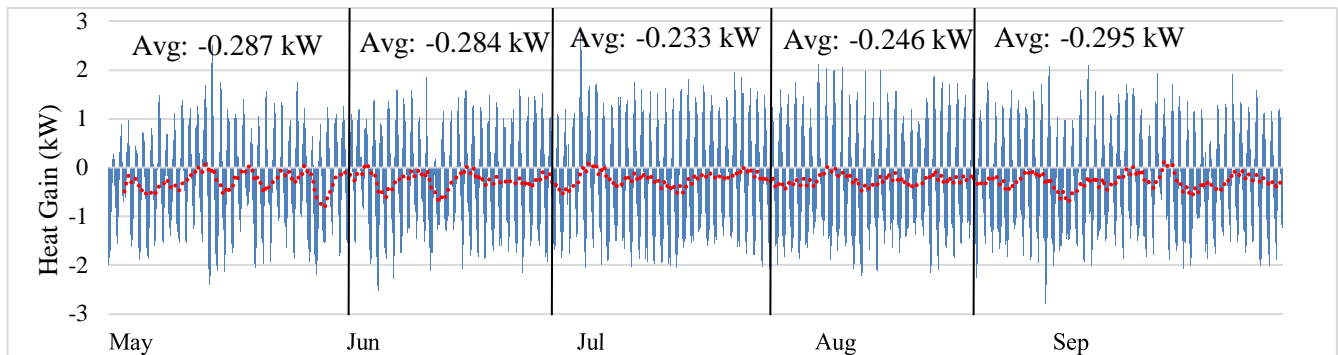


Figure 46: Heat gain through airflow entering the building’s openings.

5.1.4 Solar heat gain

The solar gain plays a significant role in the thermal balance of a building. The large value of U-value such as the external walls can dramatically transmit the absorbed heat from the solar radiation into the internal spaces in which overheating issues can be caused by the excessive solar heat gains during the hottest periods. Figure 47 shows the annual solar heat gain on the external façade of the Base Case. The diagram shows the difference in the annual heat gains during months where a fluctuation of the gained solar heat can be observed during the winter seasons, while it became a steady during summer. The average solar gain for the 1st, 2nd, and 3rd quarter of the year was 0.129 kW, 0.146 kW, and 0.13 kW, respectively.

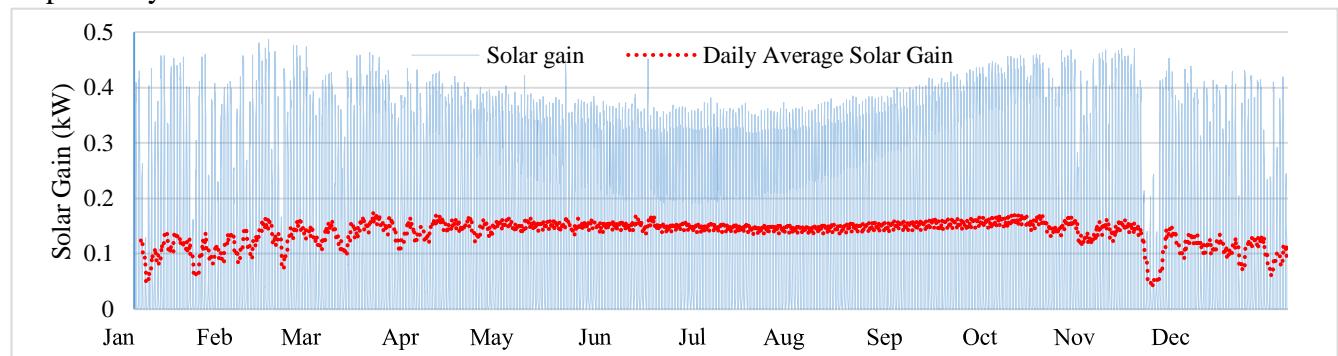


Figure 47: Monthly solar heat gain on the external facade.

5.1.5 Surface temperature

Moreover, since all the livable rooms have a direct connection with the external environment, the surface temperature of the external façades (glazed surface and solid surfaces) can play a significant role in determining the thermal behavior of rooms influenced by the temperature gain. Figure 48 shows the average maximum and minimum surface temperatures for all the external components of each façade direction. The results illustrate that the average difference between windows and wall surface temperatures have almost the same values during the year and have the equivalent thermal behavior. However, the surface temperature fluctuation for windows is higher than to the external walls' surface temperature due to the better U-value of the wall.

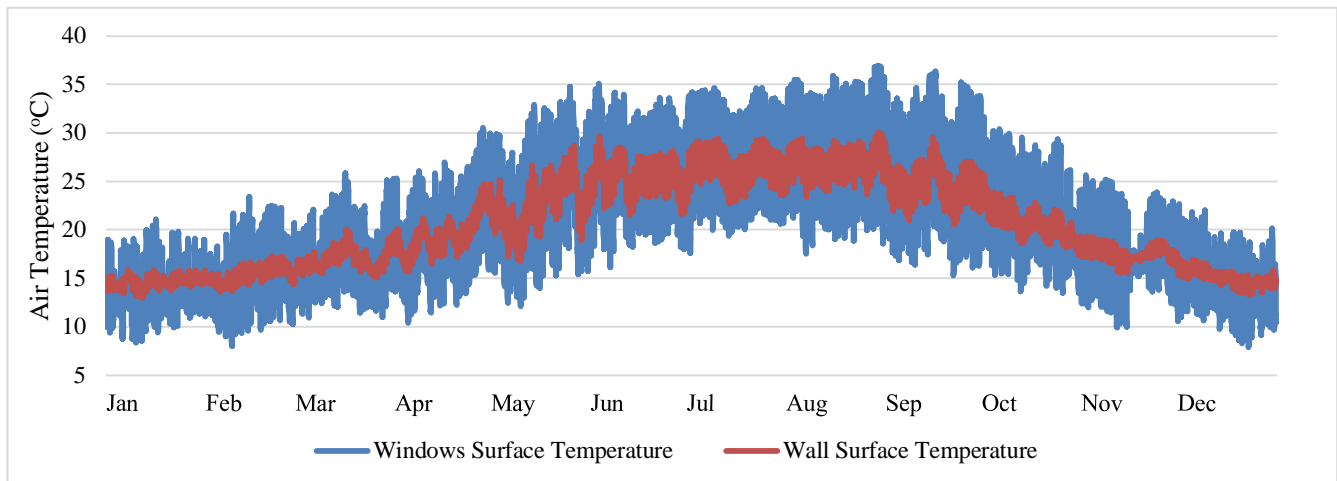


Figure 48: External walls and windows surface temperatures.

5.1.6 Heat gain through conduction.

The conduction heat gain through the external façade of the building had a significant effect on the total thermal performance of the building. The annual heat gained through conduction for all opaque walls and glazing materials is presented in Figure 49. The diagram illustrates that conduction significantly plays a role in changing the indoor conditions. However, walls are main contributor in changing the indoor air temperature, where the heat gain indicated in positive values is responsible in transferring the heat towards the building when the heat gained above zero represented from May until mid of October, while the rest months represented in winter seasons are responsible to transfer the indoor heat towards outside. Windows have a minor effect in increasing the temperature in the summer season, while a slight effect heat transfer of windows is active during winters. The average conduction gain through external walls for the 1st, 2nd, and 3rd quarter of the year is -0.16 kW, +0.07 kW, and -0.07 kW, respectively, while

the conduction gain through the external windows for the same periods are -0.08 kW, zero kW, and -0.05 kW, respectively.

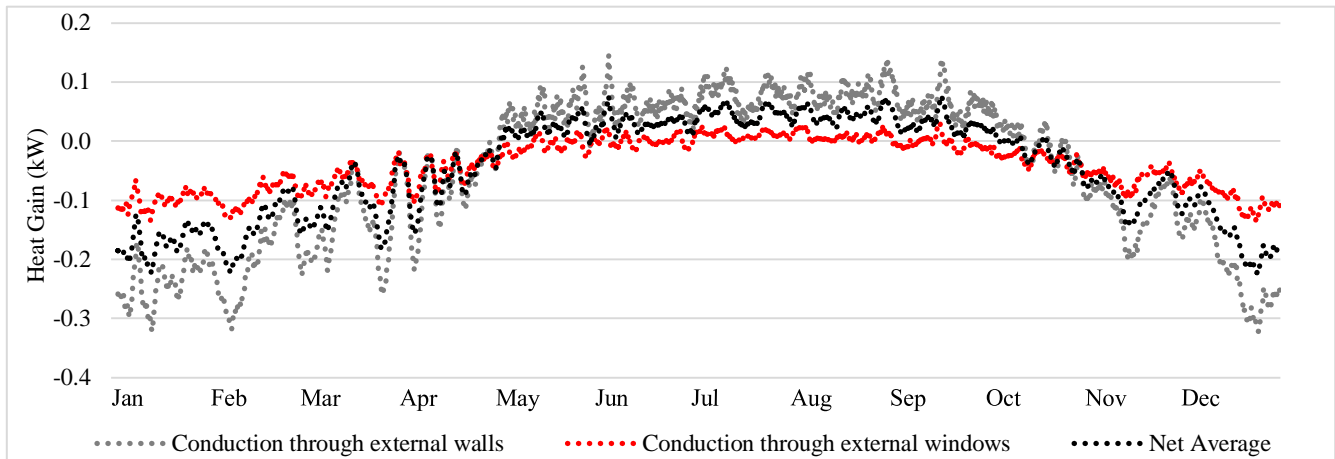


Figure 49: Heat gained through conduction

5.1.7 Energy consumption

The annual cooling and heating load required to achieve an 80% thermal satisfaction can be assessed by considering the monthly thermal comfort zone boundary according to the adaptive thermal model. Table 12 shows the monthly thermal comfort zone acceptability ranges that satisfy 80% of people. The upper and lower temperature limits in conjunction with the outdoor conditions can be evaluated according to Equation (1) and Equation (2). Thus, the designated seasonal thermal comfort is 16.25°-25.25°C (winter) and 20.75°-29.50°C.

Table 12: Monthly thermal comfort zone boundaries

Month	Average outdoor air temperature (°C)	Thermal acceptance levels	
		Lower temperature limit (°C)	Upper temperature limit (°C)
January	06.30	16.25	23.25
February	07.46	16.62	23.62
March	11.04	17.72	24.72
April	14.66	18.84	25.84
May	21.05	20.83	27.83
June	24.55	21.91	28.91
July	26.43	22.49	29.49
August	26.29	22.45	29.45
September	23.41	21.55	28.55
October	17.66	19.77	26.77
November	12.29	18.11	25.11
December	07.21	16.53	23.53

The energy profile definition can be then summarized according to the requirements in each month to obtain the desired objective of this study. However, analyzing the data obtained from Figure 44 and Table 12 help in assessing the thermal comfort in each month. The energy demand and consumption to achieve 80% acceptance thermal comfort can be then estimated. Table 13 summarizes the defined thermal variables in IES VE, where each month requires it is own criteria to be considered during the analysis. However, the energy consumption of the base case gives an indication of the possibility of the Double Skin Façades in lessening the overall energy demands along with enhancing the occupants' monthly thermal comfort.

Table 13: Summary of monthly energy profiles as defined in IES VE.

Month	Description		
	Cooling	Natural Ventilation through windows	Heating
January	N/A	Windows closed the whole time	$t_i < 16.25$
February	N/A	Windows closed the whole time	$t_i < 16.62$
March	N/A	Windows closed the whole time	$t_i < 17.72$
April	$t_i > 25.84$	$t_i < 25.84$ and $t_o < 18.84$	$t_i < 18.84$
May	$t_i > 27.83$	$t_i < 27.83$ and $t_o < 20.83$	N/A
June	$t_i > 28.91$	$t_i < 28.91$ and $t_o < 21.91$	N/A
July	$t_i > 29.49$	$t_i < 29.49$ and $t_o < 22.49$	N/A
August	$t_i > 29.45$	$t_i < 29.45$ and $t_o < 22.45$	N/A
September	$t_i > 28.55$	$t_i < 28.55$ and $t_o < 21.55$	N/A
October	$t_i > 26.77$	$t_i < 26.77$ and $t_o < 19.77$	$t_i < 19.77$
November	N/A	Windows closed the whole time	$t_i < 18.11$
December	N/A	Windows closed the whole time	$t_i < 16.53$

Note t_i : indoor air temperature, t_o : outdoor air temperature, >: greater than, <: less than, N/A: not necessarily applicable.

The result obtained for the base case simulation are analyzed from different perspectives for the comprehensive understanding of the total energy consumption of the model. However, Figure 50 shows the total chiller and heater load by assuming the model is operating the HVAC system fulfilling the 80% thermal acceptance. The figure illustrates that the months of April and October require the least attention in term of heating and cooling mechanical-based equipment. The month of July presents the highest cooling energy loads reaching 27.24 MWh. the line graph also demonstrates that August has fewer chiller loads than July due to the effect of airflow entering rooms. This fact will be discussed in the coming section. On the other hand, January and December present the highest heating loads requirements that needed to achieve thermal comfort zones in winter seasons reaching values of 17.21 MWh and 15.05 MWh, respectively.

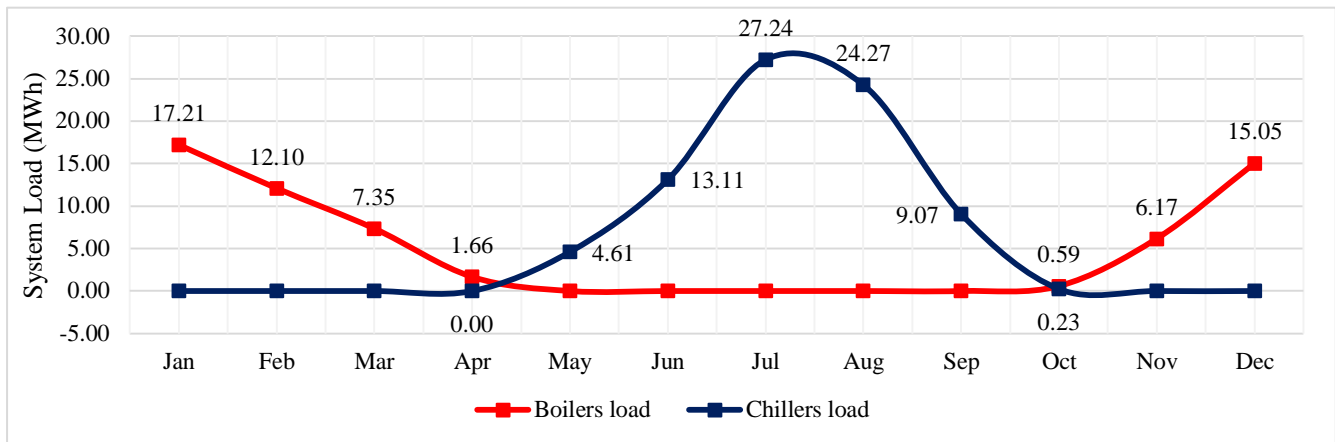


Figure 50: Boiler and chiller systems loads.

Figure 51 shows the total system energy demand of the base case building. These results illustrate the fact that the energy requirements for achieving a thermally comfort zones within the building is significantly noticeable in the winter season, where more focuses must be taken in designing the double skin façade in this season. January and December represent the highest energy demand needed to achieve an 80% thermal acceptability in the building, where the annual energy consumption can reach 19.34MWh and 16.91MWh, respectively. Nevertheless, the cooling energy consumption in summer season is highly influenced by the Seasonal Energy Efficiency Ratio (SEER). This ration indicates the total heat removed by the mean of cooling equipment during the annual cooling-season, expressed by kW/kW, divided by total electrical energy consumed during the same period (AHRI 2012). However, the assigned SEER for the building was assumed to be at a rate of 4.25 kW/kW. This explains the relatively low energy consumption during summer in spite of the higher chiller energy consumption.

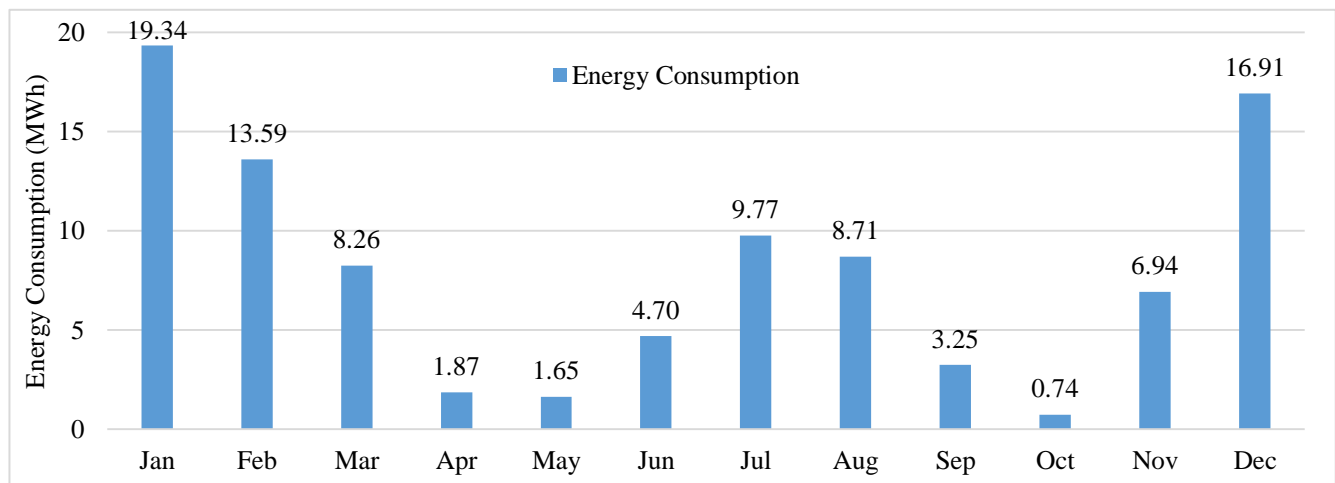


Figure 51: Energy consumption for the base case

5.2 Double skin façade simulation models results

DSF geometries types are presented to demonstrate the individual influence on the thermal performance of the building. Firstly, the obtained results of each model are discussed according to their total impact on the air movement inside the DSF cavity, air flow inside the building, the overall thermal behavior of the building. However, all the assigned thermal conditions, internal heat gain, windows and doors opening profiles, cooling and heating months are the same as defined in the base case model.

For each model, several parameters to be evaluated for a comprehensive understanding and ease comparison to base case model in order to frame the highest possible energy reduction. Variables of the same parameters are presented on the same graph generated from the base case to highlight the relative differences between cases. Variables including; rooms' temperature, cavity temperature, airflow within the cavity, and total system energy consumption. The resulting annual airflow through all windows is demonstrated by using a horizontal bar graph with positive and negatives values, where the positive values present the airflow toward the cavity, while the negative value presents the reverse flows. Moreover, at the end of each section, a summary table will be presented to highlight the most reliable option among others. However, in regards to the façade inlet and outlet opening size and opening schemes, it was assumed that the all inlet vents sizes were fixed at 300mm while the external façade's vent size is equal to the cavity width of the individual façade. However, the profile of the opening of all external windows was set to match the opening criteria defined in the baseline case.

Furthermore, this section will discuss in details the performance of the four geometry types of the DSF. Initially, the best façade performance of each type based on the lowest affords PPD will be chosen for further analysis. Due to the high content of details of describing and analysis of all data of other façade's type, this section will only elaborate results of façade geometry types based on the lowest PPD that the façade of each type according to definitions defined previously in section 4.9.2. The selection of monthly PPD of occupants in each type of the façade based on the overall behavior in which a further façade assessment will focus on one type of each façade's type that can afford the lowest PPD throughout the year. These facades are; multistory type 600mm, shaft type of 900mm cavity, corridor type of 600mm, and box-window type of 300mm.

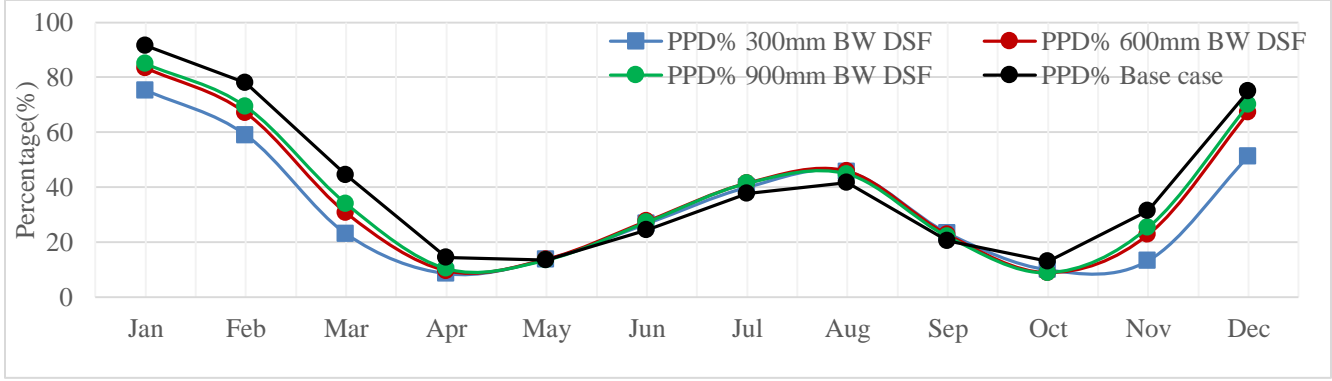
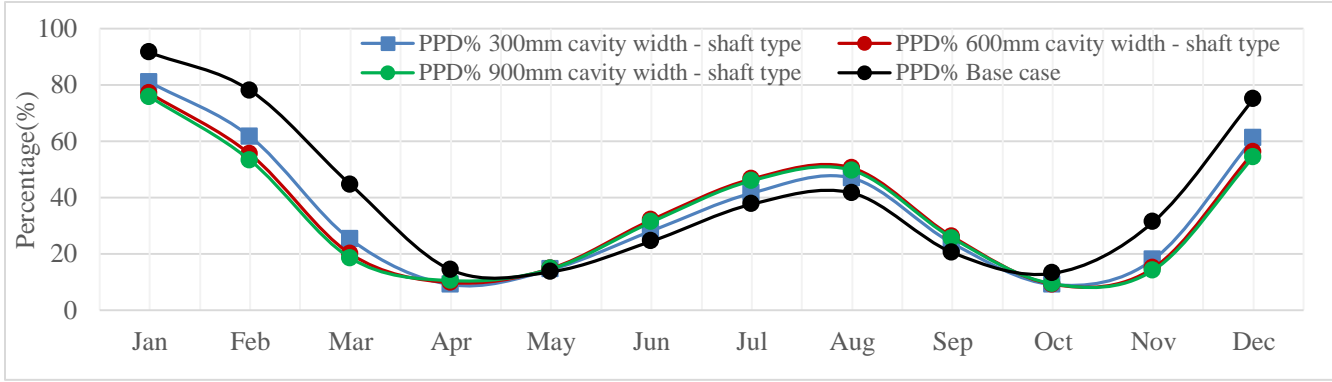
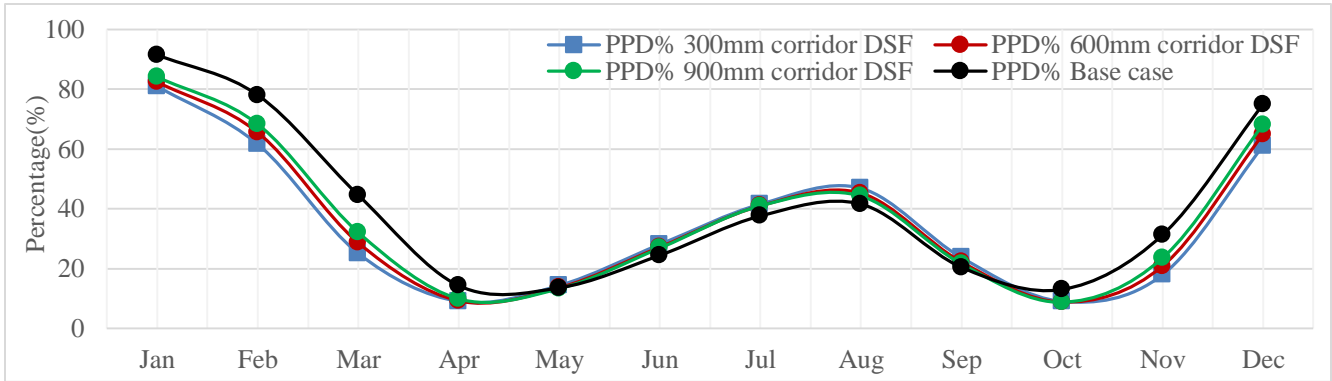
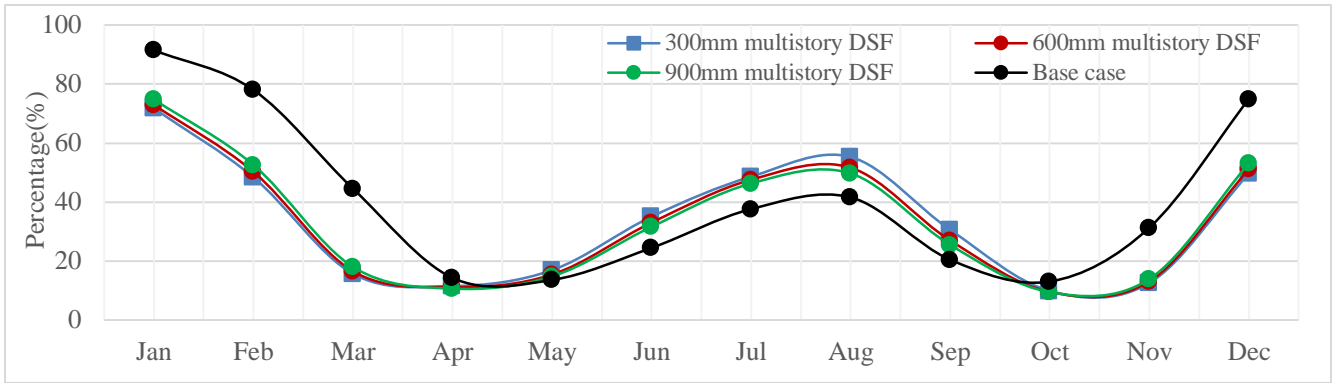
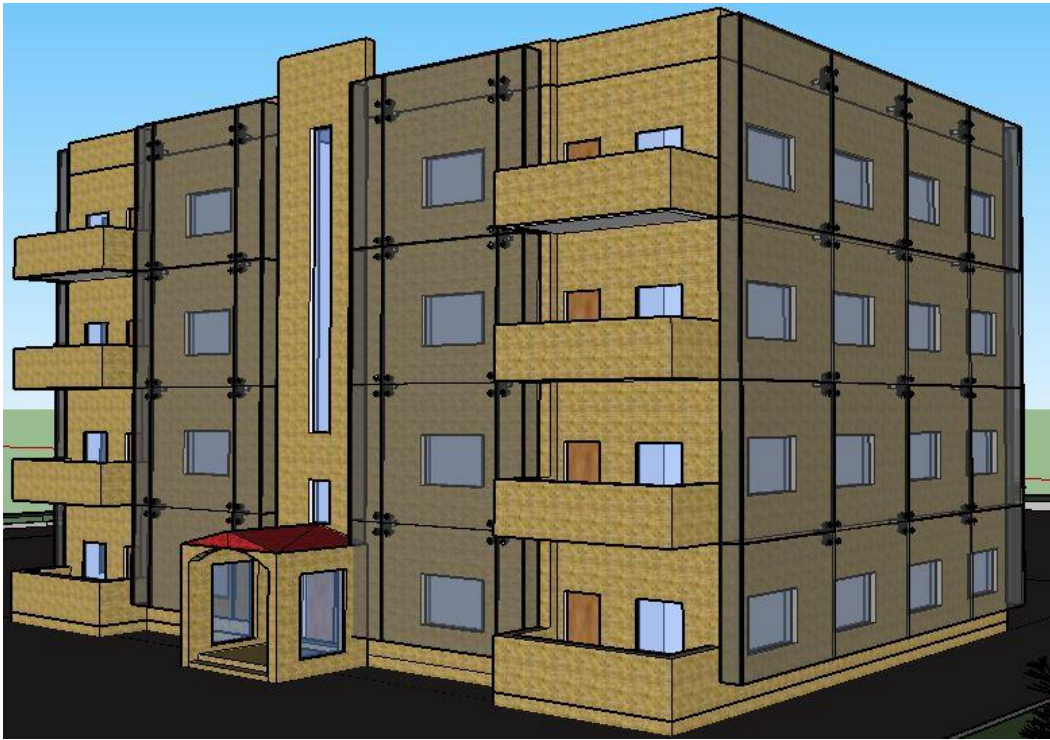
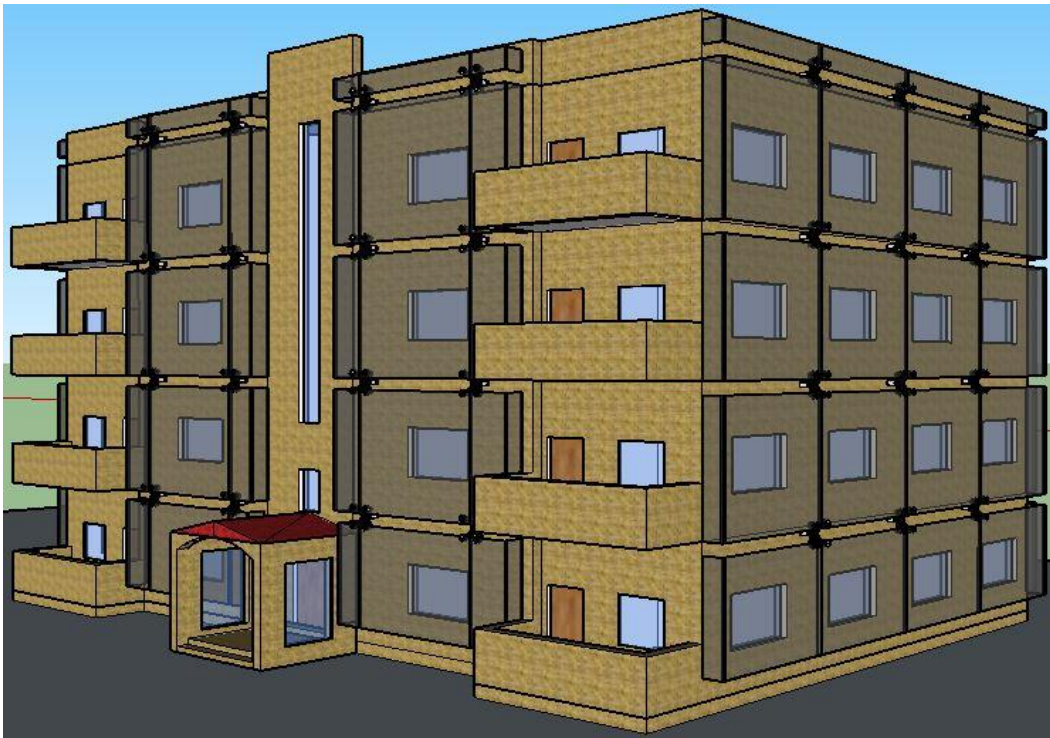


Figure 52: Comparison between base case PPD and other facade's type according to cavity widths



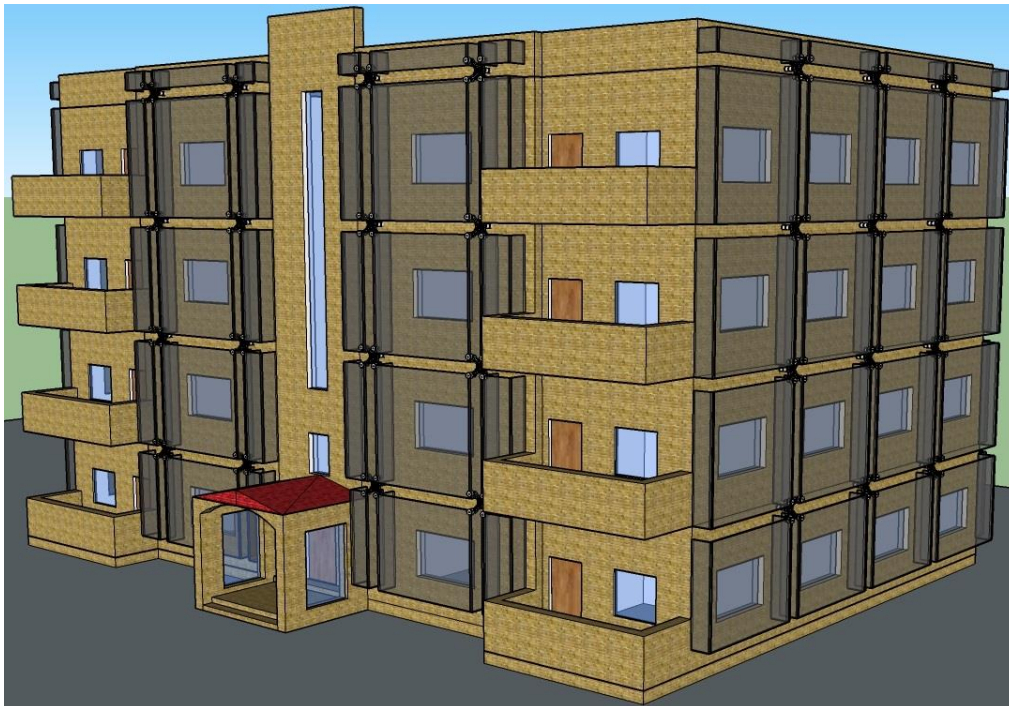
(a)



(b)



(c)



(d)

Figure 53: The development of double skin façade simulation models in Sketchup software: a) Multistory, b) Corridor, c) Shaft, and d) Box-window.

5.2.1 Multistory DSF type 600mm cavity width.

This section will elaborate and test all variables of the multistory DSF in order to achieve the maximum possible energy saving along with the highest occupant’s thermal experience in both cooling and heating months. The results will be compared with results obtained from the base case.

5.2.1.1 Airflow rates and heat gain.

According to the PPD results, the lowest PPD was accommodated in the 600mm multistory type DSF. The airflow rates entering the buildings’ windows through the 600mm Corridor façade type cavity is presented in Figure 54. As expected, the amount of airflow rates entering the windows through the façade’s cavity has fewer rates in comparison to the Base Case during the ventilation months. Table 14 shows the mean monthly net airflows entering the 600mm cavity width multistory DSF building opening during this period. The values indicate that the net average airflows have reduced entering windows through the multistory façade has been reduced by the half.

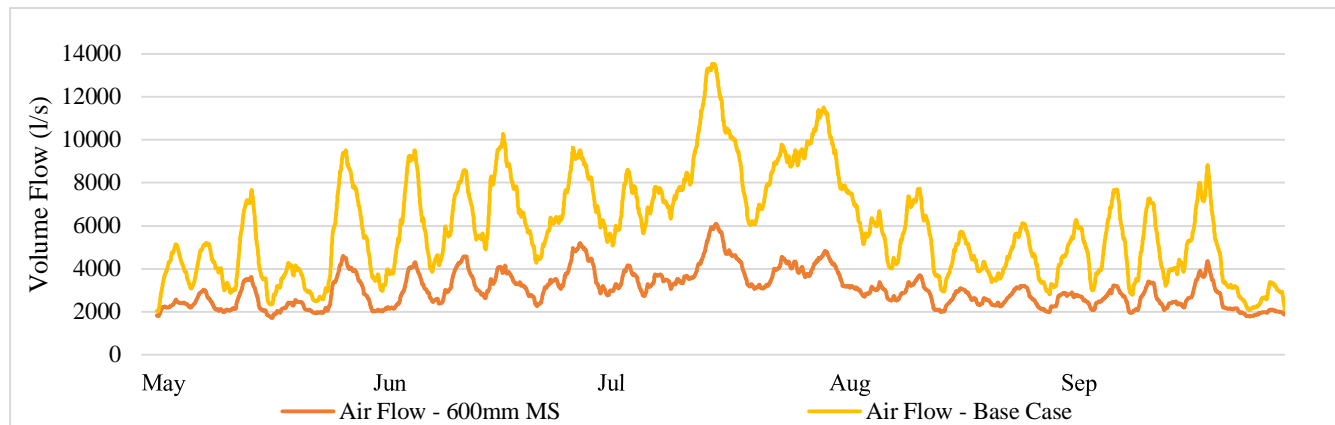


Figure 54: Volume flow rate of air entering the building and multistory DSF building

Table 14: Monthly average of airflow for Multistory and the comparison with base case in the ventilated months

Month	May	June	July	August	September
Airflow Average – Multistory 600mm	2534.29	3374.55	3945.62	2764.11	2508.06
Airflow Average - Base Case	4406.33	6700.16	8670.75	5095.07	4483.51

Specifically, Figure 55 shows the heat gain profile associated with the airflows entering the building spaces over the hottest period from May to September. The simulation results illustrate the potential of the entered air in reducing the excessive indoor heat in the base case has more effect than the multistory case, where the monthly average of the heat gain in the Base Case is -0.269 kW, while the heat gain for the 600mm cavity width multistory type DSF is -0.121 kW . The graph indicates that the airflows of the base case have a better absorption of the gained heat which has better potential to reject the excessive heat.

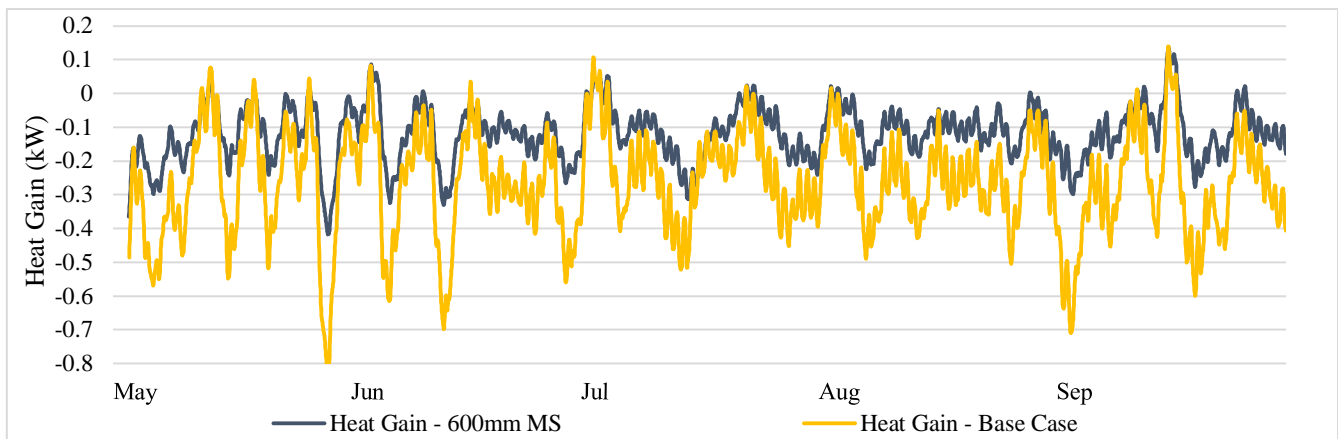


Figure 55: Heat gain through airflow entering windows openings from Multistory 600mm façade's cavity width.

5.2.1.2 Solar Gain

The benefits associated with Double Skin façades is protecting the building against direct solar gain. Proper strategies should be wisely implemented in order to maximize the advantages of reducing the solar gain during summer in lowering the heat gain while to enhance the indoor environment by storing the heat from solar radiation. Figure 56 shows the annual solar heat gain on the external façade of the multistory type DSF building. The diagram shows the massive difference of the annual solar gains between the base case and the Corridor DSF especially in summer season where lowering the solar gain is crucial. The months starting from August until October, the annual solar gain gradually increased in the Base Case while it starts to decrease in this period in case of multistory DSF type. The annual net average solar gain for the base case is 0.135 kW while the solar gain for the 600mm cavity width of the multistory DSF is 0.06 kW with an annual reduction of 44.44%.

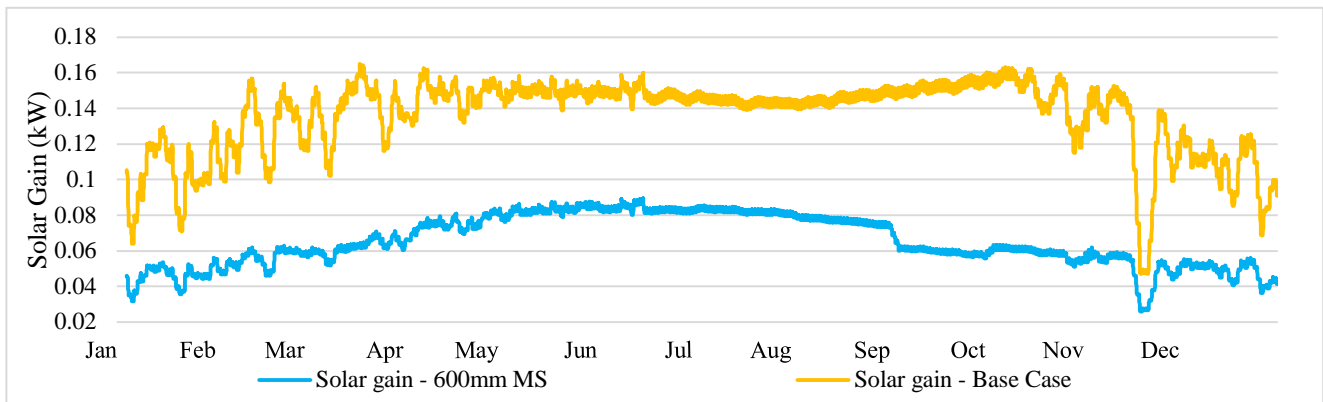


Figure 56: Annual solar gain of the multistory type DSF building

5.2.1.3 Heat gain through conduction

The heat transmitted into the building by the conduction gains through the stored heat within the cavity gain helps in understanding the DSF phenomenon in which the heat gain can be exploited passively in raising the indoor temperatures. However, the risk of overheating issues during the warm sunny days during summer is highly probable in which tend to add extra cooling loads in the building as evidenced in Figure 57. The figure shows the overall conduction heat of the building evaluated for both single and double-skin façade. Passive heat gain through conduction confirms the efficiency of this type of the DSF in regard to the energy savings is guaranteed during winter, while the excessive overheating as caused in May and June is not predictable. The annual average conduction heat gain of the 600mm cavity width of the multistory DSF is 0.036 kW, while the base case annual conduction gain was -0.047 kW.

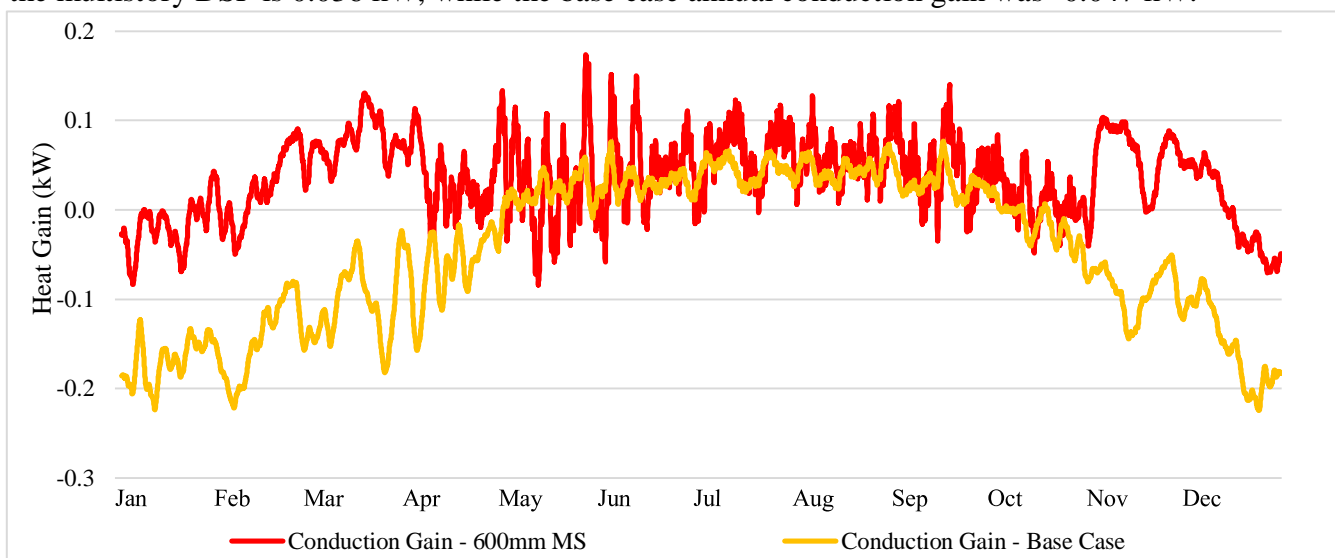


Figure 57: Conduction gain through external walls of the multistory DSF type building

5.2.2 Corridor DSF 600mm cavity width

5.2.2.1 Airflow rates and heat gain

According to the PPD results, the lowest PPD was accommodated in the 600mm corridor type. The airflow rates entering the buildings' windows through the 600mm Corridor façade type cavity is presented in Figure 58. As expected, the amount of airflow rates entering the windows through the façade's cavity has fewer rates in comparison to the Base Case during the ventilation months. Table 15 shows the mean monthly net airflows entering the 600mm cavity width Corridor DSF building opening during this period. The values indicate that the net average airflows have reduced entering windows through the Corridor façade has been reduced more than the half.

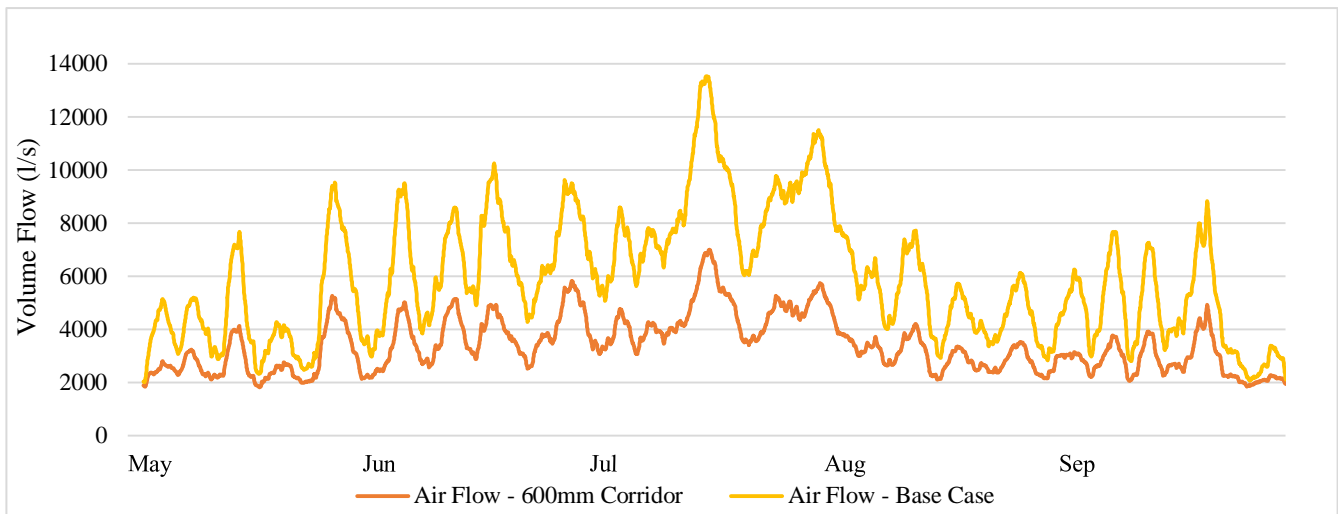


Figure 58: Volume flow rate of air entering the building and corridor DSF building

Table 15: Monthly average of airflow for Multistory and the comparison with the base case in the ventilated months

Month	May	June	July	August	September
Airflow Average – Corridor 600mm	2760.97	3826.56	4572.50	3028.48	2748.41
Airflow Average - Base Case	4406.33	6700.16	8670.75	5095.07	4483.51

Specifically, Figure 59 shows the heat gain profile associated with the airflows entering the building spaces over the hottest period from May to September. The simulation results illustrate the potential of the entered air in reducing the excessive indoor heat in the Base Case has more effect than the Corridor case, where the monthly average of the heat gain in the Base Case is -0.269 kW, while the heat gain for

the 600mm cavity width Corridor type DSF is -0.160 kW. The graph indicates that the airflows of the base case have a better absorption the gained heat which has better potential to reject the excessive heat.

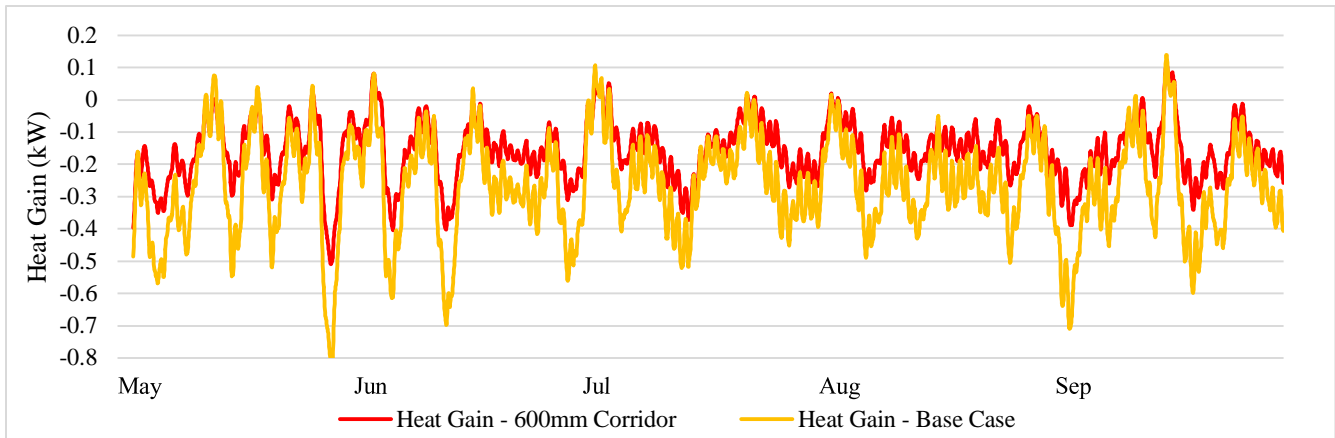


Figure 59: Heat gain through airflow entering windows openings from corridor 600mm façade’s cavity width

5.2.2.2 Solar Gain

The benefits associated with Double Skin façades is protecting the building against direct solar gain. Proper strategies should be wisely implemented in order to maximize the advantages of reducing the solar gain during summer in lowering the heat gain while to enhance the indoor environment by storing the heat from solar radiation. Figure 60 shows the annual solar heat gain on the external façade of the Corridor DSF building. The diagram shows the massive difference of the annual solar gains between the base case and the Corridor DSF especially in summer season where lowering the solar gain is crucial. The annual net average solar gain for the base case is 0.135 kW while the solar gain for the 600mm cavity width of the Corridor DSF is 0.059 kW with an annual reduction of 44.44%.

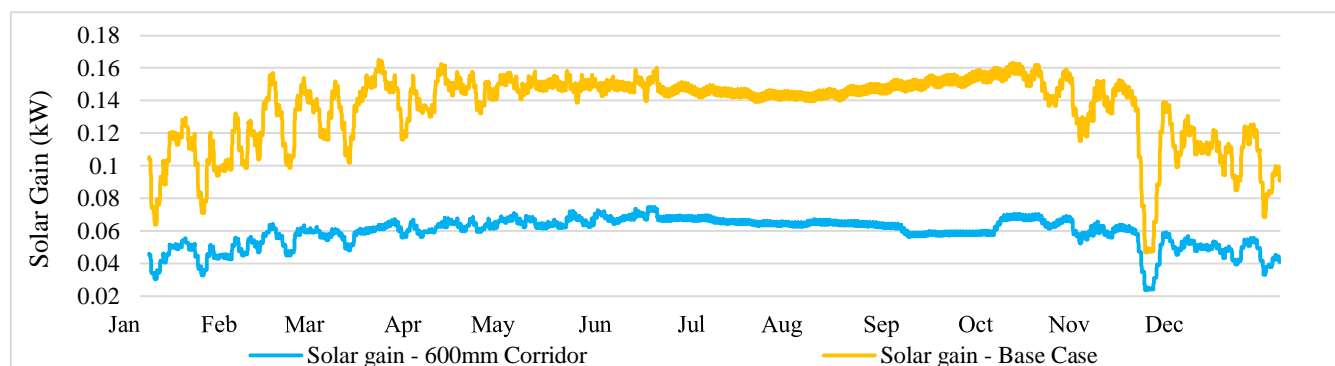


Figure 60: Annual solar gain of the corridor type DSF building

5.2.2.3 Heat gain through conduction.

The heat transmitted into the building by the conduction gains through the stored heat within the cavity gain helps in understanding the DSF phenomenon in which the heat gain can be exploited passively in raising the indoor temperatures. However, the risk of overheating issues during the warm sunny days during summer is highly probable in which tend to add extra cooling loads in the building as evidenced in Figure 61. The figure confirmed that the Double-skin façade buildings have a better thermal behavior during the winter seasons in which an energy saving is guaranteed. However, the annual average heat gain of the 600mm cavity width Corridor DSF is 0.0149 kW, while the base case annual conduction gain was -0.047 kW.

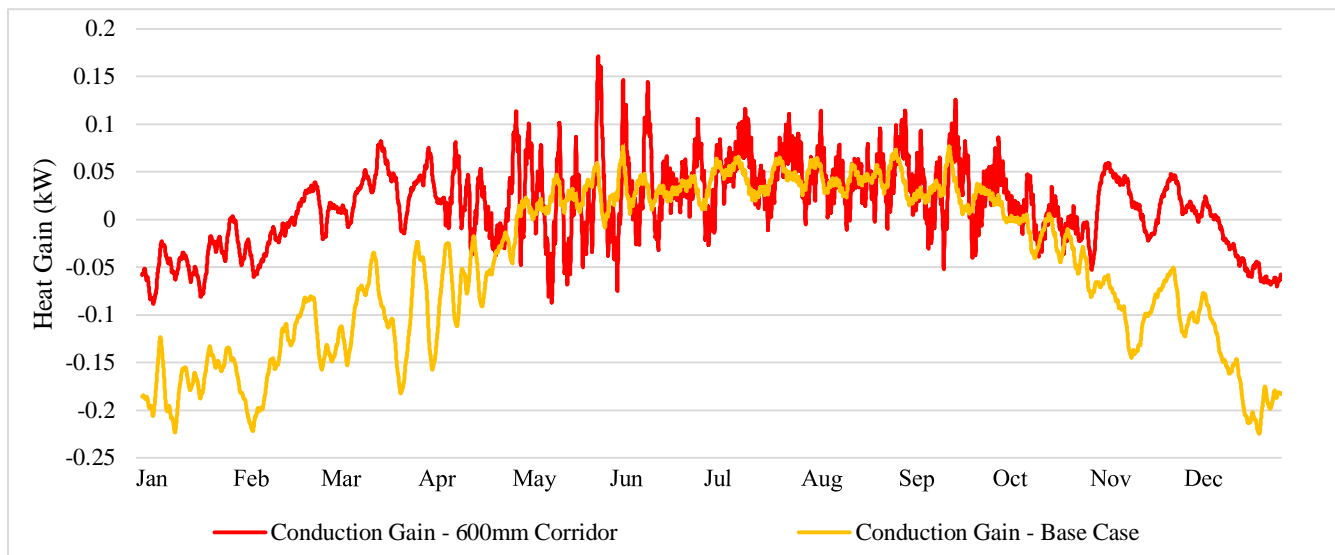


Figure 61: Conduction gain through externa walls of the corridor DSF type building

5.2.3 Shaft DSF 900mm cavity width

5.2.3.1 Airflow rates and heat gain.

According to the PPD results, the lowest PPD was accommodated in the 900mm shaft type. The airflow rates entering the buildings' windows through the 900mm Shaft façade type cavity is presented in Figure 62. As expected, the airflow rates entering the windows through the façade's cavity has dramatically reduced in comparison to the Base Case, because the airflow rates inside the façade channels were initially reduced.

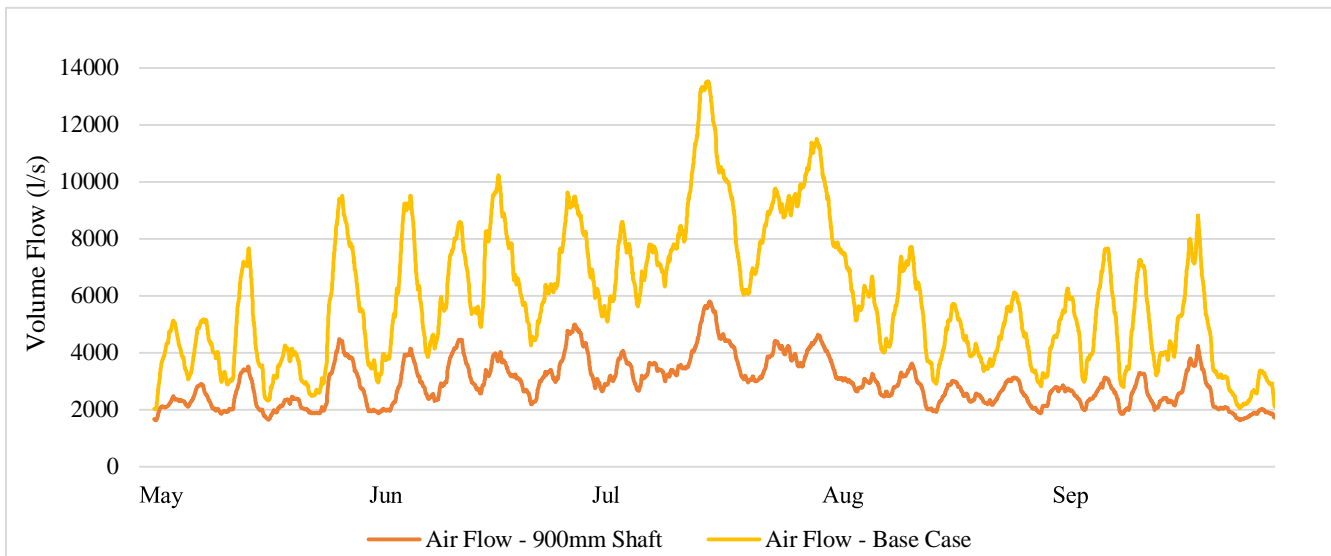


Figure 62: Volume flow rate of air entering the building and shaft DSF building

Table 16 shows the mean monthly net airflows entering the building’s opening during the ventilation period. The values indicate that the net average airflows have reduced entering windows through the Shaft façade has been reduced by the half. Furthermore, the 900mm cavity width Shaft DSF has witnessed the highest rate of airflows.

Table 16: Monthly average of airflow for Multistory and the comparison with the base case in the ventilated months

Month	May	June	July	August	September
Airflow Average - 900mm - Shaft	2450.43	3263.43	3823.54	2693.85	2423.479
Airflow Average - Base Case	4406.33	6700.16	8670.75	5095.07	4483.51

Specifically, Figure 63 shows the heat gain profile associated with the airflows entering the building spaces over the hottest period from May to September. The simulation results illustrate the potential of the entered air in reducing the excessive indoor heat in the Base Case has more effect than the Shaft case, where the monthly average of the heat gain in the Base Case is -0.269 kW, while the heat gain for the 900mm cavity width Shaft type DSF is -0.1130 kW. The negative sign indicates the ability of the entered airflow to eliminating or rejecting the heat inside the spaces.

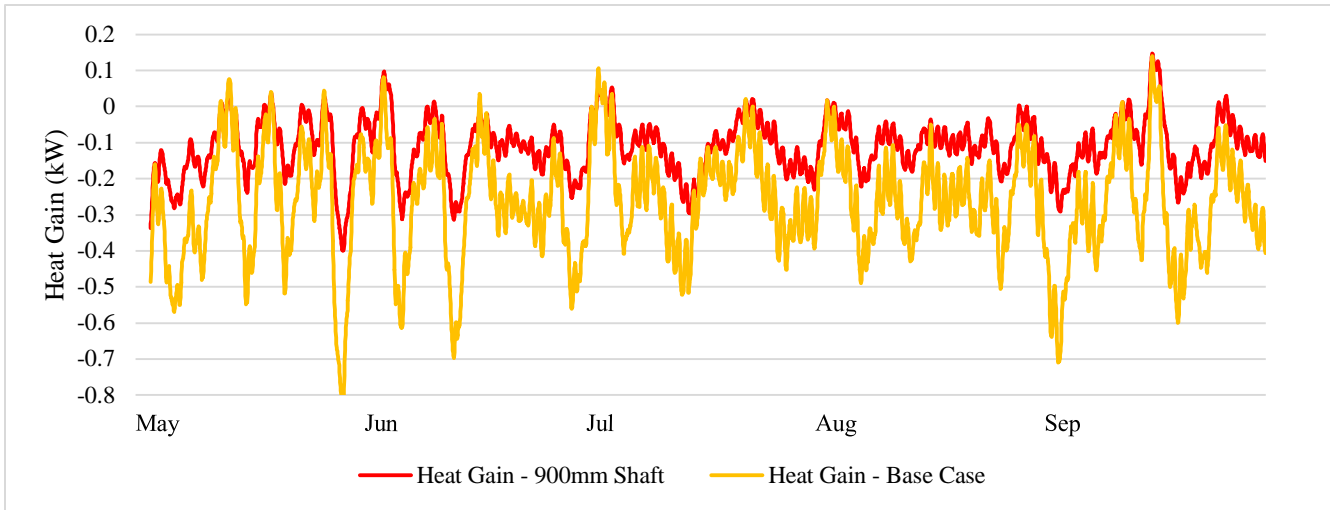


Figure 63: Heat gain through airflow entering windows openings from shaft 900mm façade’s cavity width

5.2.3.2 Solar Gain

The benefits associated with Double Skin façades is protecting the building against direct solar gain. Proper strategies should be wisely implemented in order to maximize the advantages of reducing the solar gain during summer in lowering the heat gain while to enhance the indoor environment by storing the heat from solar radiation. Figure 64 shows the annual solar heat gain on the external façade of the Shaft DSF building. The diagram shows the massive difference between the annual solar gains between the base case and the Shaft DSF. The annual net average solar gain for the base case is 0.135 kW while the solar gain for the 900mm cavity width of the Shaft DSF is 0.0559 kW with an annual reduction of 41.41%.

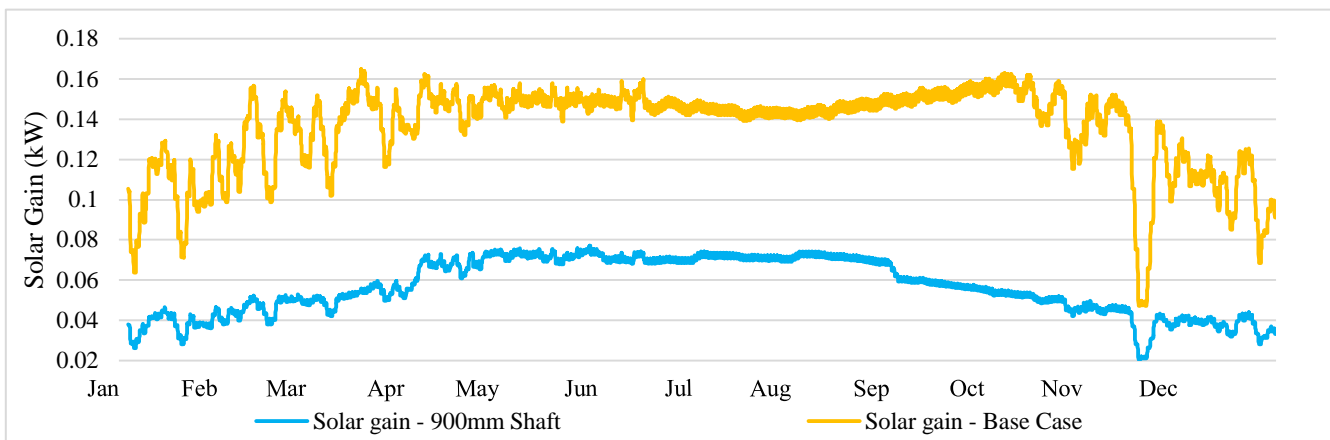


Figure 64: Annual solar gain of the shaft type DSF building

5.2.3.3 Heat gain through conduction.

The heat transmitted into the building by the conduction gains through the stored heat within the cavity gain helps in understanding the DSF phenomenon in which the heat gain can be exploited passively in raising the indoor temperatures. However, the risk of overheating issues during the warm sunny days during summer is highly probable in which tend to add extra cooling loads in the building as evidenced in Figure 65. The figure confirmed that the Double-skin façade buildings have a better thermal behavior during the winter seasons in which an energy saving is guaranteed. However, the annual average heat gain of the 900mm cavity width Shaft DSF is 0.0311 kW, while the base case annual conduction gain was -0.047 kW.

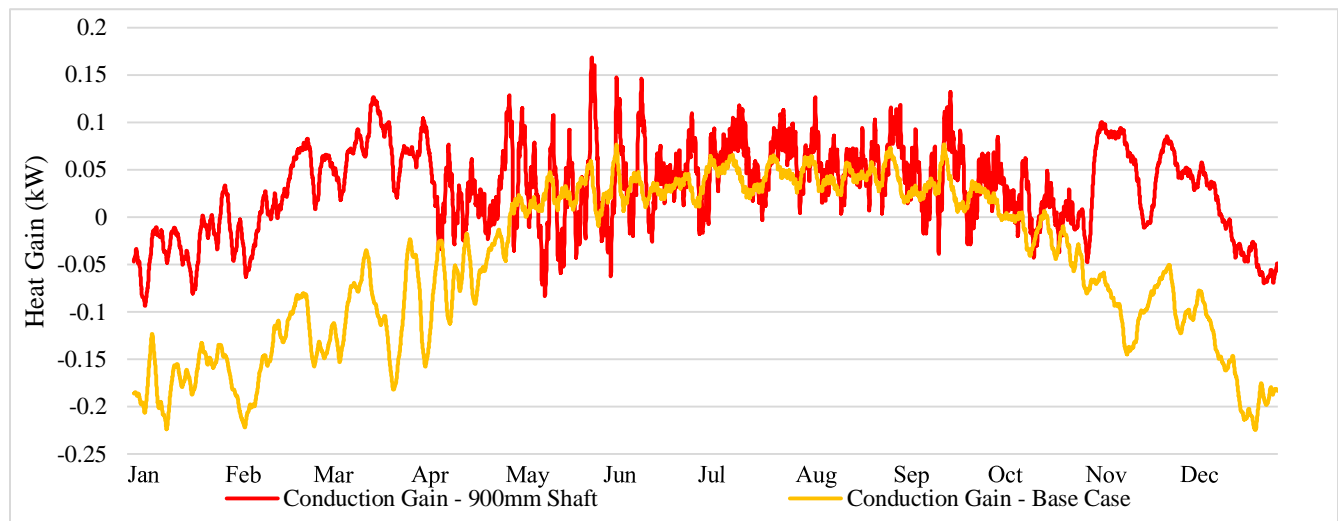


Figure 65: Conduction gain through externa walls of the shaft DSF type building

5.2.4 Box-window DSF 300mm cavity width

5.2.4.1 Airflow rates and heat gain.

According to the PPD results, the lowest PPD was accommodated in the 300mm Box-window type. The airflow rates entering the buildings' windows through the 300mm Box-window façade type cavity is presented in Figure 66. As expected, the airflow rates entering the windows through the façade's cavity has dramatically reduced in comparison to the Base Case, because the airflow rates inside the façade channels were initially reduced.

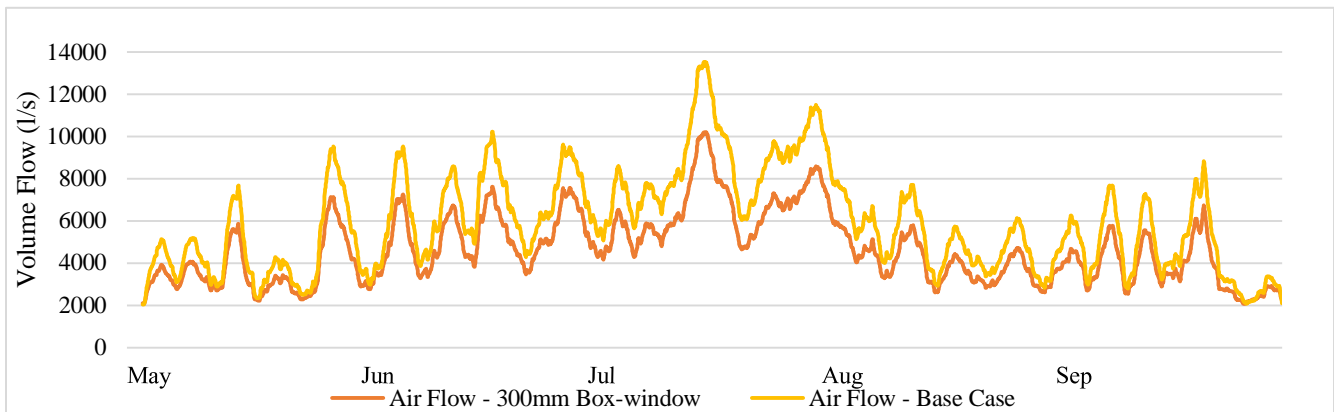


Figure 66: Volume flow rate of air entering the building and box-window DSF building

Table 17 shows the mean monthly net airflows entering the building’s opening during the ventilation period. The values indicate that the net average airflows have reduced entering windows through the Box-window façade has been reduced by the half. Furthermore, the 300mm cavity width Box-window DSF has witnessed the highest rate of airflows.

Table 17: Monthly average of airflow for box-window and the comparison with the base case in the ventilated months

Month	May	June	July	August	September
Airflow Average - 300mm - BW	3588.88	5265.96	6567.74	4017.70	3652.161
Airflow Average - Base Case	4406.33	6700.16	8670.75	5095.07	4483.51

Specifically, Figure 67 shows the heat gain profile associated with the airflows entering the building spaces over the hottest period from May to September. The simulation results illustrate the potential of the entered air in reducing the excessive indoor heat in the Base Case has more effect than the Box-window case, where the monthly average of the heat gain in the Base Case is -0.269 kW, while the heat gain for the 300mm cavity width Box-window type DSF is -0.183 kW. The negative sign indicates the ability of the entered airflow to eliminating or reject the heat inside the spaces.

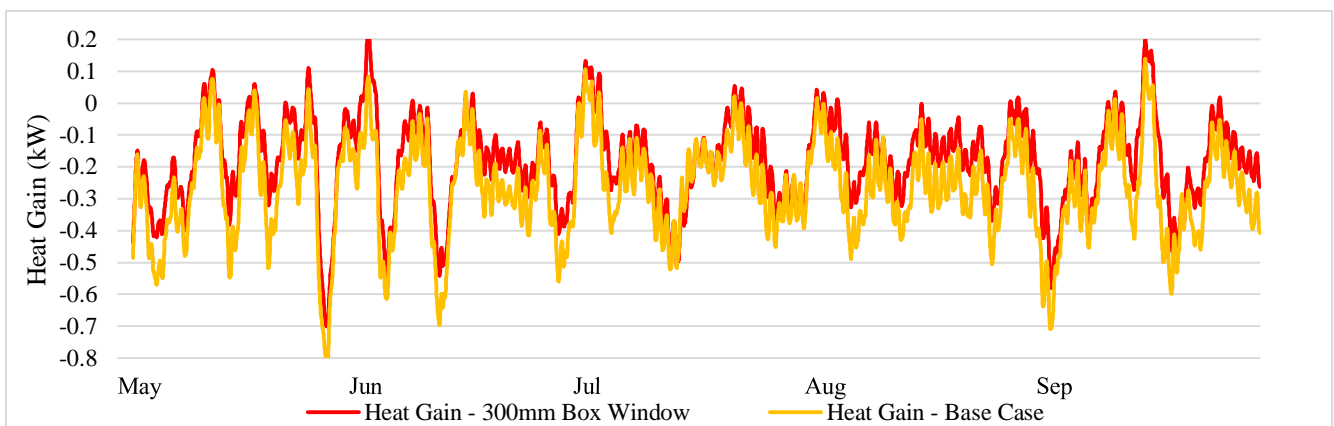


Figure 67: Heat gain through airflow entering windows openings from box-window 300mm façade’s cavity width

5.2.4.2 Solar Gain

The benefits associated with Double Skin façades is protecting the building against direct solar gain. Proper strategies should be wisely implemented in order to maximize the advantages of reducing the solar gain during summer in lowering the heat gain while to enhance the indoor environment by storing the heat from solar radiation. Figure 68 shows the annual solar heat gain on the external façade of the box-window DSF building. The diagram shows the massive difference between the annual solar gains between the base case and the Box-window DSF. The annual net average solar gain for the base case is 0.135 kW while the solar gain for the 300mm cavity width of the Box-window DSF is 0.0693 kW with an annual reduction of 51.33%.

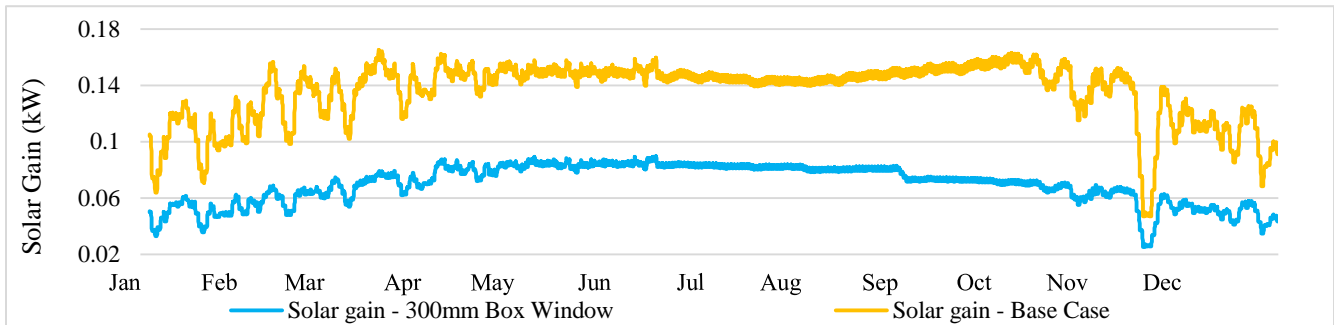


Figure 68: Annual solar gain of the box-window type DSF building

5.2.4.3 Heat gain through conduction.

However, the risk of overheating issues during the warm sunny days during summer is highly probable in which tend to add extra cooling loads in the building as evidenced in Figure 69. The figure confirmed that the Double-skin façade buildings have a better thermal behavior during the winter seasons in which an energy saving is guaranteed. However, the annual average heat gain of the 300mm cavity width Box-window DSF is 0.0262 kW, while the base case annual conduction gain was -0.047 kW.

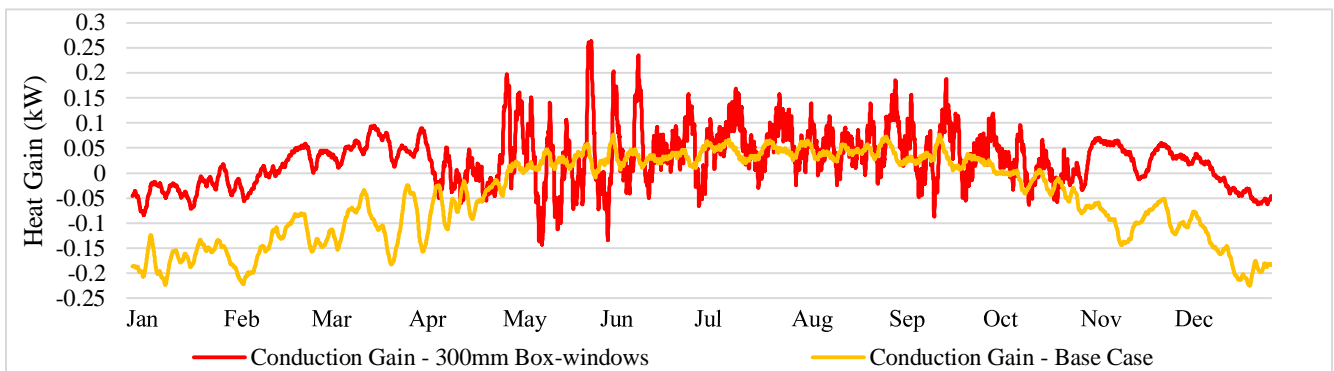


Figure 69: Conduction gain through external walls of the box-window DSF type building

6.0 Discussion

This section presents a summary of the study results and compares all findings to conclude with the most appropriate Double-Skin Façade geometry type that provides a maximum energy efficiency of the building in term of space heating and cooling reduction while maintaining the thermal comfort acceptance within 80%.

The study has shown a comprehensive level of comparison of various geometry types of the double skin façade; multistory, corridor, shaft, and box-window and different types of the path of the airflow in the cavity widths; 30mm, 60mm, and 900mm. In a total of 35 simulations were conducted to a Base Model located in Irbid, Jordan to investigate the thermal performance of the different configuration of the double-skin façade.

All the simulations were made based on that the building is totally covered with the DSF for all directions. Several hypotheses including the geometry type, cavity width, properties of glazing, and the airflow within the cavity then are evaluated for a comprehensive understanding of the performance of each component. The results are then presented in a three-dimensional perspective including the heating loads, cooling loads, and thermal satisfaction of occupants. As the main goal of these simulations is to evaluate whether the different types of DSFs can be translated into an energy saving solution, the heat transfer through the DSF is investigated in different scales. In order to simplify the Base Case mode, increase the speed of the entire simulation process, and decreasing the possibility of miscalculations in the software, the 4th floor was chosen as the area of study assuming that the last floor of the building has the highest influencing by the outer environment.

In the simulation where the HVAC systems were active, the temperature setpoints for heating and cooling was varied according to the indoor conditions in each month per the DSF geometry type per cavity width.

6.1 Thermal behavior of the double skin façade.

6.1.1 Cavity air temperature

The annual average cavity air temperature for all the selected DSF geometry types are presented in Figure 70. As expected, the average cavity temperatures during winters soared significantly in comparison to the outdoor air temperature. This is because that the solar radiation passing through the sealed façade's allows the air within the cavity to be warm. Furthermore, the Shaft 900mm and Multistory600mm which

are acting similar performance during winters in storing the radiation heat, they are preserving the highest air temperature of the cavity, approximately 92.89%, and 96.67%, respectively. This is because of their façade's geometry type in which thermal buoyancy effect produced by the dominant driven force caused by the air pressure differences in the cavity. Although the Corridor 600mm which has cavity air temperature higher by 71.52% than the outdoor air temperature, has the least ability to preserve hot air inside the cavity. Moreover, the Box-window DSF has an annual average cavity temperature higher than the outdoor air temperature by 86.93%.

In summer, the annual peak cavity air temperature of all façade showed very similar values to the average outdoor air temperatures. The average increase percentages registered as mere as 2.02% in Corridor 600mm, 2.45% in Box-window 300mm, while a slight rise in the temperature observed in both Multistory 600mm and Shaft 900mm cases representing a percentage of 5.61% and 5.44%, respectively.

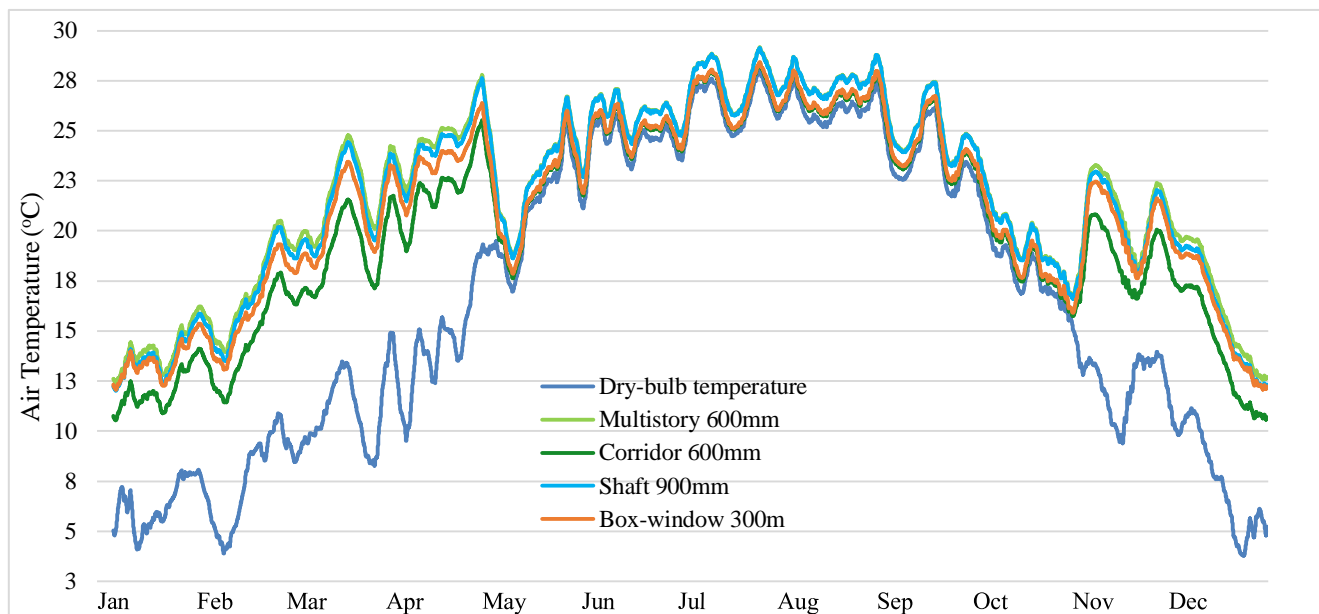


Figure 70: Annual average dry-bulb temperature vs the annual average cavity air temperature for each DSF geometry type according to the lowest PPD

Figure 72 showed that average airflow volume passing through the cavity of each façade during the cooling months. As shown, the big difference in the entering air inside the cavity for every façade despite the common outdoor boundary conditions. The Multistory and Shaft DSF are handling similar airflow within the cavity with a range oscillated between 4000 l/s to 6000 l/s, while a Corridor and the Box-window DSF are allowing a massive amount of airflows to be entering the cavity with ranges fluctuates

between 9000 l/s to 25000 l/s. However, it is interesting to note that during the cooling months, the maximum airflow is passing through the cavity, the lowest cavity air temperature is acquired. As mentioned earlier, July is the only month in which the highest flow rate in the cavity is achieved.

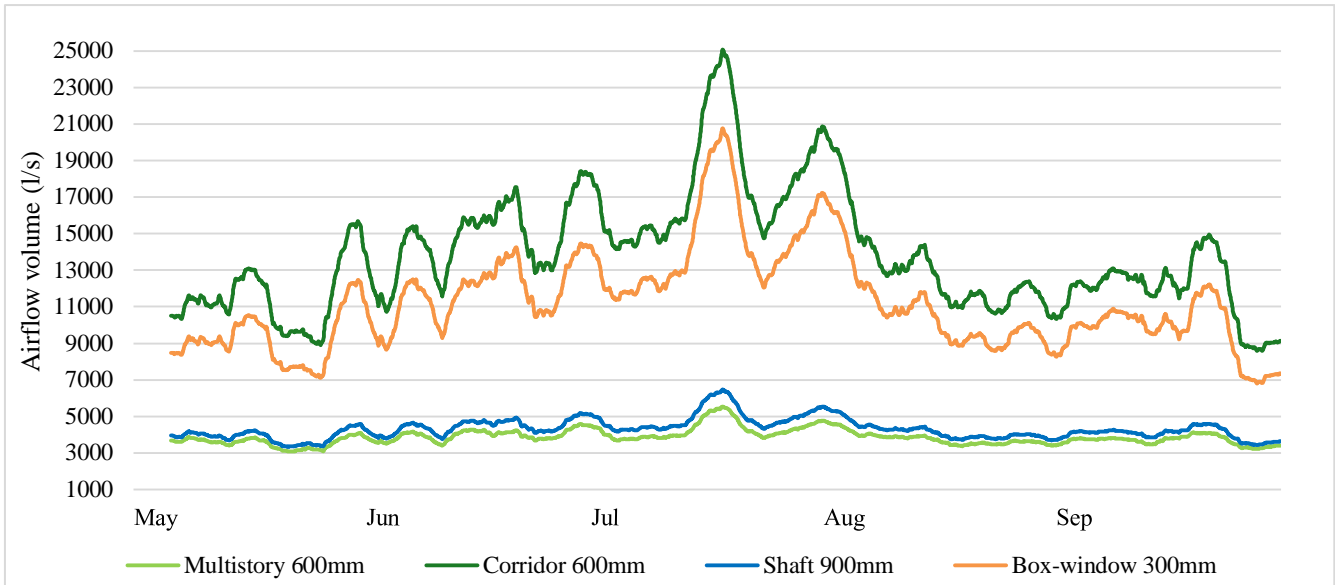


Figure 72: Average airflow inside the facade's cavity during the cooling months.

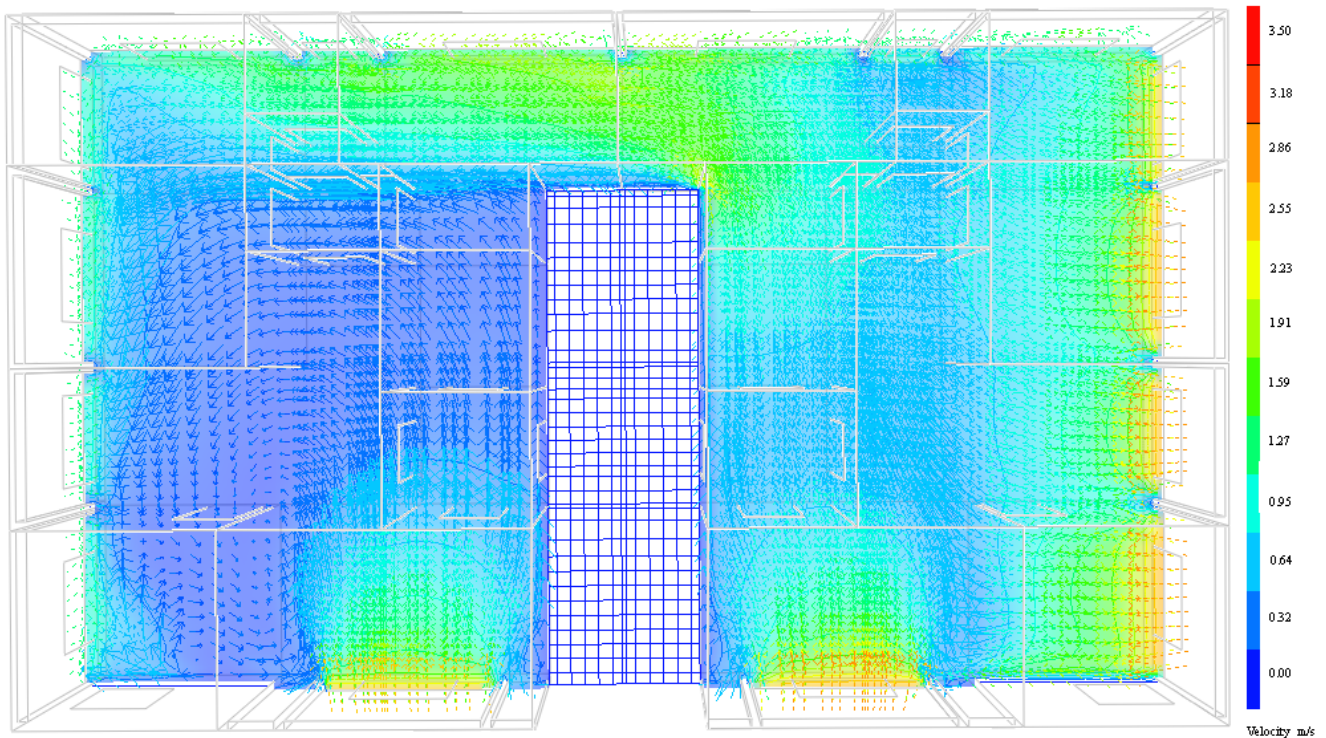


Figure 71: CFD image for the airflow velocity entering the external windows after utilizing the box-window DSF.

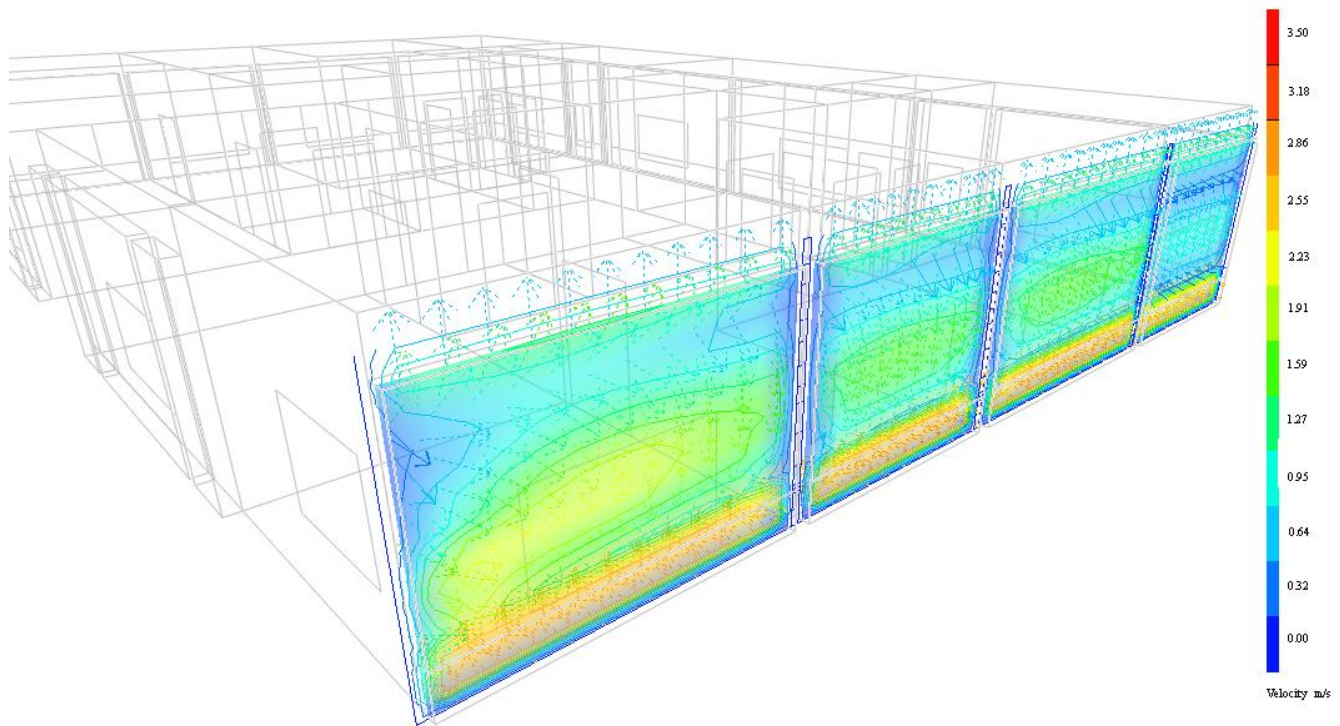


Figure 73: Velocity contour of the magnitude (m/s) of airflow entering the box-window DSF cavity

6.2 Thermal behavior of internal spaces.

The airflow rates and the temperature distributions are the most factors that affecting the performance of the DSF building. Thus, the comparison among all tested variables has been conducted based on results that the hottest month is July where temperatures could reach up to 38°C whereas the coldest month is January where the minimum temperature could drop to -6°C. For the month of August and September, the temperature might also raise to 40°C and 43.4°C. The selection of the double skin façade would be based on the lowest PPD on each case obtained in the previous section. For maximum benefit of achieving a well-designed DSF, comparisons of the various types of DSF will be carried out on the coldest winter day which is on 10 of January when outside temperature is -6°C at 5:00 A.M, and on the hottest summer day on 1 of July when the outside temperature raised to 38°C at noon 12:00 P.M. The annual relationship between the outdoor air temperature vs the average room air temperature are presented in Figure 74. The figure illustrated the indoor air temperature in all cases are higher than the outdoor air temperature which it could be beneficial during the winter season in lowering the demand for heating loads. In the summer season, where the indoor air temperatures in all DSF cases are higher than the outdoor air temperature as well as the temperatures in the Base Case, chances of overheating causing

thermal discomfort and increasing the cooling loads are expected. The schematic diagram demonstrates the complex thermal behavior of each type of the façade during the year where each type performed based on their glazing characteristics as well as the mechanism of the airflow within the cavity. As shown, the annual thermal behavior of indoor spaces air temperature in Multistory and Shaft DSFs are always the highest during all seasons despite the airflow movement inside the opened cavity during summer. However, the Corridor and the Box-windows showed a different scenario, where the Box-window is the warmer than the Corridor, but the opposite is true in case the cavity of the façade is opened, the Box-window become the colder. The figure also stated that indoor room’s temperature experiencing a drop

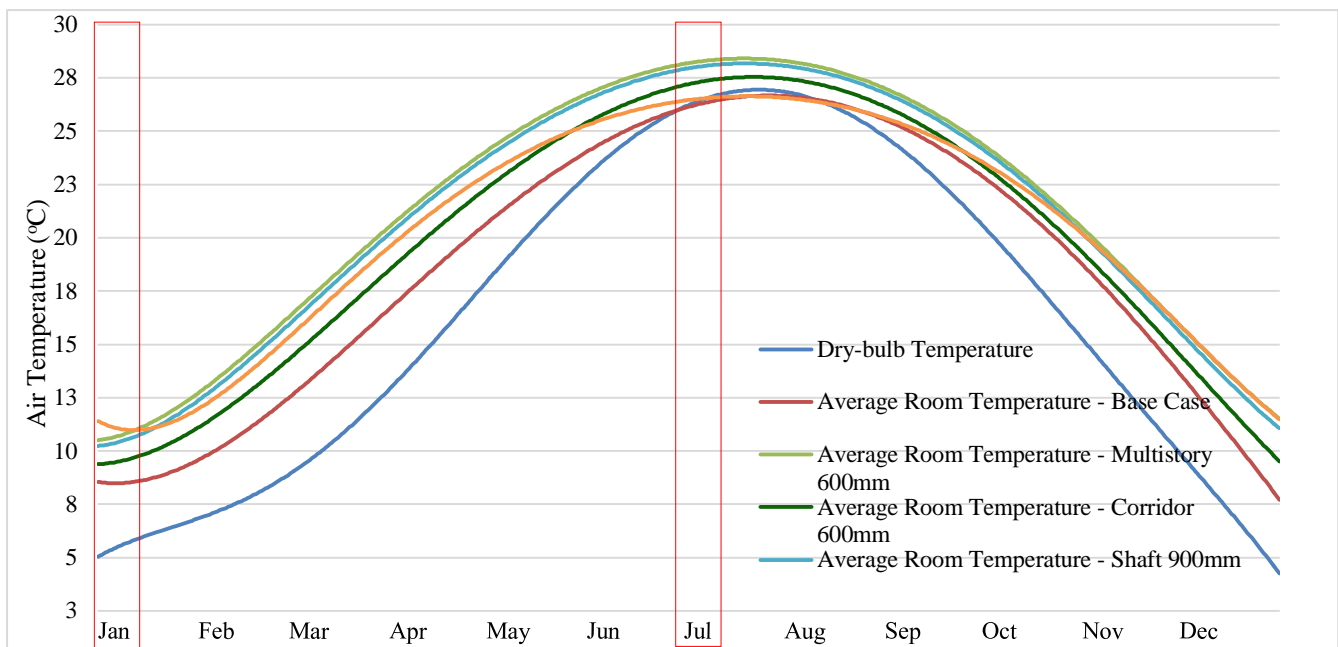


Figure 74: Annual comparison between the indoor air temperature of the Base Case and after utilizing various type of DSF with the outdoor air temperature. Red rectangles indicate the period selected for the hottest and coldest week.

in temperature in comparison with the outdoor air temperature through the Box-window DSF.

6.2.1 Average behavior in summer

6.2.1.1 Indoor air temperature

Figure 75 shows the air temperature and the solar direct irradiance on a horizontal surface from May 1st to September 30th. In this period is considered the hottest during the year, where the all the simulation results indicated the prerequisite of the façade’s cavity to be opened in this particular period. The average temperature of the period was 24.35°C. The figure also demonstrated that this period includes a day with

high direct solar irradiance that can reach sometimes 1000 W/m². The mean daily solar irradiance for the period from May to September on the horizontal surface is 314.23 W/m².

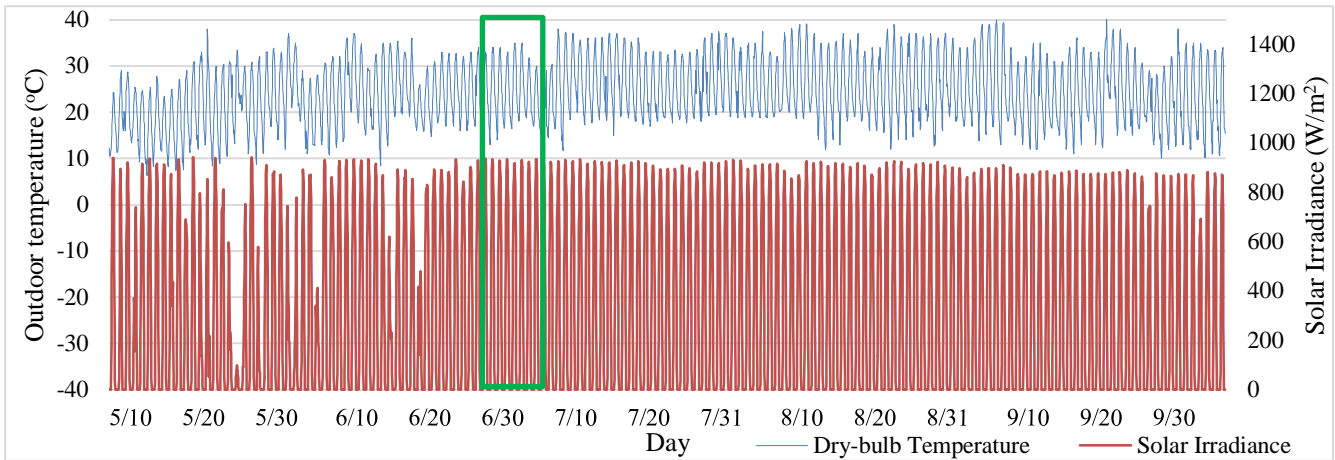


Figure 75: Air temperature and solar direct irradiance on horizontal surface for the period from May 1st to September 30th. The rectangle indicates the week selected for the detailed analysis.

Figure 76 shows the comparison between average indoor air temperature according to the façade geometry and the base case with the outdoor air temperature assuming that no HVAC equipment is running. For instance, the building room temperature with Multistory and Shaft cases registered the highest in this period in comparison to temperatures associated with the Corridor and Box-windows geometry types. Furthermore, both Corridor and Box-windows initially had similar performance (May) and then starting from June to September, the box-window registered lower indoor air temperature due

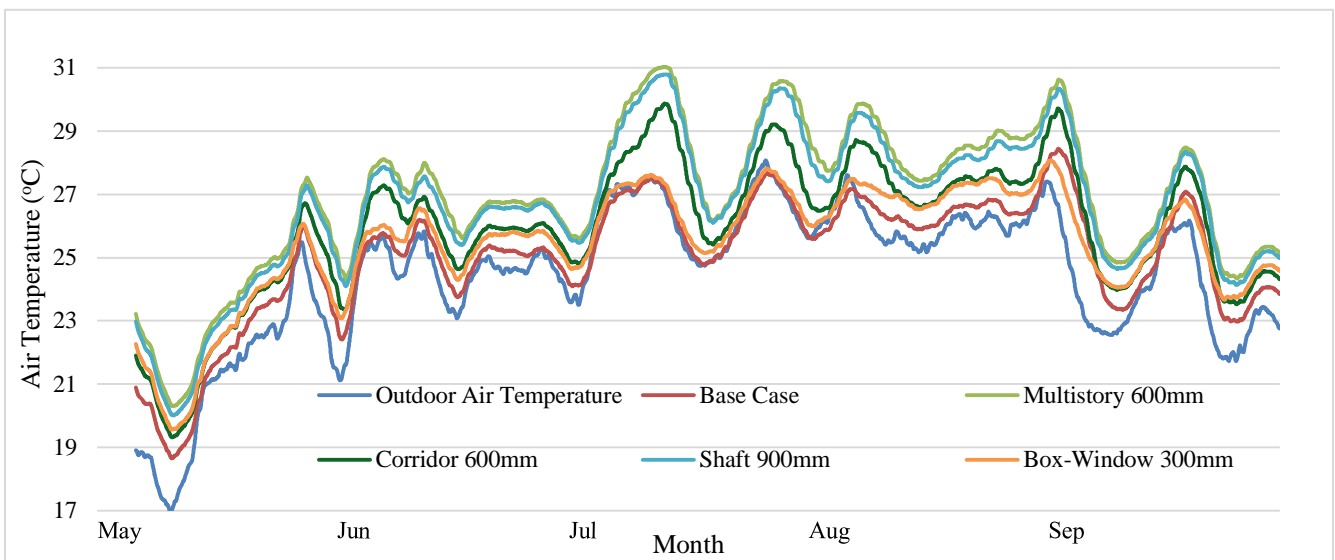


Figure 76: Indoor air temperature for the period from May 1st to September 30th.

As mentioned earlier, the hottest day (July 1st) is included in this period. The relatively high temperature caused due to the usual predominance of clear sky with intensive solar radiation. A detailed assessing will be conducted for a week interval started from June 28th to July 4th (as shown in Figure 77) in which this period was selected because it included seven sunny days that are typical of the cooling period. The average air temperature for the selected week is 25.22°C and the mean daily solar irradiance is 355.14W/m² representing values higher than the summer average values by 3.57% and 12.99% respectively.

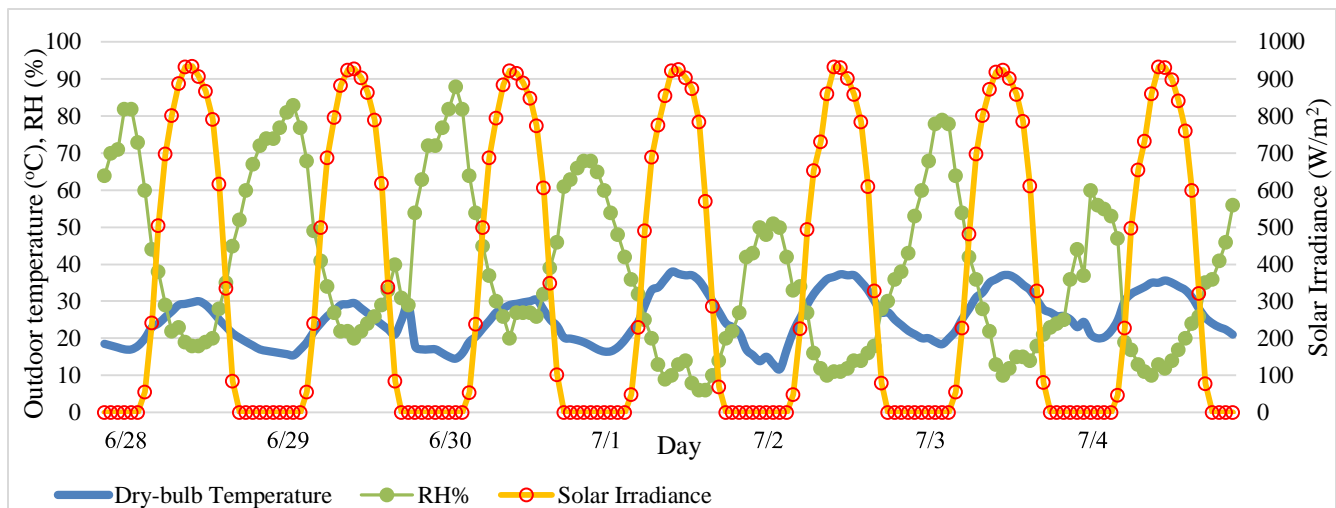


Figure 77: Outdoor air temperature, relative humidity, and solar irradiance on horizontal surface for the period between June 28th and July 4th

Figure 78 illustrates the variation of the thermal behavior of all indoor spaces after utilizing the DSF for the period from June 28th to July 4th. The average outdoor air temperature in this period was 25.22°C. Comparing the indoor thermal behavior before and after the peak day indicates the efficiency of each system. As shown prior to the peak day (July 1st), all indoor thermal behavior was followed the outdoor conditions, as the latter decreases, the former decreases. In particular, the indoor air temperature started to increase in conjunction with the jumped outdoor temperature, where they exceeded the outdoor air temperature as illustrated in Multistory and Shaft cases, while the raising in temperature remains lower than the outdoor air temperature in Corridor and Box-windows cases. However, the indoor air temperature in Multistory, Shaft, and Corridor cases kept escalating higher than the outdoor air temperature after the peak day, while on contrast, the indoor air temperature in case of Box-window DSF has descending despite the remained higher outdoor temperature. Overall, the Box-window DSF seems to be the best façade’s performance in term of releasing heat during summer. It worth to conclude, that

the building with Box-window DSF has the lowest indoor air temperature that can achieve a better energy efficiency© while the Multistory has the worst system energy efficiency.

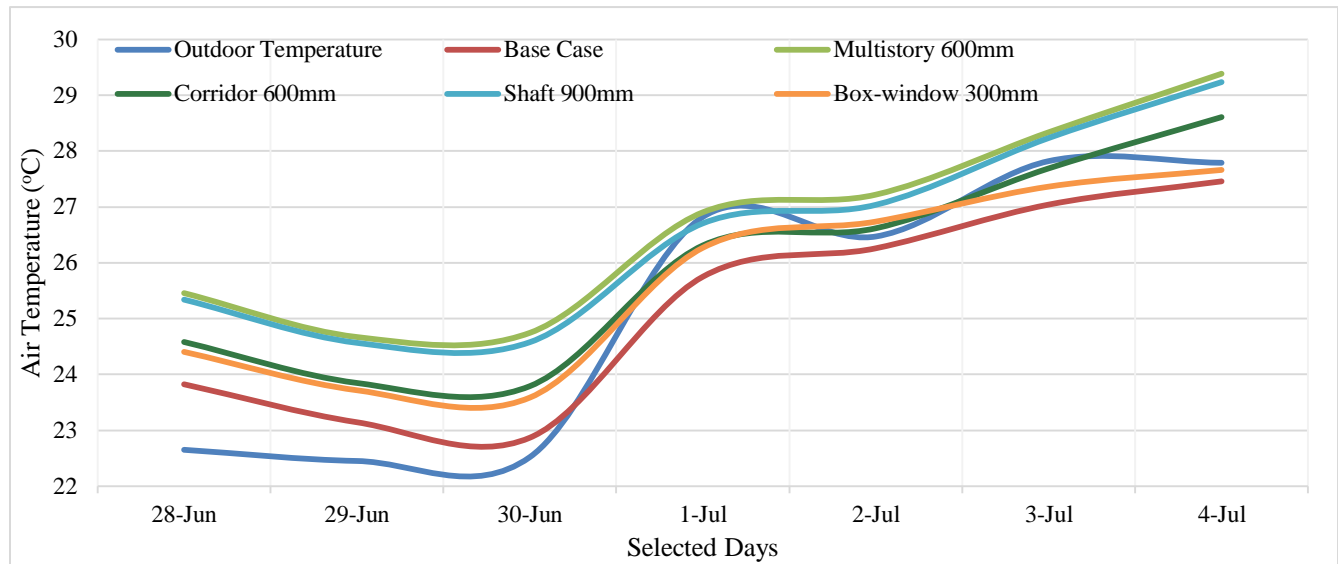


Figure 78: Indoor air temperature for the period between June 28th and July 4th.

6.2.1.2 Evaluation of the thermal level

The thermal evaluation was assessed according to ANSI/ASHRAE 55 standards (2010) through the calculation of the Predicted Mean Vote index (PMV) and Predicted Percentage of Dissatisfied (PPD). The assessment of thermal acceptance mainly based on clothing and activity level of the human body indoors. The PMV index is comprised of a 7-point thermal sensation scale that uses the heat balance principles of the human body to the average response of people to this scale. The thermal sensation scale is tabulated in the shown table.

Point	Sensation
+3	Hot
+2	Warm
+1	Slight warm
0.0	Neutral
-1	Slight cool
-2	Cool
-3	Cold

The PPD index is linked with PMV. According to ASNI/ASHRAE 55 standards, and in order to achieve the optimum thermal comfort for general application, the recommended range of $-0.5 < PMV < 0.5$ was proposed. This range strives to achieve a percentage of dissatisfied user lower than 10% as illustrated in Figure 79. As the PMV primarily uses the heat balance of the human body, the PMV could be estimated using a numerical approach. However, by assuming the clothing level for the summer period is 0.5 clo ($0.078 \text{ m}^2\text{K/W}$) (typical summer indoor clothing), metabolic rate is 1.6 Met (95 W/m^2) (typical activity

metabolic rate in residential places), and the indoor air velocity does not exceed 0.1 m/s, the following mathematical expression could be used for estimating the PMV:

$$PMV = 0.303Le^{-0.036M+0.029}$$

Where;

M: Metabolic rate

L: Variable depends on clothing level, the metabolic rate, indoor air temperature, dry-bulb temperature, relative humidity, and the mean radiant temperature.

Figure 79 represents the recommended PPD and PMV ranges for achieving a thermal acceptance level of 10%.

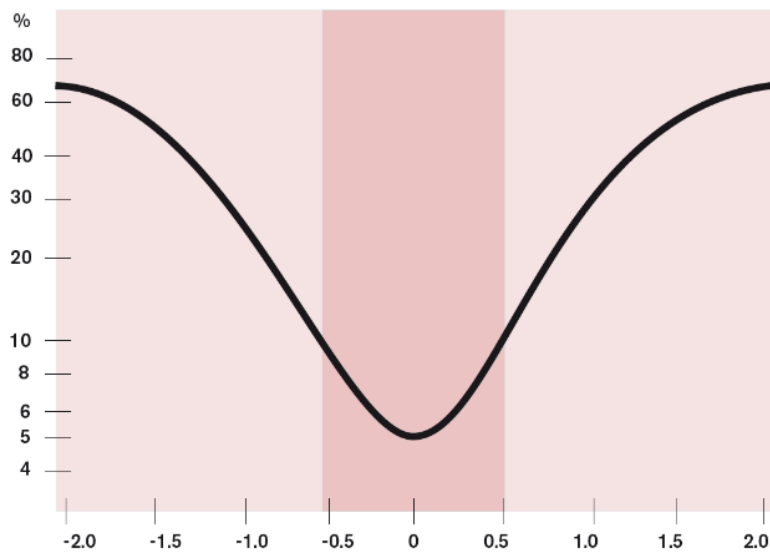


Figure 79: Predicted percentage of the dissatisfied (PPD) as a function of the predicted mean vote (PMV). (Source: Knaack et al., 2007)

In this context, the result of PMV for the summer period and the one-week interval for the hottest day is shown in Figure 80 and Figure 81. The PMV results for the entire summer period show that occupants' sensation is within the recommended ranges during May, and then constantly raising with oscillation until the beginning of September. The period from July 10th to July 20th is the most uncomfortable with PMV peak values ranged from 1.5 to 2.0 “slightly warm to warm and the majority close to warm” in case of Multistory and shaft while the PMV peak values for the same period for the Box-window DSF was ranged between 1.0 to 1.5 “slightly warm to warm and the majority close to slightly warm”.

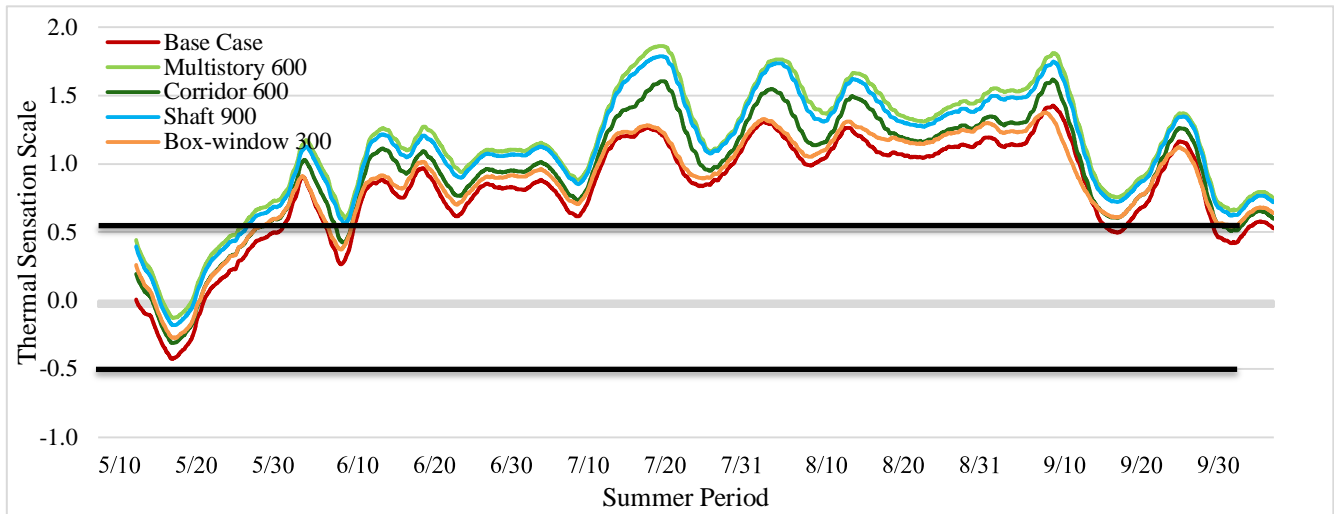


Figure 80: PMV calculated for the 4th floor for the period between May 1st and September 30th. The black bounds represent the recommended values as per ASHRAE 55 standard for general comfort.

Figure 81 shows the thermal sensation according to PMV scale during the period from June 28th to July 4th where the hottest day included in this period, all the PMV values are growing constantly during this period. In Particular, considering the PMV for all cases from the peak day (July 1st) and beyond, all PMV values indicate the typical thermal sensation for cases during the daytime. Consequently, the PMV during the night shows that the thermal sensation for indoor with Box-window DSF is the closest to the Base Case level of thermal sensation. In the whole period, the indoors' PMV average is around 0.8 for the Base Case, 1.06 for Multistory, 0.92 for Corridor, 1.03 for the shaft, and 0.88 for Box-window.

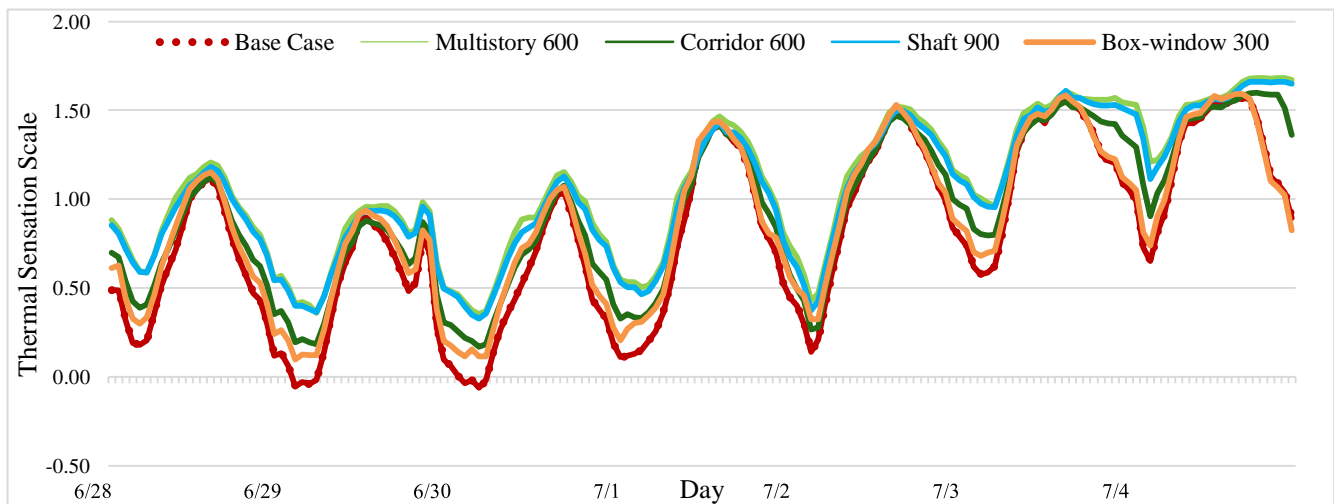


Figure 81: PMV calculated for the 4th floor for one week interval for the peak period in summer from June 28th to July 4th.

PPD of all cases behaves similarly to PMV ones, with a percentage of dissatisfied occupants that grew dramatically from the peak day until the last day of the period. On July 3rd, at peak hour at 15:30, around 54.24% were felt “slightly warm” in the Base Case, 56.57% for the Multistory, 53.06% for the Corridor, 56.74% for the Shaft, and 55.36% for the Box-window. In Contrast, and at night peak hour at 23.30, the occupant’s dissatisfied percentages at which the PMV was the lowest, was 30.36% for the Base Case, 53.42% for the Multistory, 43.35% for the Corridor, 51.64% for the Shaft, and 31.80% for the Box-window. Overall, the PPD for the whole one-week period indicates that the 4th-floor environment is comfortable for 76.52% of the week in the base case, followed by 74.54% for the Box-window, 73.13% for Corridor, 69.19% for Shaft, and the lastly 68.01% for the Multistory DSF type.

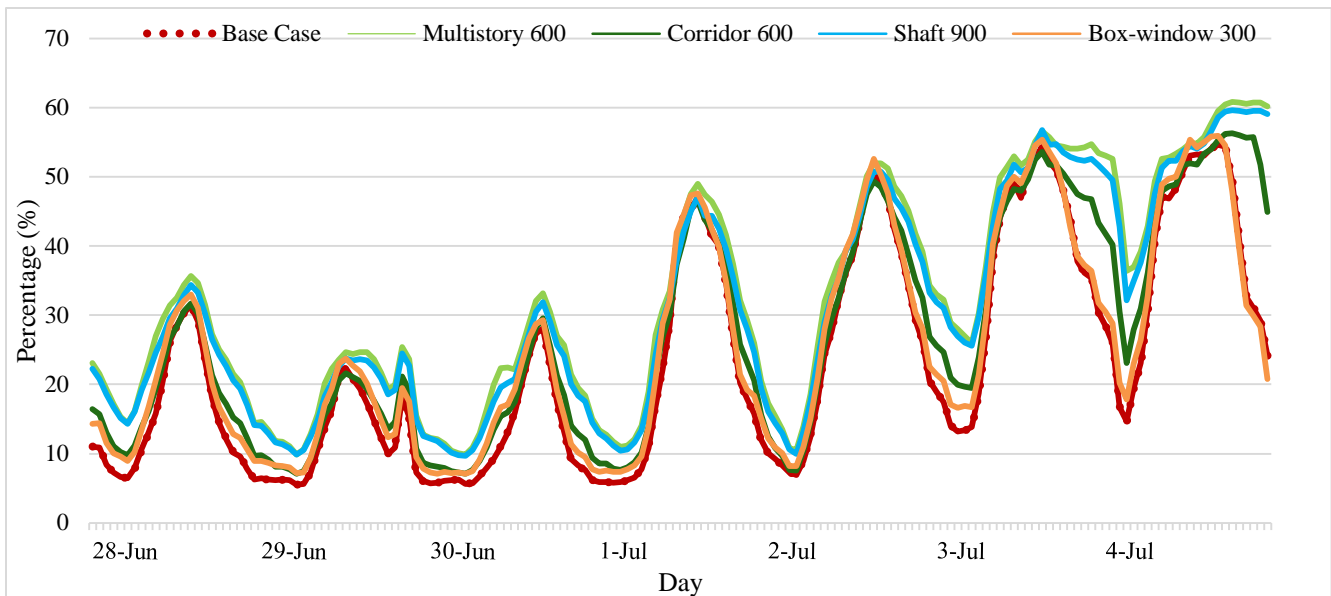


Figure 82: PPD calculated for the 4th floor for one week interval for the peak period in summer from June 28th to July 4th.

Based on the comprehensive thermal analysis for all DSF type, the study showed that the Box-window with 300mm cavity width has the optimal performance during the summer season where the indoor environment is considered comfortable 73.88% of this period

6.2.2 Average behavior in winter

6.2.2.1 Indoor air temperature

Figure 83 shows the air temperature and the solar direct irradiance on a horizontal surface for two periods starting from January 1st to April 30th and then from October 1st to December 31st. In this two periods where the predominated solar radiation is the lowest, all the simulation results specified the prerequisite of the façade's cavity to be closed in this particular period in which the maximum solar irradiation can be stored within the cavity by the radiation. The average temperature of the period was 10.97°C. The alternation of cloudy and sunny days are also dominant where the solar irradiation goes to zero even in the daytime as appears in January, November, and December. The solar direct radiation maximum value is 944 W/m² reached on Feb 20th and the average mean daily solar irradiance on a horizontal surface for this period is 180.54 W/m².

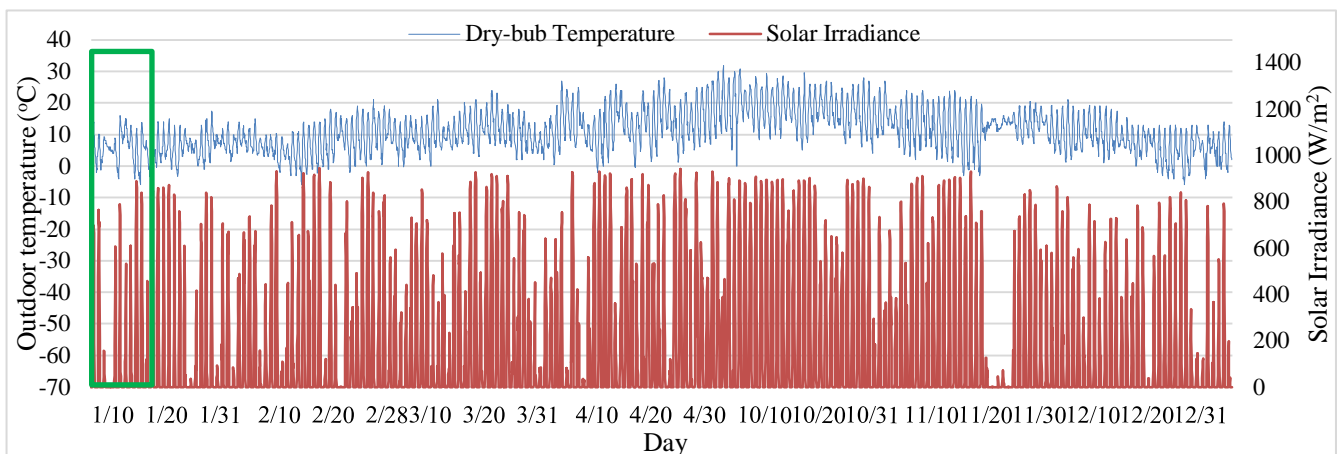


Figure 83: Air temperature and solar direct irradiance on horizontal surface for the period from January 1st to April 30th, and from October 1st to December 31st. The rectangle indicates the week selected for the detailed analysis.

Figure 84 shows the comparison between average indoor air temperature according to the façade geometry and the base case with the outdoor air temperature during the two winter's period. The average outdoor air temperature for the two periods are 10.87°C. By assuming that no heating equipment is running, the building with Box-windows DSF has the highest room temperature during January, while the higher the intensity of solar radiation, the Multistory and Shaft DSF transfer more heat to the internal spaces as shown from February until April. Furthermore, the second winter period, starting from October until December, the Multistory and Shaft DSF have initially had the best thermal efficiency in delivering the heat towards internal spaces. The Box-window DSF has a slightly lower performance in comparison with Multistory and Shaft DSF during October and November, at which the Box-window then became

the efficient case during December afterward. In the whole period, the room air temperature averaged at 17.34°C for the Multistory, 17.01°C for Shaft, and 16.8°C for the Box-window.

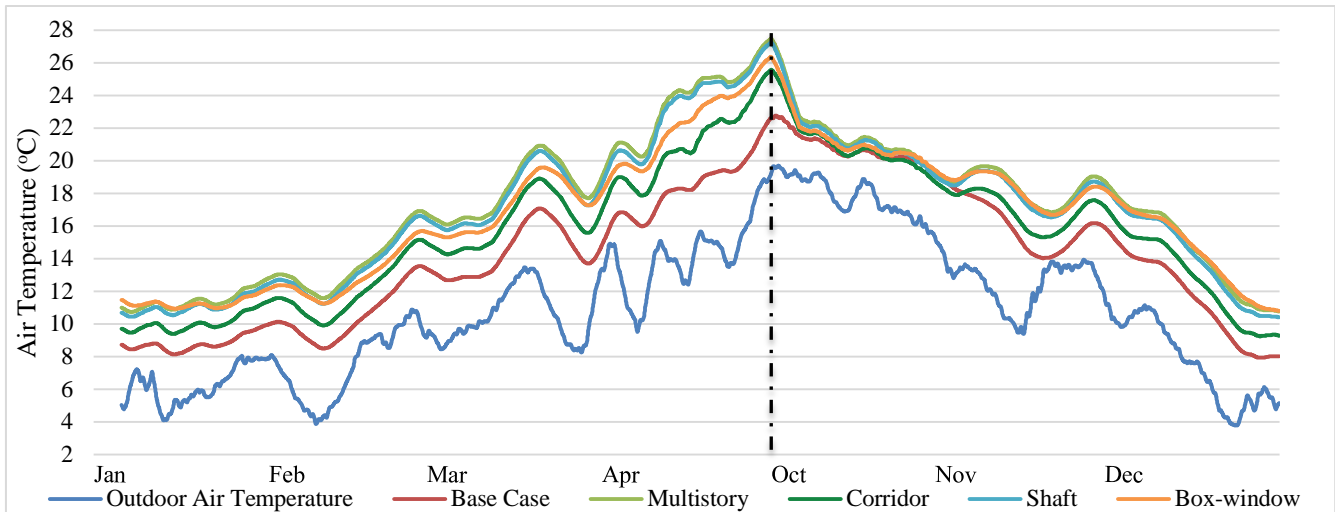


Figure 84: Indoor air temperature for the period from January 1st to April 30th, and from October 1st to December 31st

As mentioned earlier, the coldest day (January 10th) is included in this first period. A detailed assessing will be conducted for a week interval started from January 7th to January 13th (as shown in Figure 85) in which this period was selected because it included seven cloudy days that are typical of the heating period. The average air temperature for the selected week is 5.45°C and the mean daily solar irradiance is 167.58 W/m² representing values lower than the whole winter average values for both “winter to spring” and “autumn to winter” by 49.86% and 7.18% respectively.

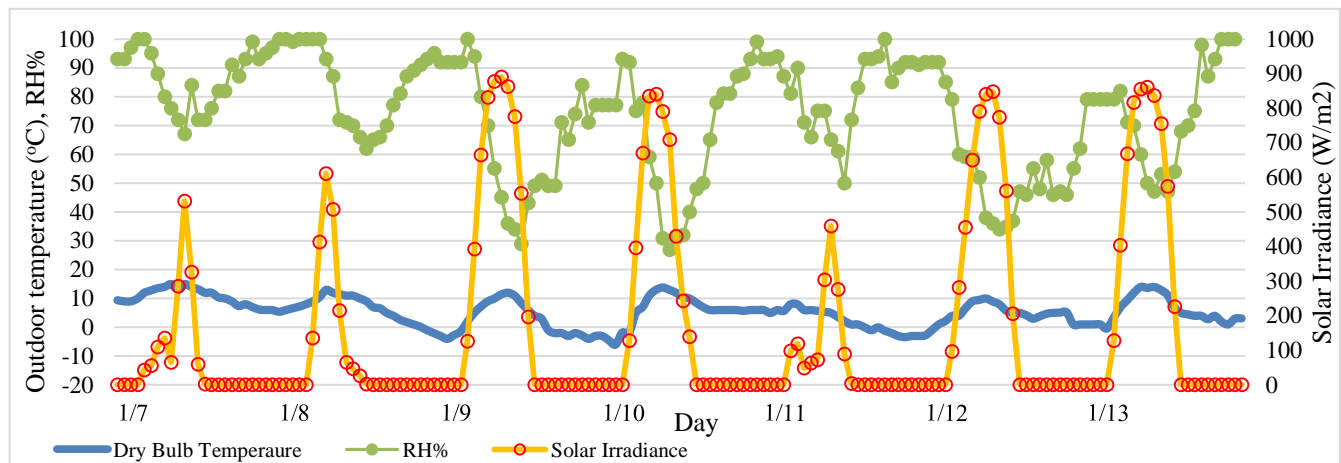


Figure 85: Outdoor air temperature, relative humidity, and solar irradiance on horizontal surface for the period January 1st to April 30th, and from October 1st to December 31st

Figure 86 illustrates the variation of the thermal behavior of all indoor spaces after utilizing the DSF in the period for the one-week interval from January 7th to January 13th. As shown, all indoor air temperature characteristics for all DSF were steady and oscillating between 1°C. Furthermore, the diagram also illustrates that benefits associated with employing the all type of DSF in preserving the indoor air temperature. Considering the period from January 7th to January 9th, where the massive dropping in outdoor air temperature, the figure show the ability of several types of DSF in maintaining the indoor air temperature within the same ranges. In particular, the Box-window DSF seems to be the best façade’s performance in term of storing heat during this period. By considering the average air temperature for this period, the average room air temperature for the Base Case was 8.53°C while the room’s indoor temperature during this period average at 11.17°C for the Box-window, 11.12°C for Multistory, 10.08°C for Shaft, and 9.77°C for the Corridor DSF. It worth to conclude that the building with Box-window DSF has the highest ability in preserving the indoor air temperature in which it achieves a better energy efficiency© while the Corridor DSF has the worst system energy efficiency.

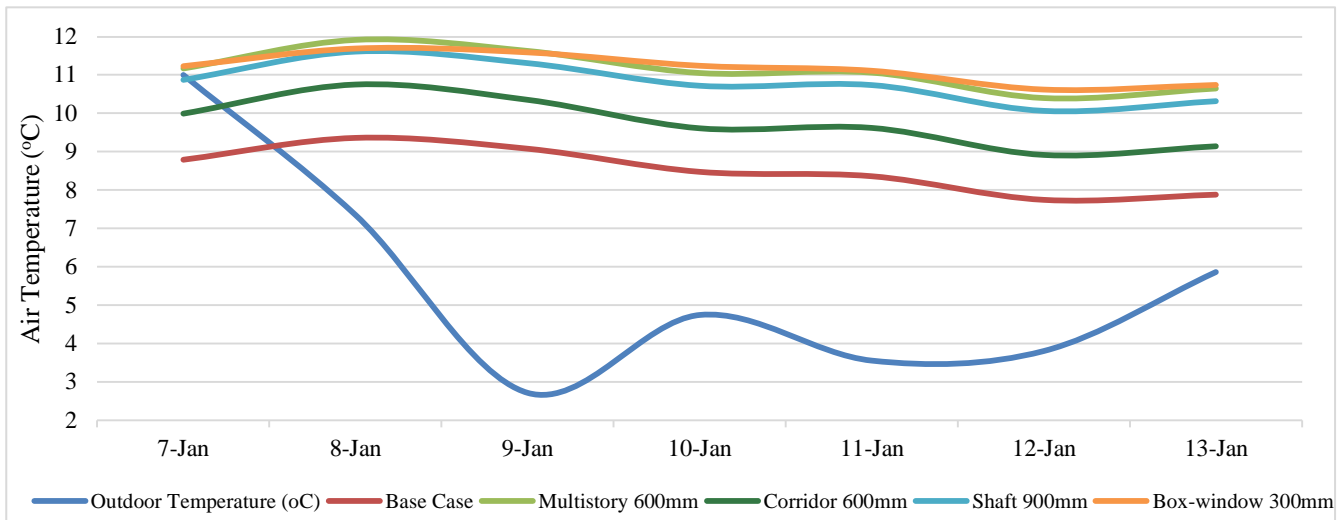


Figure 86: Indoor air temperature for the period between January 7th and January 13th

6.2.2.2 Thermal comfort evaluation

The thermal comfort of this period adopted from the standards defined in section 8.2.1.2. The result of PMV for the entire two winter periods and the one-week interval from January 7th to January 13th are illustrated in Figure 87 and Figure 88. Considering the clothing level insulation during the coldest period is equal to 1 clo (0.156m²K/W), the PMV lines indicated in Figure 87 shows that the occupants’ sensation

for all DSF types is within the recommended ranges during April and October Only. As shown, all PMV values are below the recommendation values in which the sense of coldness is highly apparent in January and December as the PMV values between 2.0 and 2.5 (“cool to cold”). Subsequently, a slight drop appears during February and then they started to constantly ascending until the end of March. In contrast, the PMV constantly descending from November until the end of December.

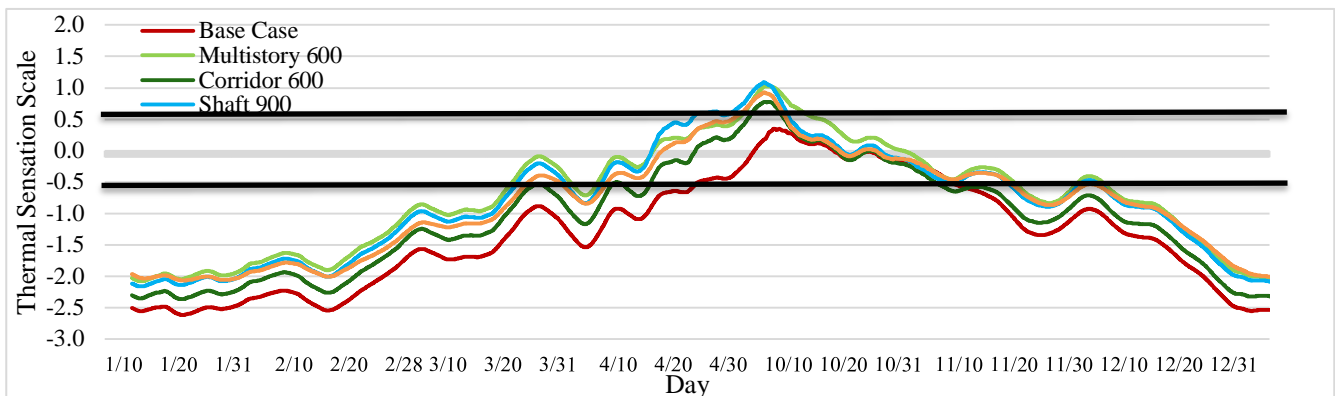


Figure 87: PMV calculated for the 4th floor for the period between January 1st to April 30th, and from October 1st to December 31st. The black lines bounds the recommended values as per ASHRAE 55 standard for general comfort.

Figure 88 shows the thermal sensation according to PMV scale during the period from January 7th to January 13th where the coldest day included in this period, all the PMV values are growing constantly during this period. In Particular, considering the PMV for all cases before and after the peak day (January 10th), all PMV values showed almost stable conditions of thermal sensation. Consequently, no significant differences indicated between daytime and nighttime during the entire period. The PMV showed that the Box-windows and Multistory DSF have similar performance during the coldest period. In the whole period, the indoors’ PMV average is around -2.54 for the Base Case, -2.0 for Multistory, -2.02 for Box-window, -2.09 for the shaft, and -2.29 for Corridor.

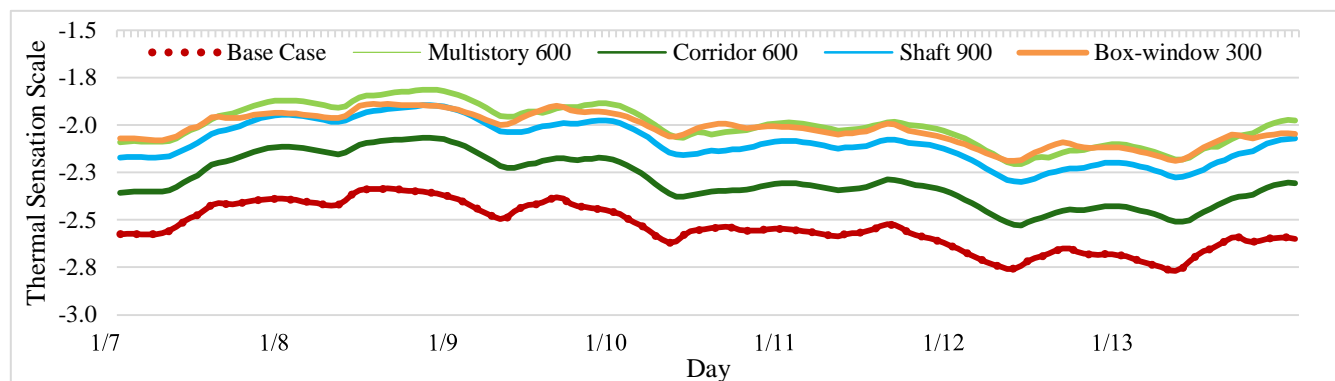


Figure 88: PMV calculated for the 4th floor for one week interval for the peak period in summer from January 7th to January 13th.

PPD of all cases behaves similarly to PMV ones, where the percentages remain almost steady during the week interval. In the whole period, around 93.33% were felt “cold” in the Base Case, 75.31%, 76.38%, 79.21% are feeling “slightly cool” to “cool” for both Multistory, Box-window, and Shaft, respectively, and 86.71% of occupants were felt “cool” to “cold” in case of Corridor DSF. Overall, the PPD for the whole one-week period indicates that, considering the indoors’ environment is comfortable was only 6.67% in Base Case, the 4th floor environment is comfortable for by 24.69% for the Multistory, followed by 23.62% for Box-window, 20.79% for Shaft, and the lastly 13.29% for the Corridor DSF.

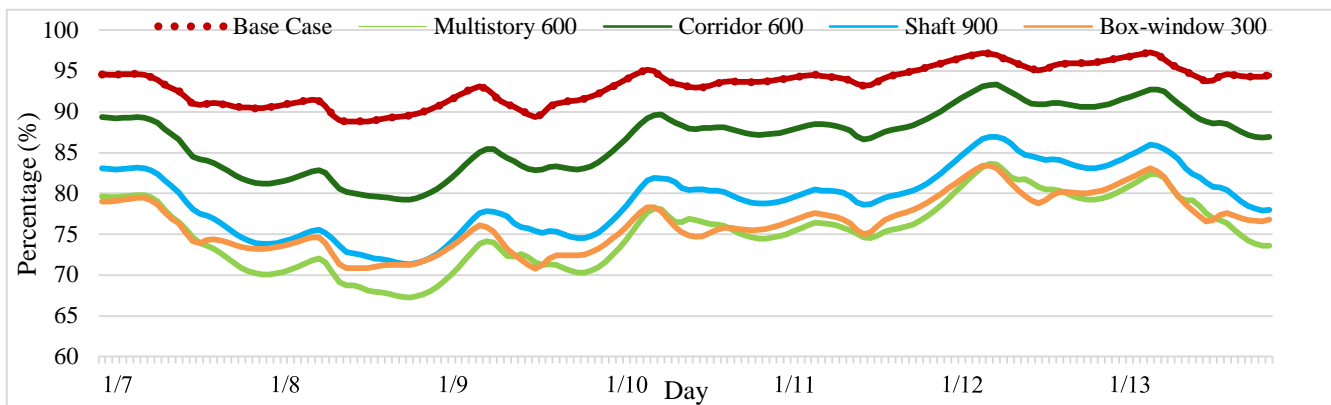


Figure 89: PPD calculated for the 4th floor for one week interval for the peak period in winter from January 7th to January 13th.

Based on the findings, the comprehensive thermal analysis for all DSF type showed that the Box-window with 300mm cavity width has the optimal performance during the winter season where the indoor environment is considered comfortable 66.46% of this period.

In summary, Table 18 shows the annual average PPD% of all the DSF based on the previous findings. The selection of the double skin façade would be upon the most façade at which it can afford the most thermal comfort to the occupants during a full year. As tabulated, the Box-windows with 300mm cavity width DSF can deliver the highest thermal comfort throughout the year, where this façade afford a comfortable indoors’ environment averaged at 71.16% per annum©.

Table 18: Average PPD for summer, winter, and annual.

Case	PPD% - Summer	PPD% - Winter	Average PPD%	Comfortable percentages
Base Case	24.78%	47.40%	36.09%	63.01%
Multistory 600mm	36.15%	31.03%	33.59%	66.41%
Corridor 600mm	29.39%	39.97%	34.68%	65.32%
Shaft 900mm	34.42%	33.60%	34.01%	65.99%
Box-window 300mm	26.13%	33.54%	28.84%	71.16%

Figure 90 and Figure 91 shows the typical floor plan of the building after utilizing the box-window on four sides of the building.

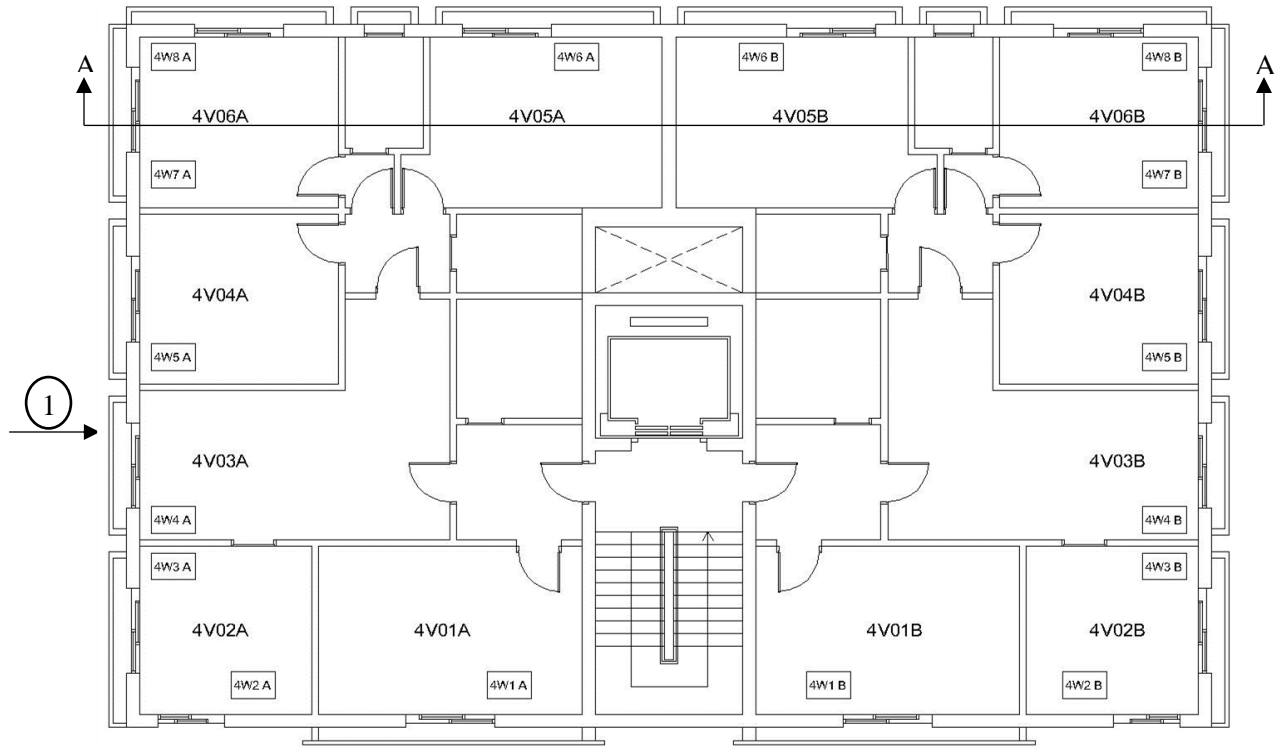


Figure 90: Typical plan floor of Al Majd 1 building. The box-window DSF is situated on all building sides.

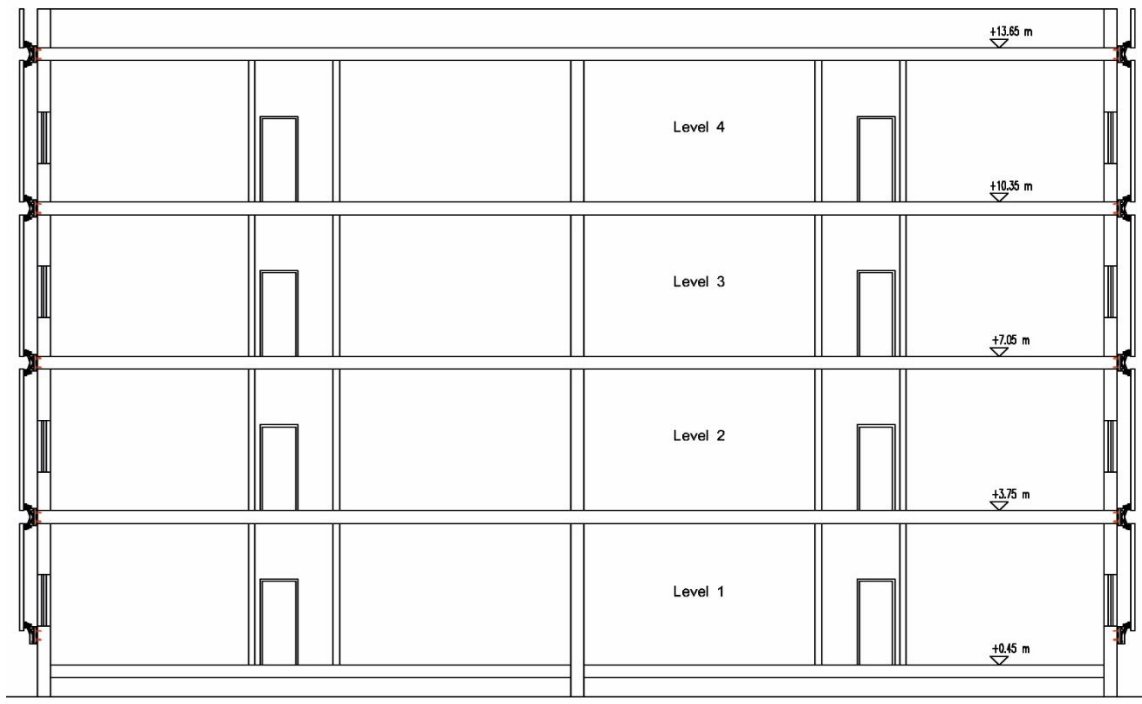


Figure 91: Section A-A

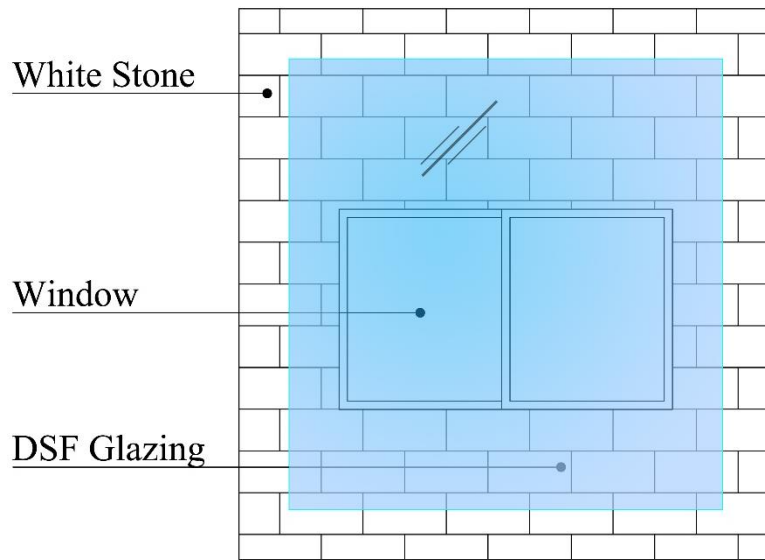


Figure 92: View 1 details.

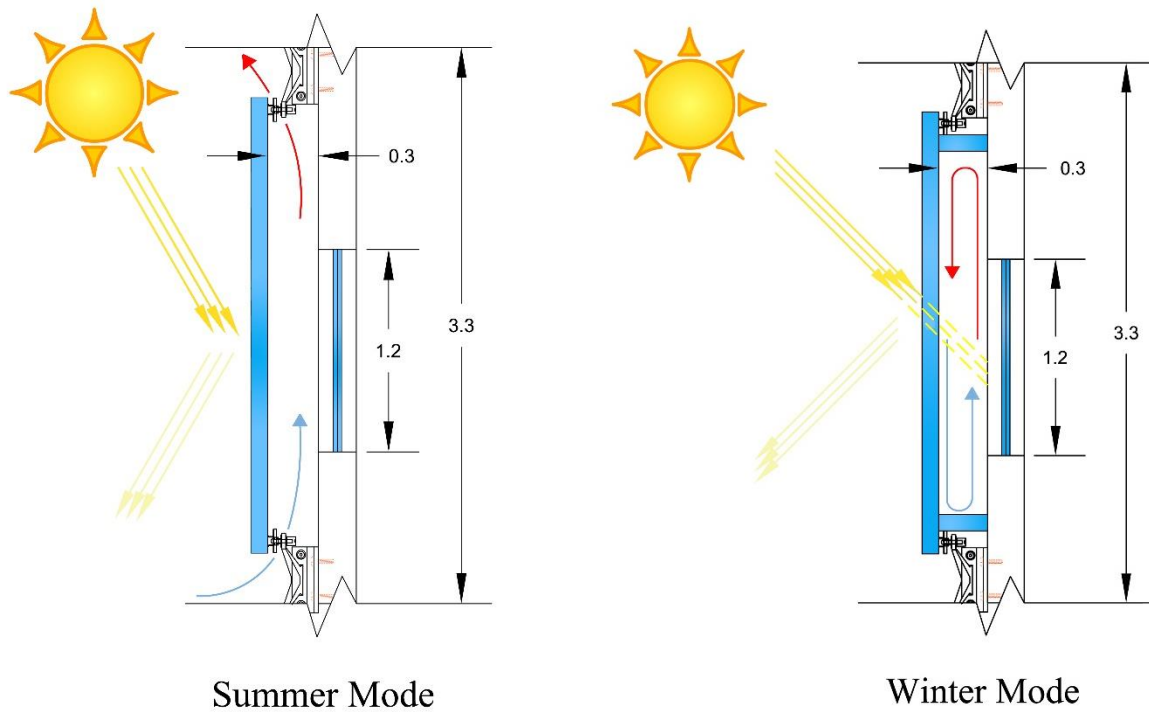


Figure 93: Cross-section diagram of the box-window for both summer and winter modes.

Figure 94 shows a rendered image of the case study building after utilizing the box window DSF type with 300mm cavity width.



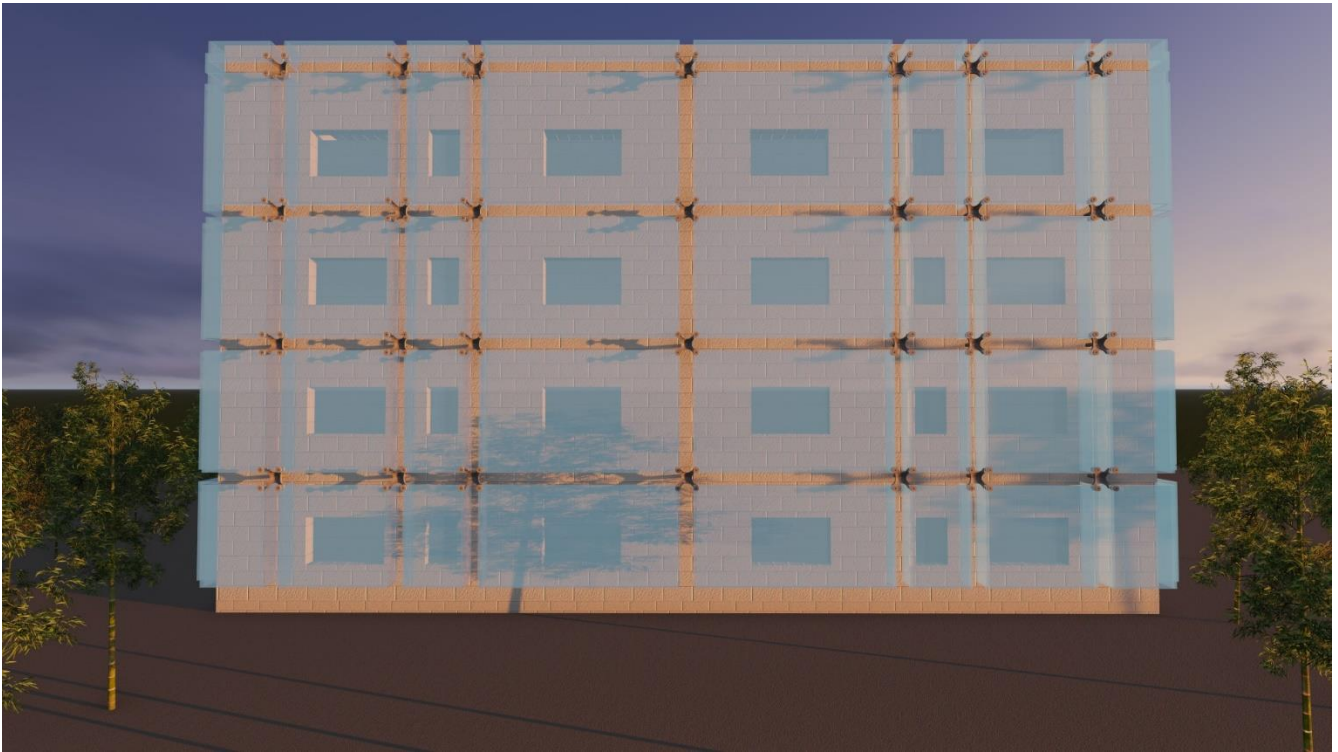


Figure 94: Rendered image of the building with box window type DSF.

6.3 Cooling and heating loads summary.

The Box-window double skin façade showed an acceptable thermal satisfaction in both winter and summer regime with indoors’ environment comfortable rates around 66.46% and 73.88%, respectively. However, assuming the lowest PPD percentages in every month for the Box-window 300mm cavity width case are the conditions at which the energy consumption needed to assure a thermal comfort for 80% of occupants, the energy consumption can then be evaluated. In fact, since the inner skin of the building is no longer in contact with the outer conditions, the façade’s cavity thermal conditions became the main influencer on the room thermal performance. However, the upper and lower temperature limits, in this case, will be related to air temperature inside the cavity as it is the ambient temperature. The upper and lower temperature limits in conjunction with the outdoor conditions can be evaluated according to Equation (1) and Equation (2). Table 19 shows the acceptable comfort zones based on the individual monthly average temperature of the cavities for box-window DSF type.

Table 19: Upper and lower temperature limits for the box-window DSF building type.

Month	Average outdoor air temperature (°C) “average cavity’s temperature”	Thermal acceptance levels	
		Lower temperature limit (°C)	Upper temperature limit (°C)
January	13.37	18.44	25.44
February	15.77	19.19	26.19
March	20.31	20.60	27.60
April	24.60	21.93	28.93
May	21.65	21.01	28.01
June	25.06	22.07	29.07
July	26.88	22.63	29.63
August	26.84	22.62	29.62
September	24.05	21.76	28.76
October	18.47	20.03	27.03
November	21.16	20.86	27.86
December	15.24	19.02	26.02

The energy profile definition can be then summarized according to the requirements in each month to obtain the desired thermal comfort according to definitions previously discussed in section 4.9.4. Table 20 summarizes the defined thermal variables in IES VE for each month individually, where each month requires it is own criteria to be considered during the analysis such as façade’s openings profile, external windows openings profile, cooling set points, and heating set points. However, the cooling, heating, and the total energy consumption of the building after utilizing the Box-window gives an indication of the

possibility of the Double Skin Façades in lessening the overall energy demands along with enhancing the occupants' monthly thermal comfort.

Table 20: Temperature and ventilation profiles defined in IES VE for the assessment of box-window DSF.

Façade	Month	Description			
		Cooling	Natural Ventilation through DSF	Natural Ventilation through Windows	Heating
Box-window DSF – 300mm Cavity width	January	N/A	Façade closed the whole time	Windows closed the whole time	$t_i < 18.44$
	February	N/A	Façade closed the whole time	Windows closed the whole time	$t_i < 19.19$
	March	N/A	Façade closed the whole time	Windows closed the whole time	$t_i < 20.60$
	April	$t_i > 28.93$	Façade closed the whole time	$21.93 < t_i < 28.93$ and $21.93 < t_{CAVITY} < 28.93$	$t_i < 21.93$
	May	$t_i > 28.01$	Façade opened the whole time	$t_i < 28.50$ and $t_{CAVITY} < 28.50$	N/A
	June	$t_i > 29.07$	Façade opened the whole time	$t_i < 29.50$ and $t_{CAVITY} < 29.50$	N/A
	July	$t_i > 29.63$	Façade opened the whole time	$t_i < 30.00$ and $t_{CAVITY} < 30.00$	N/A
	August	$t_i > 29.62$	Façade opened the whole time	$t_i < 30.00$ and $t_{CAVITY} < 30.00$	N/A
	September	$t_i > 28.76$	Façade opened the whole time	$t_i < 29.25$ and $t_{CAVITY} < 29.25$	N/A
	October	$t_i > 27.03$	Façade opened the whole time	Windows closed the whole time	$t_i < 20.03$
	November	N/A	Façade closed the whole time	Windows closed the whole time	$t_i < 20.86$
	December	N/A	Façade closed the whole time	Windows closed the whole time	$t_i < 19.02$

Note t_i : indoor air temperature, t_{CAVITY} : cavity air temperature, >: greater than, <: less than, N/A: not necessarily applicable.

Figure 95 shows the total chiller and heater systems load required for the building with Box-window 300mm cavity width in order to achieve the 80% thermal acceptability demands. Due to summer overheating, the cooling energy required to maintain the indoor temperature within the acceptable ranges, the cooling loads peaks in July with total system loads around 19.39MW_h. The figure also showed that January is the coldest month where the heating system loads reach 12.21 MW_h. Furthermore, April and October are the two months where the energy consumption is very minimal.

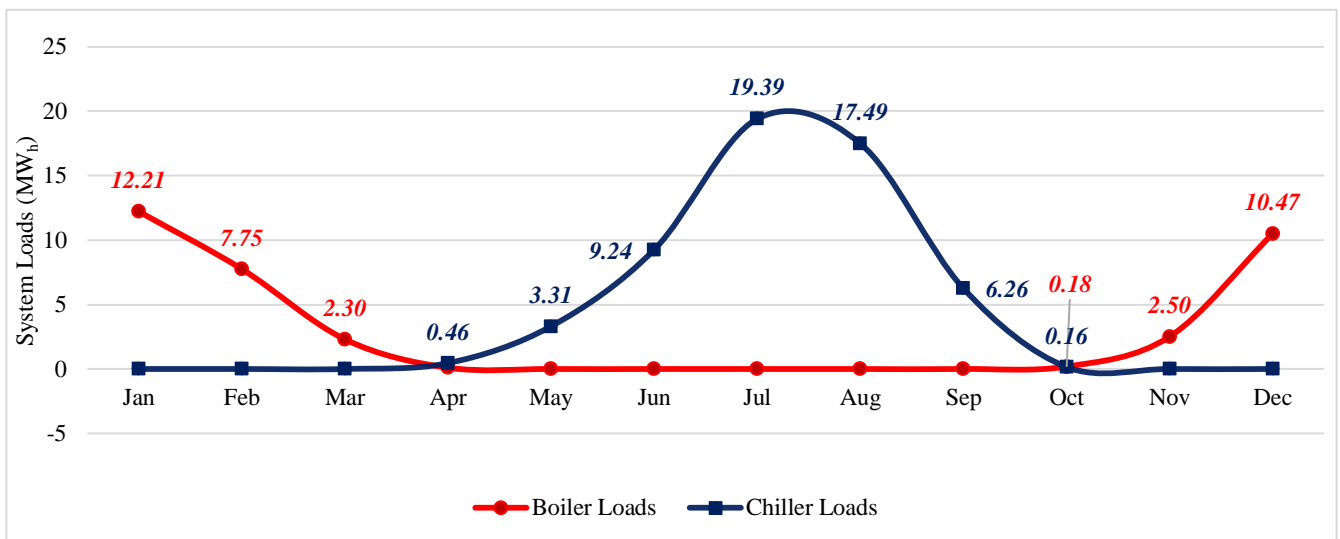


Figure 95:Boiler and chiller systems loads for the box-window DSF..

The electricity consumption (chiller + boiler) of each case is presented in Figure 96. To be specific, utilizing the box-window DSF on the external façade built a difference of 300mm cavity width contribute to annual heating and cooling energy saving by 40.95% and 28.28%, respectively. The percentage of total energy consumption savings compared to the Base Case was 37.22% is also achievable.

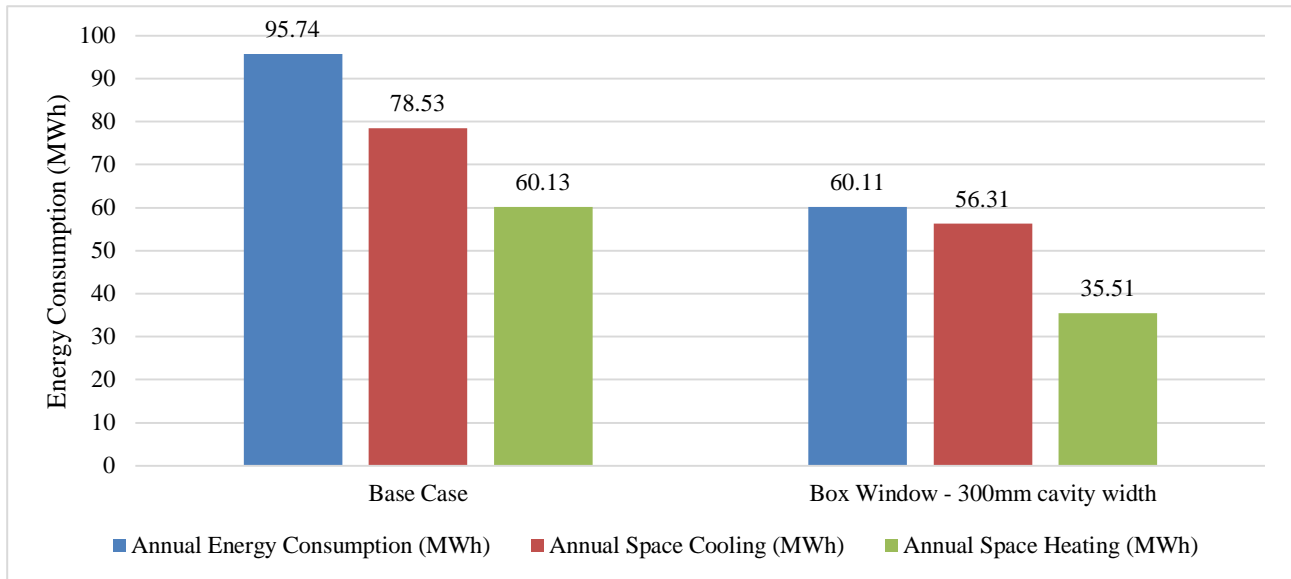


Figure 96: Comparison between base case building and box-window DSF building for final energy consumption

7.0 Conclusion

Demand for environmentally-responsive and sustainable buildings is on the rise. Apparently, the double skin façade which stands for to an additional skin built with a several distances from the existing building's façade has many advantages that put it as a promising passive solution for building façades. Nevertheless, the concept of the DSF has corroborated by many studies, the system efficiency for an existing building with a conventional facade built with mainly Whitestone is not clear and never been investigated. Hence, this study would fill the knowledge gap in this field.

The research main purpose was to investigate whether the double skin façade is passive building technology that can adapt to the prevailing climatic condition of Jordan. Accordingly, the benefits associated with the double skin façade in the building sector in general and the residential sector, in particular, were investigated under both summer and winter scenarios.

This article focused on the assessment of different types of double skin façade geometry types in Irbid city in which the selection of the appropriate façade was based on the overall energy efficiency that can deliver the highest energy saving and improve the indoor thermal comfort simultaneously. The research addressed several aspects: 1) energy performance of different type of DSFs (multistory, corridor, shaft, and box-window); 2) the energy performance associated with the various cavity width of the façade; 2) the effect of façade's and external window vents on the energy performance of the DSF; 3) occupants' thermal acceptance level enhancement; and 4) the effects of DSFs on the annual energy consumption. The chosen research methodology is the computer simulation. A series of simulations were conducted in order to quantify the effects of the DSF. After analyzing the results obtained from all the conducted simulations, the most façade configuration that able to deliver acceptable energy performance along with thermal acceptance level is the box-window type double skin façade that has a 300mm cavity width.

In this paper, the results of the comprehensive study conducted on a double skin façade applied in building with a residential type occupation were analyzed. As the DSF performance is highly dependent on the physics of façade geometry, the main inferences from this study on the performance of the DSF in Mediterranean climate conditions can be summarized as the following:

- (1) The cavity air temperatures for all geometry façade types were higher than the outdoor air temperature during both summer and winter scenarios. Despite the higher cavity air temperature

of multistory and shaft DSF that can be achieved during winter, a summer overheating was their major issue. Box-window DSF has a compromise cavity air temperature registering an 86.94% higher temperature during winter and a mere of 2.45% during summer.

- (2) Results showed that the cavity air temperature in case of box-window DSF is higher, on average than the outdoor air temperature by 6-8°C during heating months, while the difference in cooling months is slightly higher than the outdoor air temperature. In the same context, the difference between the air temperature of indoors in relative to outdoor air temperature registered at 3-5°C during heating months, while during the cooling months the average between the two air temperature had almost no difference.
- (3) In regards to the indoor air temperature in relation to outdoor air temperature, the results show that the difference between the indoor to outdoor air temperature maintained as the outdoor ambient temperature and remained lower than the outdoor temperature in the peak day. While the difference soared by 7-8°C during winter and could reach to 9°C during the peak winter day.
- (4) The airflow volume inside the cavity gives an indicator for the type of façade that can deliver a higher flow rate of air that can then extract the heated air inside the cavity towards the outdoor. However, the maximum the airflow passes through the cavity, the lower the cavity air temperature is acquired. The ascending order of façade in regard to airflow passing the thought the cavity are multistory, shaft, box-window, and the corridor type DSF.
- (5) Results show that the façade's geometry that would able to supply sufficient fresh air towards indoor rooms is the box-window DSF. The volume flow rate of the air entering through the external windows from the naturally ventilated cavity during the cooling months played a significant role in replacing the unwanted ambient hot air indoors. Although the supplied air from the ventilated cavity is often lower than the airflow towards indoor room in the base case, the box-window DSF has reduced the airflow entering from the external cavity by 21.35%, followed by 42.31% for corridor type, 48.47% for the multistory type, and then 50.17% for the shaft type. Furthermore, in regards to heat gain, the most façade that helped to extract warm air from the indoor rooms is the box-window by a rate of 0.183 kW, followed by a corridor with a rate of 0.16 kW, 0.121 kW for multistory, and 0.113 kW for shaft DSF type.
- (6) The analysis of the parametric results of the predicted percentage of dissatisfied (PPD) in regards the façade thermal performance indicated that the multistory DSF functions effectively during

winter seasons, and the shaft and the corridor DSF performed well during summer seasons, while the box-window has a compromise thermal efficiency during both summer and winter seasons.

- (7) The annual energy savings of different geometry types with several cavity widths have significantly reduced after applying the DSF. Although the multistory DSF able to achieve an energy saving about 48.15%, the annual thermal acceptable limits are relatively low due to its poor performance during summer seasons. In the same context, the poor performance of the shaft DSF to trap the solar radiation during winter seasons made the selection of this type of façade less preferable. Despite box-window DSF able to achieve an energy saving around 37.22%, but its adequate performance during both summer and winter seasons stimulate achieving approximately 71.16% of occupied hours within thermal acceptable levels compared to 63.01% in the base case.
- (8) Double skin façade has significantly reduced the direct solar gain in the building. The solar gain of the base case has a value 54.78% higher, on average, of the annual solar gain for all tested DSF geometry types.
- (9) Considering the energy savings potential, the box-window DSF enhances the building energy efficiency as the cooling loads were reduced by 28.28% while the heating loads were also reduced by 40.95% making the overall energy reduction to achieve a percentage of 37.22% annually.

Overall, the construction style of the housing sector in Jordan seems to be poorly designed as the highest thermal comfort that can be achieved is 63.01% that's required around 95.74 MWh of energy to achieve the desired thermal comfort, whilst implementing the Box-Window DSF on the same building has boosted the thermal comfort to reach 71.16% with shrinking consuming an energy rate of 60.11 MWh simultaneously. In conclusion, the utilization of DSF systems in a conventional building type under the Irbid climate conditions deemed to be an efficient application in such city and it is expected to be widely growing in time and socially accepted due to their high interest including: cost-benefit saving, thermal efficiency, and aesthetic appearance. Table 21 presents the summary of this research evaluated findings and the comparison with the related cases findings:

Table 21: The similarity between findings from the literature and their relation to this research findings

Parameter	Author/year	Location	Tool	Ventilation Mode	Finding/observation
Cavity opening	Torres et al. (2007)	Spain	TAS (BES)	HVAC	Larger façade's vents help in the extraction of unwanted warm air inside the cavity.
Cavity Height	Radhi et al. (2013)	UAE	Design Builder	HVAC	A difference of 3.2°C in the indoor air temperature for a height of 3-stories building was maintained when the outside temperature below 31°C.
Structure	Hong et al. (2013)	S.Korea	Design Builder	HVAC	The multistory DSF type had the highest ability in preheating the air inside the cavity. But overheating is more predictable.
Cavity Width	Radhi et al. (2013)	UAE	Design Builder	HVAC	Narrow cavity width decreases the heat transfer towards indoors due to higher ventilation rates.
Energy saving	Ghadamian et al. (2012)	Iran	Mathematical model	Mechanical	Mechanically ventilated DSF could provide energy savings by 21% to 26% and 41% to 59% in both season summer and winter, respectively.
Energy Saving	Kim et al. (2012)	N/A	IES VE	Natural	A gross of 38% of energy saving after utilizing the DSF on renovation or refurbishment of the old residential building.
Energy Saving	Chan et al. (2009)	China	Design Builder +CFD	HVAC	DSF could cut up to 26% of the total building cooling loads
Energy Saving	Cakmanus (2007)	Turkey	IES VE	Natural	A gross of 38% of energy saving after utilizing the DSF on renovation or refurbishment of the old residential building.
Thermal Comfort	Barbosa et al. (2015)	Brazil	IES + Design builder	Natural	Utilization of DSF on the west elevation of a naturally ventilated building assures a 70% of the occupied hours are thermally comfortable.
Summer Overheating	Singh et al. (2008)	India	Experimental	Natural	Although DSF made from glass and being glass the main contributor to heat gain, DSF can significantly reduce the transmitted direct solar gain towards internal spaces.

7.1 Recommendation and future works

Double skin façade is the fastest worldwide trend in the building architectural. To keep pace with this boom, more studies and suggestions for future works are summarized as follows:

- (1) As this study had conducted based on a simulation approach, the absence of the on-site experimental data for the validation of the computational simulation results would be significantly affect the precision of this study results. Therefore, an experimental work should be taking place in future in order to deliver more comprehensive data to validate the simulation outcomes.
- (2) More accurate results would be generated if the average cavity air temperature was computed based on a shorter time interval instead of a one-month interval in calculating the upper and lower temperature limits in determining the thermal acceptable limits for the indoor environment.
- (3) In regards of the design days, the simulation shall be expanded considering more design days and weather conditions of Irbid city.
- (4) Expand the work to cover the whole building apartments rather than considering the simulation of the 4th floor only.
- (5) Future works should consider the influences that may occur due to the effect of any adjacent buildings and study their shading effect and the wind barrier influences on the building.
- (6) Study whether applying the DSF on the north direction would have the least impact on the overall building's thermal performance.
- (7) Investigate the probability of obtaining more positive results by apply various geometry types on the individual existing facade of the building as well as widening the investigation into more façade's cavity widths.
- (8) Expand the work by exploring the benefits of creating on site electricity generation by installing PV panels on the glazed facade while considering not affecting the final visual experience of the habitants.
- (9) Conducting a comprehensive feasibility study for the total constructional cost of DSF, maintenance cost, operational cost, the life-cycle of the system, and any other issues that might affect the system performance (e.g. condensation of inner glazed surface).

8.0 References

- Agrawal, P.C. (1989). A review of passive systems for natural heating and cooling of buildings, *Solar & Wind Technology*, vol. 6 (5), pp. 557-567.
- Air Conditioning, Heating, and Refrigeration Institute (2012). AHRI 210/240:2012. Performance of rating of unitary air-conditioning & air-source heat pump equipment [online]. Arlington: AHRI. [Accessed 11 February 2018]. Available at: http://www.ahrinet.org/App_Content/ahri/files/STANDARDS/AHRI/AHRI_Standard_210-240_2017.pdf
- Alberto, A., Ramos, N., and Almeida R. (2017). Parametric study of double-skin façades performance in mild climate countries, *Journal of Building Engineering*, vol. 12, pp. 87-98.
- Andelkovic, A., Urosevic, B., Kljajic, M. (2015). Experimental research of the thermal characteristics of a multi-story naturally ventilated double skin façade, *Energy and Buildings*, vol. 86 (2015), pp. 766-781.
- Arons, D. (2000). *Properties and application of double-skin building façades*. MSc. Thesis. Massachusetts Institute of Technology.
- Astorqui, J. and Porrás-Amores, C. (2016). Ventilated façade with double chamber and flow control device, *Energy & Buildings*, vol. 149, pp. 471-482.
- Barbosa, S., Ip, K., and Southall, R. (2015). Thermal comfort in naturally ventilated buildings with double skin façades under the tropical climate conditions: the influence of key design parameters, *Energy & Buildings*, vol. 109 (2015), pp. 397-406.
- Cakmanus, I. (2007). Optimization of double skin façade for buildings: an office building example in Ankara-Turkey. *Proceedings of Clima 2007 Wellbeing Indoors*. Helsinki, Finland. 10-14 June.
- Campen, D. (2009). *Research methods-experimental & correlation* [online]. Viewed 24 December 2018. Available at: <https://youtu.be/MrBSNE-GDUI>
- Chan, A., Chow, T., Fong, K., & Lin, Z. (2009). Investigation on energy performance of double skin façade in Hong Kong, *Energy Building*, vol. 42, pp. 1135-1142.

- Choi, W., Joe, J., Kwak, Y., & Ho Huh, J. (2012). Operation and control strategies for multi-story double skin façades during the heating season, *Energy & Building*, vol. 59, pp. 454-465.
- Darkwa, J., Li, Y., and Chow D. (2014). Heat transfer and air movement behavior in a double-skin façade, *Sustainable Cities and Society*, vol. 10 (2014), pp. 130-139.
- Department of Land and Survey. (1979). *Building and organization system in Amman city system No. (67) for the year of 1979*. Amman: Department of Land and Survey.
- Department of Statistics. (2016). *General population and housing census 2015* [online]. Amman: Population and Housing Census. [Accessed 29 May 2018]. Available at: http://www.dos.gov.jo/dos_home_e/main/population/census2015/Main_Result.pdf
- Djunaedy, E., Hansen, J.L.M, & Loomans M. (2002). Towards a strategy for airflow simulation in building. Paper presented at Design Center for Building & Systems, Technische Universiteit Eindhoven.
- Fallahi, A., Haghghat, F., & Elsadi, H. (2013). Development of a double-skin façade for sustainable renovation of old residential buildings, *Indoor Built Environment*, vol. 22, pp. 180-190.
- Ghadamian, H., Ghadimi, M., Shakouri, M., Moghadasi, M., & Moghadasi, M. (2012). Analytical solution for energy modeling of double skin façade building, *Energy & Building*, vol. 50, pp. 158-165.
- Goia, F., Haase, M., and Perino, M. (2013). Optimizing the configuration of a façade module for office buildings by means of integrated thermal and lighting simulations in a total energy perspective. *Applied Energy*, vol. 108, pp. 515-527.
- Haase, M., Marque da Silva, F. & Amato, A. (2009). Simulation of ventilated façade in hot and humid climates. *Energy and Buildings*, vol. 41 (4), pp. 361-373.
- Hamza, N. (2008). Double versus single skin façades in hot arid areas, *Solar Energy and Buildings*, vol. 40, issue 3, pp. 240-248.
- Hong, T., Kim, J., Lee, J., Koo, C., & Park, H., (2013). Assessment of seasonal energy efficiency strategies of a double skin façade in a Monsoon climate region, *Energies*, vol. 6, pp. 4352-4376.
- Inan, T., Basaran, T., and Ezan M. (2016). Experimental and numerical investigation of natural convection in a double skin façade. *Applied Thermal Engineering*, vol. 106, pp. 1225-1235.

- Jager, W. (2003). Double skin façade – sustainable concepts. Paper presented at Hydro and Syd Bygg, Malmo.
- Jarad, H. and Ashhab, M. (2017). Energy savings in the Jordanian residential sector, *Jordan Journal of Mechanical and Industrial Engineering*, vol. 11 (1), pp. 51-59.
- Jiru, T., Haghghat, F. (2008). Modeling ventilated double skin façade – A zonal approach, *Energy Build*, vol. 40, pp. 1567-1576.
- Joe, J., Choi, W., Kwak, Y., and Huh, J. (2014). Optimal design of a multi-story double skin façade, *Energy and Buildings*, vol. 76(2014), pp. 143-150.
- Kothari, C.R. (2004). *Research methodology: methods & technique*. New Delhi: New Age International Publisher.
- Kottek, M., Grieser, J., Beck, C., Rudolf, B., & Rubel, F. (2006). World map of the Koppen-Geiger climate classification update. *Meteorologische Zeitschrift*, vol. 15, pp. 259-264.
- Kragh, M. (2000). Building envelope and environmental systems. Paper presented at Modern Façades of Office Buildings, Delft Technical University.
- Larsen, S., Rengifo, L. and Filippin, C. (2015). Double skin glazed façades in sunny Mediterranean climates, *Energy and Buildings*, vol. 102 (2015), pp. 18-31.
- Lee, J., & Chang, J. (2015), Influence on vertical shading device orientation and thickness on the natural ventilation and acoustical performance of a double skin façade, *International Conference on Sustainable Design, Engineering and Construction 2015*, vol. 118, pp. 304 – 309.
- Lee, J., Alshayeb, M., and Chang, D. (2015). A study of shading device configuration on the natural ventilation efficiency and energy performance of a double skin façade, *International Conference on Sustainable Design, Engineering and Construction 2015*, vol. 118, pp. 310-317.
- Magali, b. (2001). *Proposition of climatic façades classification, case 2: double envelope systems*. MSc. University of Leuven.

- Matouq, M., El-Hasan, T., Al-Bilbisi, H., Abdelhadi, M., Hindiyeh, M., Eslamian, S., and Duheisar, S. (2014). The climate change implication on Jordan: A case study using the GIS and Artificial Neural Networks for weather forecasting, *Journal of Taibah University for Science*, vol. 8, pp. 44-55.
- Nimlyat, P.S., Dassah, E., Allu, E.L.A. (2014). Computer simulation in buildings: implication for building energy performance, *International Organization of Scientific Research; Journal of Engineering*, vol. 4 (3), pp. 56-62.
- Oesterle, E., Lieb, R-D., Luts, M., & Heusler, W. (2001). *Double skin façade – integrated planning*. Munich, Prestel Verlag.
- Pasut, W. and Carli, M. (2012). Evaluation of various CFD modeling strategies in predicting airflow and temperature in a naturally ventilated double skin façade, *Applied Thermal Engineering*, vol. 37, pp. 267-274.
- Poirazis, H. (2006). *Double skin façade: a literature review*. Lund: Lund University.
- Pomponi, E., Piroozfar, P., Southall, R., & Sdhton P. (2016). Energy performance of Double-Skin Façades in temperate climates: a systematic review and Meta-analysis, *Renewable and Sustainable Energy Review*, vol. 54, pp.1525-1536.
- Radhi, H., Sharples, S. & Fikiry, F., (2013). Will multi-façade systems reduce cooling energy in fully glazed building? A scoping study of UAE buildings, *Energy & Buildings*, vol. 56, pp. 179-188.
- Royal Scientific Society. (2009). *Energy Efficient Building for Jordan: Conference in Jerusalem*. November.
- Sahlin, P. (2000) The Methods of 2020 for Building Envelope and HVAC Systems Simulation - Will the Present Tools Survive? [online]. Stockholm: Västerlånggatan. [Accessed May 27, 2018]. Available at: <https://www.equa.se/dncenter/Dublin2000.pdf>
- Schofield, J. (2012). Case study: Capital Gate, Abu Dhabi, *International Journal on Tall Buildings and Urban Habitant* [online], (2). [Accessed 22 June 2018]. Available at: <http://global.ctbuh.org/resources/papers/download/21-case-study-capital-gate-abu-dhabi.pdf>

- Shameri, M., Alghoul, M., Sopian, K., Zain, M., & Elayeb, O. (2011). Perspectives of double skin façade systems in buildings and energy saving, *Renewable and Sustainable Energy Review*, vol. 15, pp. 1468-1475.
- Shariah, A., Tashtoush, B., & Rousan A. (1997). Cooling and heating loads in residential buildings in Jordan, *Energy and Buildings*, vol. 26, pp. 137-143.
- Shen, C. & Li, X. (2016). Solar heat gains reduction of double glazing façade with cooling pipes embedded in venetian blinds by utilizing natural cooling, *Energy & Buildings*, vol. 112 (2016), pp.173-184.
- Sing, M., Garg, S., & JHA, R. (2008). Different glazing system and their impact on human thermal comfort – Indian scenario, *Building and Environment*, vol. 43, pp. 1596-1602.
- Sousa, J. (2012). Energy Simulation Software for Buildings: Review and Comparison. *Information Technology for Energy Application 2012: Proceedings of the First International Workshop on Information Technology for Energy Applications* [online]. Lisbon, Portugal. 6-7 September. [Accessed 2 June 2018] Available at: <http://ceur-ws.org/Vol-923/paper08.pdf>
- Suliman, S., and Beithou, N. (2011). Residential building walls and environment in Amman, Jordan. *International Journal of Thermal & Environment Engineering*, vol. 3 (2), pp. 101-107.
- Tashakkori, A. & Teddlie, C. (2003) *Handbook of Mixed Methods in Social & Behavioral Research* [online]. Viewed 27 December 2016 available at: <http://www3.uakron.edu/arm/resources/education/Books%20IID.pdf>
- Torres, M., Alavedra, P., Guzman, A., Cuerva, E., Planas, C., Clemente, R., & Escalona, V., (2007). *Double skin façade – cavity and exterior dimensions for saving energy on Mediterranean climate, Building Simulation*. Beijing: China.
- Walliman, N. (2011). *Research methodology: the basics*. Abington: Routledge.
- Zerefos, S. (2008). On the performance of double skin façade in different environmental conditions, *Internal Journal of Sustainable Energy* [online], vol. 26 (4), [Accessed 5 May 2018]. Available at: <https://doi.org/10.1080/14786450701803239>

